

## Effects of Actinide Burning on Waste Disposal at Yucca Mountain

By

Jessica Hirschfelder

DOE/OR/00033--T484

DE92 016228

B.S. (Massachusetts Institute of Technology) 1989

1982-1992

## THESIS

Submitted in partial satisfaction of the requirements for the degree of

MASTER OF SCIENCE

in

NUCLEAR ENGINEERING

in the

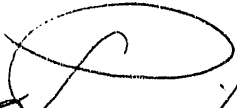
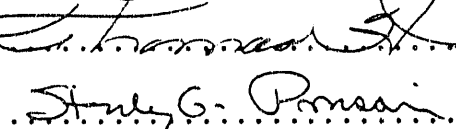
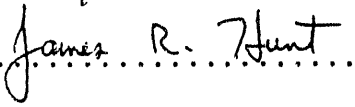
GRADUATE DIVISION

of the

UNIVERSITY OF CALIFORNIA at BERKELEY

Approved:

Chair: .....

 Dr. Thomas J. Dugay ..... April 7, 1992  
 Date  
 .....  
 Stanley G. Pearson ..... 3/25/92  
 .....  
 James R. Hunt ..... 4/20/92

\* \* \* \* \*

MASTER

JMF

DISTRIBUTION OF THIS DOCUMENT IS UNLIMITED

# **Effects of Actinide Burning on Waste Disposal at Yucca Mountain**

by

**Jessica Hirschfelder**

## **Abstract**

Release rates of 15 radionuclides from waste packages expected to result from partitioning and transmutation of Light-Water Reactor (LWR) and Actinide-Burning Liquid-Metal Reactor (ALMR) spent fuel are calculated and compared to release rates from standard LWR spent fuel packages. The release rates are input to a model for radionuclide transport from the proposed geologic repository at Yucca Mountain to the water table. Discharge rates at the water table are calculated and used in a model for transport to the accessible environment, defined to be five kilometers from the repository edge. Concentrations and dose rates at the accessible environment from spent fuel and wastes from reprocessing, with partitioning and transmutation, are calculated.

Partitioning and transmutation of LWR and ALMR spent fuel reduces the inventories of uranium, neptunium, plutonium, americium and curium in the high-level waste by factors of 40 to 500. However, because release rates of all of the actinides except curium are limited by solubility and are independent of package inventory, they are not reduced correspondingly. Only for curium is the repository release rate much lower for reprocessing wastes.

The only actinides that reach the water table are U-234, U-238, Np-237, and Pu-242. Their discharge rates at the water table from spent fuel are only about one to six times higher than those from reprocessing wastes, due mainly to radionuclide placement in a larger number of spent fuel packages. The discharge rates at the water table of Tc-99 and I-129, from both spent fuel and reprocessing wastes, are

about  $10^6$  times higher than those of the actinides with the highest discharge rates. Dose rates of Tc-99 and I-129 at the accessible environment are about  $10^5$  times higher than the dose rates of these actinides. The Tc-99 and I-129 peak dose rates from spent fuel are about two and one times higher, respectively, than those from reprocessing wastes. This is due to a combination of factors including their inventories, waste forms, and waste package types, which differ for spent fuel and reprocessing wastes.

“You've got to take on a more serious attitude.”

-Thor, God of the Sky

## Contents

List of Figures . . . . .	iv
List of Tables . . . . .	vii
Acknowledgements . . . . .	ix
1. Introduction	
1.1. The Yucca Mountain Project . . . . .	1
1.2. The ALMR Program . . . . .	5
1.3. Basis for this Study . . . . .	8
2. Release Rates from the Repository	
2.1. Release Rate Model . . . . .	15
2.2. Waste Packages and Inventories . . . . .	17
2.2.1. Spent Fuel . . . . .	17
2.2.2. Reprocessing Wastes . . . . .	19
2.3. Radionuclide Release Rates . . . . .	35
2.3.1. Normalized Per-Package Release Rates . . . . .	35
2.3.2. Repository Release Rates . . . . .	50
2.4. The Borosilicate Glass Option . . . . .	62
3. Transport in the Unsaturated Zone	
3.1. Transport Model . . . . .	68
3.2. Discussion of Parameters . . . . .	74
3.3. Discharge Rates at the Water Table . . . . .	77
4. Transport in the Saturated Zone	
4.1. Transport Model . . . . .	84
4.2. Discussion of Parameters . . . . .	89
4.3. Concentrations at the Accessible Environment . . . . .	92
5. Conclusions . . . . .	103
References . . . . .	107

## List of Figures

Figure 1.1. Location of Proposed Repository at Yucca Mountain, from Ref. 4	3
Figure 1.2. Cross-Section of Proposed Repository at Yucca Mountain, from Ref. 4	4
Figure 1.3. Comparison of Disposal Schemes: Spent Fuel and Reprocessing Wastes	10
Figure 2.1. LWR Spent Fuel Pyroprocess Flowsheet, from Ref. 28	20
Figure 2.2. ALMR Spent Fuel Pyroprocess Flowsheet, from Ref. 28	21
Figure 2.3. Normalized Release Rates of Alteration-Controlled Species from Spent Fuel	36
Figure 2.4. Normalized Release Rates of Uranium and Np-237 from Spent Fuel	37
Figure 2.5. Normalized Release Rates of U-234 and Daughters from Spent Fuel	38
Figure 2.6. Normalized Release Rates of Plutonium and Americium from Spent Fuel	39
Figure 2.7. Normalized Release Rates of Tc-99 from Reprocessing Wastes	41
Figure 2.8. Normalized Release Rates of I-129 and Cs-135 from Reprocessing Wastes	42
Figure 2.9. Normalized Release Rates of Uranium from Reprocessing Wastes	43
Figure 2.10. Normalized Release Rates of U-234 and Daughters from Reprocessing Wastes	44
Figure 2.11. Normalized Release Rates of Np-237 from Reprocessing Wastes	45
Figure 2.12. Normalized Release Rates of Plutonium from Reprocessing Wastes	46
Figure 2.13. Normalized Release Rates of Americium from Reprocessing Wastes	47
Figure 2.14. Normalized Release Rates of Curium from Reprocessing Wastes	48

Figure 2.15. Per-Package Release Rates of Uranium from Spent Fuel and Reprocessing Wastes . . . . .	49
Figure 2.16. Repository Release Rates of Fission Products from Spent Fuel and Reprocessing Wastes . . . . .	51
Figure 2.17. Repository Release Rates of Uranium from Spent Fuel and Reprocessing Wastes . . . . .	52
Figure 2.18. Repository Release Rates of U-234 and Daughters from Spent Fuel and Reprocessing Wastes . . . . .	53
Figure 2.19. Repository Release Rates of Np-237 from Spent Fuel and Reprocessing Wastes . . . . .	54
Figure 2.20. Repository Release Rates of Plutonium from Spent Fuel and Reprocessing Wastes . . . . .	55
Figure 2.21. Repository Release Rates of Americium from Spent Fuel and Reprocessing Wastes . . . . .	56
Figure 2.22. Repository Release Rates of Curium from Spent Fuel and Reprocessing Wastes . . . . .	57
Figure 2.23. Normalized Release Rates of I-129 and Cs-135 in Borosilicate Glass and Salt/Zeolite Wastes . . . . .	66
Figure 2.24. Repository Release Rates of I-129 and Cs-135 in Borosilicate Glass and Salt/Zeolite Wastes, Without Sr/Cs Separation . . . . .	67
Figure 3.1. Unsaturated Zone Radionuclide Transport Model . . . . .	69
Figure 3.2. Tc-99 and I-129 Discharge Rates at the Water Table for Spent Fuel and Reprocessing Wastes . . . . .	78
Figure 3.3. Uranium Discharge Rates at the Water Table for Spent Fuel and Reprocessing Wastes . . . . .	79
Figure 3.4. U-234 and Daughters Discharge Rates at the Water Table for Spent Fuel and Reprocessing Wastes . . . . .	80
Figure 3.5. Np-237 and Pu-242 Discharge Rates at the Water Table for Spent Fuel and Reprocessing Wastes . . . . .	81

Figure 4.1. Saturated Zone Radionuclide Transport Model . . . . .	85
Figure 4.2. Source Point Locations for the Saturated Zone Transport Model	86
Figure 4.3. Tc-99 and I-129 Concentrations at the Accessible Environment for Spent Fuel and Reprocessing Wastes . . . . .	93
Figure 4.4. Uranium Concentrations at the Accessible Environment for Spent Fuel and Reprocessing Wastes . . . . .	94
Figure 4.5. U-234 and Daughters Concentrations at the Accessible Environment for Spent Fuel and Reprocessing Wastes . . . . .	95
Figure 4.6. Np-237 and Pu-242 Concentrations at the Accessible Environment for Spent Fuel and Reprocessing Wastes . . . . .	96
Figure 4.7. Tc-99 and I-129 Dose Rates at the Accessible Environment for Spent Fuel and Reprocessing Wastes . . . . .	97
Figure 4.8. Uranium Dose Rates at the Accessible Environment for Spent Fuel and Reprocessing Wastes . . . . .	98
Figure 4.9. U-234 and Daughters Dose Rates at the Accessible Environment for Spent Fuel and Reprocessing Wastes . . . . .	99
Figure 4.10. Np-237 and Pu-242 Dose Rates at the Accessible Environment for Spent Fuel and Reprocessing Wastes . . . . .	100

## List of Tables

Table 1.1. Radionuclides Included in this Study . . . . .	11
Table 1.2. ALMR Characteristics by Breeding Ratio . . . . .	13
Table 2.1. Spent Fuel Container Characteristics . . . . .	17
Table 2.2. Spent Fuel Radionuclide Inventories . . . . .	18
Table 2.3. Solubilities of Actinides in Spent Fuel . . . . .	19
Table 2.4. Waste Stream Heat Generation Rates at 10 Years . . . . .	25
Table 2.5. Reprocessing Waste Package Characteristics . . . . .	27
Table 2.6. Reprocessing Waste Packages . . . . .	28
Table 2.7. 1000-Year Inventories: Waste Stream A1-1,2 . . . . .	29
Table 2.8. 1000-Year Inventories: Iodine and Cesium Waste Streams . . . . .	29
Table 2.9. 1000-Year Inventories: Waste Stream A1-6 . . . . .	30
Table 2.10. 1000-Year Inventories: Waste Stream A1-8 . . . . .	30
Table 2.11. 1000-Year Inventories: Waste Stream A3-2,5 . . . . .	31
Table 2.12. Repository Inventories at 1000 Years, Reprocessing Schemes . . . . .	32
Table 2.13. Reduction Factors of Reprocessed LWR Spent Fuel at 10 Years . . . . .	33
Table 2.14. Reprocessing Waste Forms . . . . .	34
Table 2.15. Reprocessing Waste Release Mechanisms . . . . .	34
Table 2.16. Total Top Areas of Waste Packages Containing Solubility-Limited Species . . . . .	59
Table 2.17. Peak Release Rates from Spent Fuel in $10^5$ Years . . . . .	60
Table 2.18. Peak Release Rates from Reprocessing Wastes in $10^5$ Years, Without Sr/Cs Separation . . . . .	61
Table 2.19. Cumulative Releases from Spent Fuel and Reprocessing Wastes Without Sr/Cs Separation, in $10^5$ Years . . . . .	63
Table 2.20. Borosilicate Glass Per-Package Inventories at 1000 Years, Without Sr/Cs Separation . . . . .	64

## **Acknowledgements**

I would like to thank Professor Pigford very much for all of his help and guidance on this project. I would also like to thank Dr. Lee for much miscellaneous help. Mr. Light and Mr. Sadeghi generously helped with programming, and calculating many of the waste package release rates, respectively. I also thank Professor Chambré and Dr. Choi for their helpful discussions.

I would also like to thank Professors Hunt and Prussin, the other two members of my thesis committee. I also thank Mr. Hwang, Ms. Zhou, and Mr. Zwahlen for their helpful comments. Finally, I would like to thank Dr. Bear and Mr. Fong for their distinguished silliness, which they have demonstrated most superbly, and which remains unsurpassed in both quantity and quality.

This research was performed under appointment to the Environmental Restoration and Waste Management Fellowship program administered by Oak Ridge Associated Universities for the U. S. Department of Energy.

Table 3.1. Properties of Yucca Mountain Tuff Layers . . . . .	75
Table 3.2. SCP Unsaturated Zone Sorption Experiment Data: $K_D$ in ml/g . . . . .	76
Table 3.3. Unsaturated Zone Retardation Parameters . . . . .	77
Table 3.4. Radionuclide Travel Times to the Water Table . . . . .	82
Table 4.1. Source Points for the Saturated Zone Transport Model . . . . .	88
Table 4.2. Saturated Zone Hydrologic Parameters . . . . .	89
Table 4.3. SCP Saturated Zone Sorption Experiment Data: $K_D$ in ml/g . . . . .	90
Table 4.4. Saturated Zone Retardation Parameters . . . . .	91
Table 4.5. Radionuclide Dose Conversion Factors . . . . .	91

## Chapter 1

### Introduction

#### 1.1 The Yucca Mountain Project

For over 40 years, the United States has been stockpiling radioactive wastes from commercial nuclear power reactors, defense activities and research institutions. Since the first U. S. commercial nuclear power plant began operation in 1957, radioactive spent fuel has been stored in pools and dry casks at nuclear plant sites across the country. Spent fuel accounts for over 90% of the radioactivity of stored nuclear wastes.<sup>1</sup>

By the end of 1991, these storage facilities will contain approximately 23,400 Mg of spent fuel.<sup>2</sup> One Mg of spent fuel refers to one Mg of initial heavy metal fueled to the reactor. By the year 2000, the U. S. spent fuel inventory is expected to exceed 40,000 Mg.<sup>2</sup> By then there is also expected to be about  $3.5 \times 10^5$  m<sup>3</sup> of defense high-level wastes (before processing for disposal).<sup>2</sup> Defense nuclear wastes are currently stored primarily at three U. S. Department of Energy (DOE) facilities: the Savannah River Site in South Carolina, the Idaho National Engineering Laboratory, and the Hanford Site in Washington State.

Much of these wastes consists of long-lived, highly toxic species which pose a direct threat to human health. The DOE has chosen deep geologic disposal as its method of isolating these wastes from humans. Radioactive waste will be packaged in special containers designed to resist corrosion for 300 to 1000 years,<sup>3</sup> and will then be buried in an underground repository. The wastes to be emplaced are commercial spent fuel, defense high-level wastes, and a small amount of commercial high-level waste. Radionuclides that are released from the containers can migrate into the flowing groundwater in the surrounding rock, becoming diluted and eventually reaching human living areas. The combined barriers of the waste package, backfill

(filler material which may be placed between the waste package and the surrounding rock), and the rock itself, are expected to contain radionuclides for thousands of years, preventing them from reaching humans until after they have decayed to safe levels.

In 1982, Congress established the Nuclear Waste Policy Act, which assigned to DOE the responsibility for locating, building, and operating a nuclear waste repository. In 1983, DOE selected nine locations in six states for consideration as potential repository sites. After preliminary studies of all nine sites, three were selected for intensive site characterization: the Hanford Reservation; Deaf Smith County, Texas; and Yucca Mountain, Nevada. In December 1987, Congress amended the Nuclear Waste Policy Act to designate Yucca Mountain as the only site for study. If Yucca Mountain is found suitable, DOE will recommend the site to the president. If the site receives presidential approval, DOE will then seek a license from the Nuclear Regulatory Commission (NRC) to begin construction of the repository. If Yucca Mountain is found unsuitable, it will be restored to its natural condition and a new site will be found.

Yucca Mountain is located in Nye County in southern Nevada, about 160 km northwest of Las Vegas. The site is situated on three federal lands, the Nellis Air Force Range, the Nevada Test Site, and lands managed by the Bureau of Land Management. Figure 1.1 shows the location of the proposed repository. It lies in an arid region with little rainfall, sparse vegetation and sparse population.

Yucca Mountain consists of layers of tuff, a dense form of compacted volcanic ash. The proposed repository horizon is located in the Topopah Spring Member, a part of the Paintbrush Tuff rock formation. It lies in the unsaturated zone, about 300 m below the land surface and 200 m above the water table. Figure 1.2 shows a cross-section of the repository and the rock layers of Yucca Mountain. Because rainfall is very low (about six inches per year<sup>4</sup>) and the evaporation rate is high, little water is expected to percolate downward from the ground surface and contact

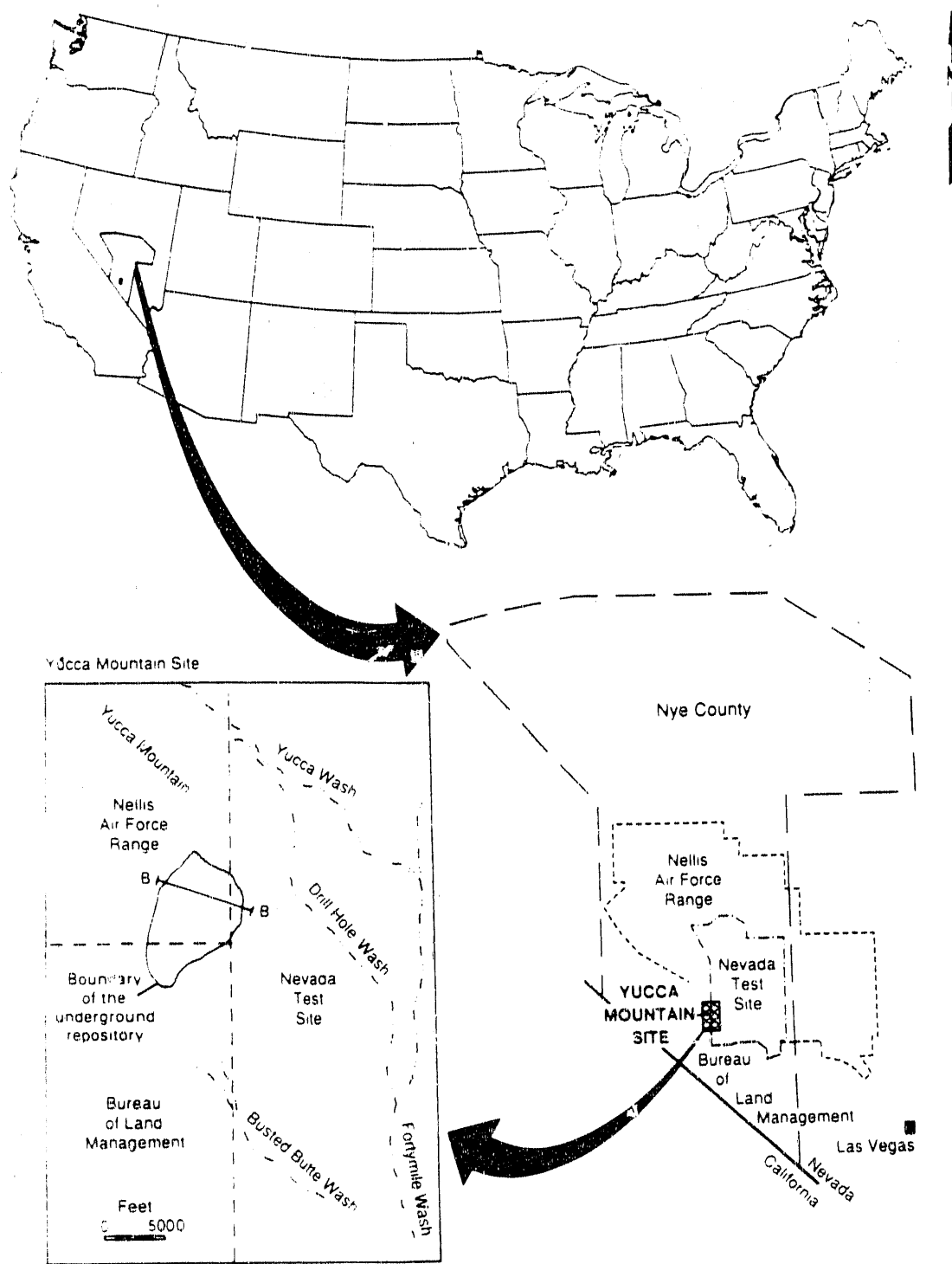


Figure 1.1. Location of Proposed Repository at Yucca Mountain, from Ref. 4

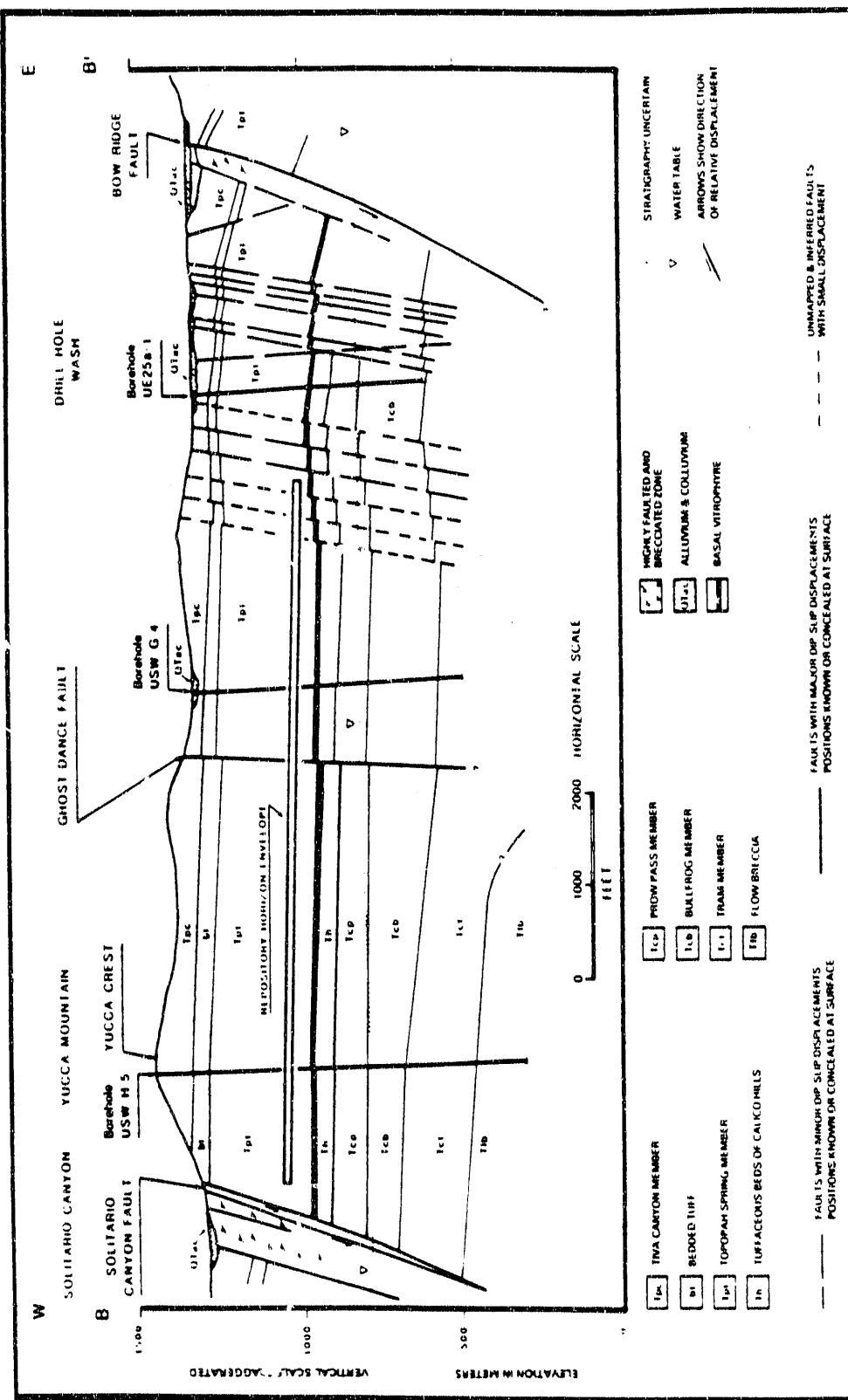


Figure 1.2. Cross-Section of Proposed Repository at Yucca Mountain, from Ref. 4

the waste packages.

Water that does flow downward through the rock layers can dissolve radionuclides in the wastes and carry them away from the repository. The water is expected to travel primarily in the rock matrix and to take thousands of years to reach the water table. Water in the saturated zone is believed to flow horizontally through fractures, at a much faster rate than in the unsaturated zone. Eventually, contaminated water can reach the "accessible environment," any area where it could be used by humans. DOE defines the accessible environment as all locations at least 5 km from the repository perimeter.

The NRC<sup>3</sup> has specified for each radionuclide its maximum allowable release rate at the waste surface. The Environmental Protection Agency (EPA)<sup>5</sup> has set limits on the allowable cumulative radionuclide releases at the accessible environment in 10,000 years. In this thesis, release rates and cumulative releases of radionuclides in a variety of wastes are calculated and compared with the NRC and EPA limits.

## 1.2 The ALMR Program

Partitioning the actinides in spent fuel and transmuting them in actinide-burning liquid-metal reactors (ALMRs) has been proposed as a method of reducing the public risks from geologic disposal of nuclear waste.<sup>6</sup> Spent fuel can be reprocessed, and the actinides can be recovered and then transmuted into stable or short-lived isotopes by bombardment with neutrons. Actinide burning refers to the concept of using ALMRs fueled with the actinides recovered from light-water reactor (LWR) spent fuel to generate electricity as well as perform transmutation. Transmuting the actinides in particle accelerators has also been proposed.<sup>7</sup>

A detailed history of partitioning and transmutation concepts is given by Croff.<sup>8</sup> He states that Steinburg<sup>9</sup> first suggested transmutation as a waste management option in 1964. Subsequent U. S. and international studies<sup>10-14</sup> in the 1970's and early 1980's generally concluded that, while technologically feasible, actinide burning offered little improvement in the safety of a geologic repository and would be very

costly to implement. For example, Burkholder<sup>10</sup> found that removal of actinides from high-level waste placed in a geologic repository did not appreciably reduce the radiation doses to future humans. Croff *et. al.*<sup>12</sup> found no cost or safety incentives for partitioning and transmuting actinides for waste management purposes.

Interest in actinide burning waned after the mid-1980's but in the past few years has been renewed for a number of reasons. New pyrochemical reprocessing techniques designed to recover up to 99.999% of the actinides in spent fuel are being explored at Argonne National Laboratory (ANL). Improved conventional aqueous processes are also expected to achieve this high actinide recovery rate. Earlier studies<sup>12</sup> concluded that the increase in short-term doses to reprocessing facility workers, and to the public from release of gaseous radionuclides during reprocessing, would equal or exceed the long-term dose reduction from removal of actinides from high-level wastes. However, advances in robotics and remote-handling methods, and new technologies for trapping and storing gasses, could decrease short-term doses.

Other reasons for the renewed interest in actinide burning include the availability of an accelerator at Los Alamos National Laboratory which may be suitable for transmuting nuclear waste, and increased public and political opposition to the Yucca Mountain repository. It has been suggested that public acceptance of the repository will be easier to obtain if most of the actinides are removed from the wastes. It has also been suggested that site characterization and repository licensing would be simplified, and that the waste forms resulting from reprocessing would be less reactive than spent fuel in the oxidizing environment of Yucca Mountain.

The proposed DOE ALMR program specifies treating LWR spent fuel with either an aqueous or pyrochemical process in which 99.9% to 99.999% of the actinides would be removed and fabricated into ALMR fuel. This fuel would support the annual introduction of 1.4 GWe of ALMRs, beginning sometime between 2005 and 2012. Spent ALMR fuel would also be reprocessed and the recovered actinides would be recycled into more ALMR fuel. Wastes from reprocessing LWR and

ALMR spent fuel would be placed in the repository. By the year 2045, all of the LWR fuel now destined for the repository would be reprocessed. Profits from the sale of electricity produced by the ALMRs would be used to pay for their construction and for the reprocessing plant(s).

A variation of the program includes separation of strontium and cesium, the primary heat producers in the wastes from reprocessing both LWR and ALMR spent fuel. With this option, strontium and cesium would be separated from the other reprocessing wastes and stored above ground for 200-300 years. The remaining wastes would be placed in the repository. After the heat-producing Sr-90 and Cs-137 have decayed, the remaining long-lived Cs-135 would also be emplaced in the repository.

The General Electric Company's PRISM (Power Reactor, Innovative Small Module) actinide burner, along with the Integral Fast Reactor (IFR) metal fuel pyroprocess being developed at ANL, is the reference DOE ALMR program.<sup>15,16</sup> One PRISM consists of nine modules organized in three identical 465 MWe power blocks for an overall electrical production of 1395 MWe. The reactor uses as fuel uranium and plutonium, as well as the minor actinides neptunium, americium and curium. Because only a small fraction of the uranium recovered from LWR spent fuel can be used in an ALMR, some plan for dealing with the excess uranium must be devised.

An ALMR may be operated as a burner, in which it consumes more actinides than it produces, or a breeder, in which it supports a net production of actinides which can be used to repeatedly fuel itself or other ALMRs. Development of the PRISM began prior to renewed interest in actinide burning as a waste management strategy; the design includes features unrelated to waste management, such as modular construction, improved fuel economy, and passive safety features.

The ALMR program is currently highly controversial. A few of its suggested benefits are mentioned above. Proposed drawbacks of the program include its projected high cost,<sup>17,18</sup> increased risks from reprocessing facilities, and nuclear proliferation

issues. The desirability of strontium and cesium separation is also disputed. It has been suggested that the reduced heat generation rates may reduce technical uncertainty about the performance of the repository,<sup>19,20</sup> and would allow greater areal loading of wastes, thus eliminating the need for a second repository. However, decay heat from emplaced wastes is expected to keep the surrounding rock at temperatures above the boiling point of water for over one thousand years,<sup>21,22</sup> thereby preventing liquid water from contacting and corroding the waste packages during this time. A number of papers<sup>8,18,23,24</sup> discuss in more detail the many issues involved with the ALMR program.

### 1.3 Basis for this Study

Studies conducted in the mid-1980's and earlier, which found little benefit to waste disposal from partitioning and transmutation, addressed only uranium and plutonium recycle. At least two recent studies<sup>25,26</sup> have investigated the effects on long-term radiation doses to humans of recovering other actinides as well. However, the effects of actinide removal on wastes buried in the Yucca Mountain repository have not been fully analyzed. In this study, we compare the radiation doses to future humans resulting from burial at Yucca Mountain of LWR spent fuel and of wastes from reprocessing, with actinide recycle, both LWR and ALMR spent fuel.

Two waste disposal schemes are considered. In each, the heat generation rate of the wastes at emplacement is  $1.1 \times 10^8$  watts, the maximum for the repository. Existing information about the Yucca Mountain site indicates that 2,095 acres would be available for underground waste emplacement, and current plans call for using 1,380 acres.<sup>4</sup> We assume that for economic considerations, the entire available area will be used. With a heat generation limit of 57 kW/acre,<sup>4</sup> the repository can hold wastes generating  $1.1 \times 10^8$  watts. We assume that wastes in both disposal schemes are ten years old at emplacement.

In the first disposal scheme, the repository contains only unprocessed LWR spent fuel. Ten year old spent fuel from a pressurized water reactor (PWR) with a burnup

of  $33,000 \text{ MWd/Mg}$  generates  $1.14 \times 10^3 \text{ W/Mg}$ ,<sup>27</sup> so the repository will contain  $96,500 \text{ Mg}$ . This is 38 percent greater than the current legal limit of  $70,000 \text{ Mg}$ . However, this limit was not established from any technical limitation of the site, so it is reasonable to assume that it may be changed. We also note that, because a substantial amount of the spent fuel currently stored at reactor sites is already ten to twenty years old, by the time the repository is constructed the average age of U. S. spent fuel will probably be greater than ten years. If the repository were filled with thirty year old spent fuel, which generates  $723 \text{ W/Mg}$ ,<sup>27</sup> it could contain  $1.52 \times 10^5 \text{ Mg}$ . Although only the  $96,500 \text{ Mg}$  case is investigated, it will be shown later that radionuclide release rates and radiation dose rates from spent fuel are approximately proportional to the number of Mg placed in the repository.

In the second disposal scheme, all current U. S. LWRs operate for 40 year lifetimes, producing a total of  $84,000 \text{ Mg}$  of LWR spent fuel. No additional LWRs are built; instead we assume that ALMRs are then used to produce electricity indefinitely. The LWR spent fuel is treated using the ANL pyrochemical process: 98.4% of the U and 99.8% of the Np, Pu, Am, and Cm<sup>28</sup> are extracted and fabricated into ALMR fuel, with the reprocessing wastes destined for the repository. Spent ALMR fuel is also pyrochemically reprocessed: 99.8% of the actinides is recovered and recycled into ALMR fuel, and the wastes are placed in the repository. Thus in the second scheme, the repository contains wastes from reprocessing  $84,000 \text{ Mg}$  of LWR spent fuel, plus the maximum amount of ALMR reprocessing wastes allowed in the repository, based on its heat generation limit. We consider the wastes that would be emplaced both with and without strontium and cesium separation.

Figure 1.3 illustrates the two disposal schemes. In both schemes we ignore defense wastes, which must also be placed in the repository. For each scheme, we calculate release rates from the repository for 15 radionuclides, listed in Table 1.1. These species have been chosen due to their roles in the actinide burning process and/or their importance to waste disposal. We then calculate mass discharge rates at the water table, and concentrations and dose rates at the accessible environment. The

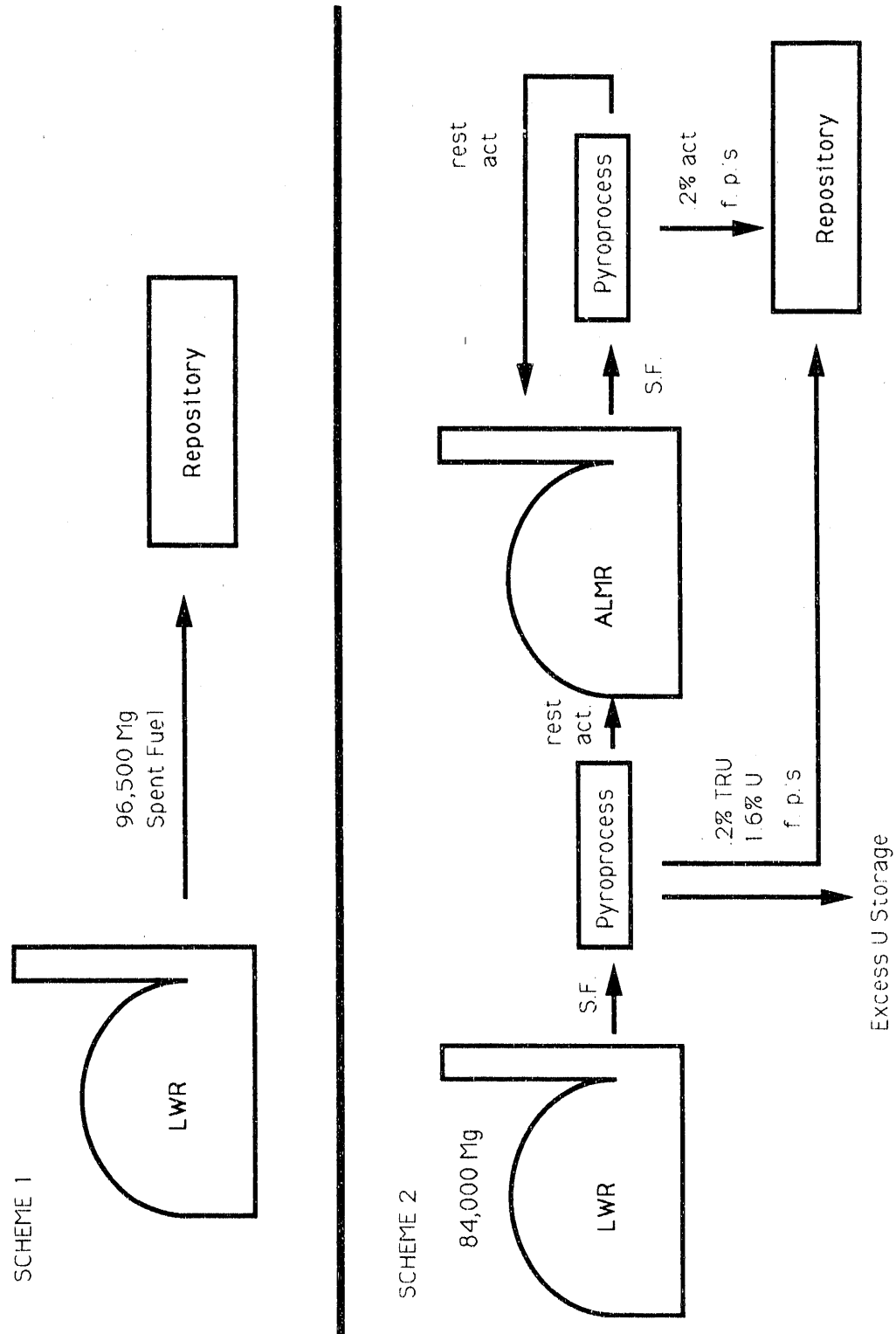


Figure 1.3. Comparison of Disposal Schemes: Spent Fuel and Reprocessing Wastes

results provide a comparison of the risks to future humans from disposal at Yucca Mountain of unprocessed spent fuel and of wastes resulting from a program of actinide partitioning and transmutation in ALMRs.

Table 1.1. Radionuclides Included in this Study (Data from Ref. 2)

Species	Half Life (years)	Decay Constant (per year)	Specific Activity (Ci/g)
Tc-99	$2.13 \times 10^5$	$3.25 \times 10^{-6}$	$1.695 \times 10^{-2}$
I-129	$1.57 \times 10^7$	$4.41 \times 10^{-8}$	$1.765 \times 10^{-4}$
Cs-135	$3.0 \times 10^6$	$2.3 \times 10^{-7}$	$1.151 \times 10^{-3}$
Ra-226	$1.600 \times 10^3$	$4.332 \times 10^{-4}$	$9.887 \times 10^{-1}$
Th-230	$7.54 \times 10^4$	$9.19 \times 10^{-6}$	$2.109 \times 10^{-2}$
U-234	$2.454 \times 10^5$	$2.824 \times 10^{-6}$	$6.248 \times 10^{-3}$
U-238	$4.468 \times 10^9$	$1.551 \times 10^{-10}$	$3.362 \times 10^{-7}$
Np-237	$2.140 \times 10^6$	$3.239 \times 10^{-7}$	$7.049 \times 10^{-4}$
Pu-239	$2.411 \times 10^4$	$2.874 \times 10^{-5}$	$6.216 \times 10^{-2}$
Pu-240	$6.563 \times 10^3$	$1.056 \times 10^{-4}$	$2.279 \times 10^{-1}$
Pu-242	$3.763 \times 10^5$	$1.842 \times 10^{-6}$	$3.818 \times 10^{-3}$
Am-241	$4.327 \times 10^2$	$1.601 \times 10^{-3}$	3.432
Am-243	$7.380 \times 10^3$	$9.392 \times 10^{-5}$	$1.993 \times 10^{-1}$
Cm-245	$8.5 \times 10^3$	$8.1 \times 10^{-5}$	$1.717 \times 10^{-1}$
Cm-246	$4.73 \times 10^3$	$1.46 \times 10^{-4}$	$3.072 \times 10^{-1}$

An ALMR can be fueled in many ways with recycled LWR and ALMR actinides. We assume that transuranics (TRU) recovered from LWR spent fuel will be used for the initial load and first two reloads of the ALMR. If the ALMR is operated as a breeder, with a breeding ratio of at least unity, the transuranics for subsequent reloads will be those recycled from discharged ALMR core and blanket fuel. If the ALMR is operated as a burner, transuranics from LWR spent fuel will be needed

for partial makeup of subsequent reloads.

Pigford and Choi<sup>29</sup> tabulate, for ALMRs with capacity factor 0.8 and various breeding ratios, the length of a refueling cycle, the net transuranic depletion rate, and the transuranic inventory in the reactor and fuel cycle, approximately equal to the transuranics needed for startup and the first two reloads. Here the breeding ratio is defined as the ratio of Pu-239,241 production to Pu-239,241 destruction. A breeding ratio of 0.22 corresponds to no production of new transuranics, and 0.96 corresponds to no net production or depletion of transuranics. The net transuranic depletion rate, the difference between the refueling and discharge rates at steady state, is the transuranics needed from LWR spent fuel for one reactor cycle. The total amount of LWR transuranics needed to fuel one ALMR is the amount needed for startup and the first two reloads, plus makeup for the rest of its 40 year life. With one Mg of LWR spent fuel proving 9.72 kg transuranics, we may also calculate the number of ALMRs needed to burn 84,000 Mg of LWR spent fuel. These data are given in Table 1.2.

The U. S. DOE prefers a breeding ratio of 0.62,<sup>30</sup> although lower fuel cycle costs are found for breeding ratios near unity.<sup>31</sup> A breeding ratio of at least 0.76 is needed to preserve the passive safety features of the PRISM design. The composition of ALMR reprocessing wastes does not change appreciably with different breeding ratios. Since the amount of reprocessing wastes placed in the repository is determined only by their heat generation rates, it is not necessary to specify a breeding ratio for this study. However, in Chapter 2 we elaborate on the number and type of ALMRs that might be used with our reprocessing scheme.

Lee *et. al.*<sup>32</sup> calculate release rates of technetium and plutonium from waste packages using a comparison basis proposed by Pigford<sup>33</sup> in which the wastes from both disposal schemes have resulted in the production of the same amount of electrical energy. One scheme involves disposal of LWR spent fuel. In the other scheme, the 63,000 Mg of LWR spent fuel currently planned for the first repository<sup>34</sup> is re-

Table 1.2. ALMR Characteristics by Breeding Ratio (Data from Ref. 29)

Breeding Ratio	Cycle Time (yr)	TRU Needed Startup +2 Reloads (kg)	Net TRU Depletion Rate (kg/yr)	Total TRU Needed (kg)	No. ALMRs to Burn 84,000 Mg LWR S.F.
1.11 <sup>a</sup>	1.88	27,200	-115	27,200	30
0.96 <sup>a</sup>	1.61	19,400	0	19,400	42
0.76 <sup>b</sup>	1.88	27,600	250	36,700	22
0.62 <sup>a</sup>	1.16	14,400	373	28,500	29
0.40 <sup>b</sup>	1.25	20,200	487	38,500	21
0.22 <sup>c</sup>	0.700	34,900	1090	77,000	11

<sup>a</sup> Data for a PRISM with core and blanket.

<sup>b</sup> Data for a PRISM with a homogeneous core and no blanket.

<sup>c</sup> Data for an Argonne 450 MWe IFR with no blanket and core charged entirely with transuranics, scaled to 1395 MWe. Discharged IFR fuel is cooled two years before reprocessing, but reprocessing time is ignored.

processed and used to fuel 40-year ALMRs. The number of ALMRs needed to use up the 63,000 Mg depends on their capacity factor and breeding ratio. Lee *et. al.* choose 0.8 and 0.76, so that 16 ALMRs are needed. These ALMRs would produce a total of  $9.1 \times 10^5$  MWe-yr. In the reprocessing scheme, the repository contains the wastes from reprocessing 63,000 Mg LWR spent fuel and from reprocessing the spent fuel from 16 ALMRs. In the spent fuel scheme then, the repository will contain 63,000 Mg LWR spent fuel, plus the amount of spent fuel that would result from the production of an additional  $9.1 \times 10^5$  MWe-yr. This amount is 25,400 Mg, so in the spent fuel scheme the repository contains 88,400 Mg.

This basis of comparison also ignores the repository's current legal limit of 70,000 Mg. The spent fuel inventory in the spent fuel scheme is close for both comparison

bases. However, it will be shown in Chapter 2 that the number of ALMRs, with capacity factor 0.8 and breeding ratio 0.76, used in the reprocessing scheme considered in this thesis is 43, over twice the number used by Lee *et. al.* Thus in their reprocessing scheme the wattage of reprocessing wastes is substantially below that allowed at Yucca Mountain.

In the equal-energy comparison basis, the amount of waste in the repository in both schemes depends on the type of ALMR chosen. The reprocessing scheme used by Lee *et. al.* ignores the in-reactor transuranics left over after the 16 ALMRs have ceased operation. However, it is possible that the breeding ratios of later ALMRs will be higher than those of the ALMRs first built, in order to burn up the actinides left in the reactors at the end of their operation. In fact, Pigford and Choi<sup>29</sup> show that it will be necessary to operate ALMRs for hundreds of years to achieve an appreciable reduction in the transuranic inventory in the ALMR, its fuel cycle, and the wastes from reprocessing LWR and ALMR spent fuel.

With the heat-generation comparison basis, the amount of wastes in the repository depends on the storage time of the wastes before emplacement, which is not yet known. In addition, the 57 kW/acre site limit is not established and may be conservatively low. Neither comparison basis addresses the need for a second repository, which is implicit in the heat-generation basis' assumption that ALMR operation continue indefinitely. A second repository would be needed in the equal-energy basis if operation of current LWRs is not to be ended prematurely, or if it is decided that nuclear energy production continue beyond just burning up the transuranics in LWR spent fuel.

## Chapter 2

### Release Rates from the Repository

#### 2.1 Release Rate Model

Radionuclide release rates in both disposal schemes are calculated using the wet-drip water-contact mode model.<sup>35,36</sup> According to current repository design, each cylindrical, vertically emplaced waste package is expected to be surrounded by an air gap. The air gap prevents any diffusive release of dissolved radionuclides from the waste packages. Groundwater from rock above drips onto the waste packages and penetrates cracks or holes in a failed container. Radionuclides in the waste form dissolve into the water as it accumulates in the container's void volume and eventually fills the container. At this point the contaminated water overflows through the cracks in the top of the waste package and drips onto the rock below. Water in the container is assumed to always be well mixed due to diffusion and thermal convection. Overflow occurs only at the top of the container, and we assume that all waste packages fail 1000 years after emplacement. This model conservatively neglects water evaporation, which would limit water contact with the waste. The volumetric flow rate into (and out of) the container is the product of the groundwater flux and the cross-sectional area of the container. The time from container failure to overflow depends on the volumetric flow rate and the void volume inside the container. The groundwater Darcy velocity at Yucca Mountain is estimated to be about 0.5 mm/year or less.<sup>34</sup> For all calculations, the value 0.5 mm/year is used.

Radionuclide dissolution inside the waste package occurs via three different mechanisms: solubility-limited dissolution, alteration of the waste form, and immediate dissolution of readily soluble species. For solubility-limited species, we assume the waste form constituents are in chemical solubility equilibrium with the water that

has accumulated in the container. The concentration of each dissolved element is at a maximum given by the solubility of that element, until all of the element is dissolved and fresh water continues to dilute the container contents. The release rate of a solubility-limited element is given by the product of its solubility, the groundwater flux, and the cross sectional area of the waste package. The release rate of an individual radionuclide is given by the product of the elemental release rate and the time-dependent isotopic fraction of that species in the waste. For all calculations, we ignore any isotopes, such as U-235 and U-236, that are present in the waste but not included in the study. The solubility-limited release rates of radionuclides in a chain are calculated assuming that the release rate of the first member is limited by its elemental solubility and the daughters dissolve congruently with the first member. Here the only chain of interest is U-234→Th-230→Ra-226. All other decay chains are ignored.

Dissolution of alteration-controlled species occurs simultaneously with the reaction of the waste matrix with the water in the container, and is controlled by the alteration rate of the specific waste form.

For readily soluble species in certain waste forms, some or all of the inventory can immediately dissolve as soon as water enters the container and contacts the waste. The dissolved radionuclides remain in the water accumulating in the container until it overflows. The inventory fraction that is not instantly dissolved may dissolve via other mechanisms in the time between first water contact and overflow. Although it would be impossible to distinguish the processes upon overflow, release rates may be calculated separately for each mechanism and summed to obtain the total release rate from the container.

For a given species for given parameters, when more than one type of release is occurring at once, the mechanism that results in the lowest release rate is adopted as the rate-controlling mechanism for that species. Analytic expressions for the release rates of each type of species are given in Sadeghi *et. al.*<sup>36</sup>

## 2.2 Waste Packages and Inventories

In the first scheme, the repository contains only spent fuel waste packages. In the second scheme, pyrochemical reprocessing of both LWR and ALMR spent fuel results in a variety of waste streams. In this section the waste forms, waste packages, radionuclide inventories, and release mechanisms are described for both disposal schemes.

### 2.2.1 Spent Fuel

The reference spent fuel package<sup>27,34</sup> contains three PWR spent fuel assemblies. Since each assembly contains 0.5 Mg, each container holds 1.5 Mg of initial uranium. A repository filled with 96,500 Mg contains 64,333 packages. The spent fuel package characteristics are given in Table 2.1. Per-package and repository inventories are given in Table 2.2.

Table 2.1. Spent Fuel Container Characteristics (Data from Ref.s 27 and 34)

Container height (m)	4.76
Container radius (m)	0.33
Cross-sectional area (m <sup>2</sup> )	0.342
Waste volume (m <sup>3</sup> )	.155
Internal void volume (m <sup>3</sup> )	1.48
Volumetric flow rate (m <sup>3</sup> /yr)	$1.71 \times 10^{-4}$
Time to fill container (year)	8650

The dissolution of spent fuel in water from the J-13 exploratory well at Yucca Mountain has been studied in the laboratory<sup>37,38</sup> and with geochemical simulation codes.<sup>39</sup> The fractional alteration rate of spent fuel is estimated from these experiments to be  $10^{-3}$  per year.<sup>40</sup> In spent fuel the soluble technetium, iodine, and cesium that exist in the fuel-cladding gap, fuel plenum, and grain boundaries are treated as instant-dissolution species. It is assumed that two percent of these fission

Table 2.2. Spent Fuel Radionuclide Inventories

Species	Package Inventory at 10 Years (g)	Repository Inventory at 1000 Years (Ci)
Tc-99	$1.16 \times 10^3$	$1.25 \times 10^6$
I-129	$2.67 \times 10^2$	$3.04 \times 10^3$
Cs-135	$4.50 \times 10^2$	$3.33 \times 10^4$
Ra-226	$5.60 \times 10^{-7}$	$3.01 \times 10^2$
Th-230	$9.48 \times 10^{-3}$	$1.66 \times 10^3$
U-234	$2.86 \times 10^2$	$1.96 \times 10^5$
U-238	$1.42 \times 10^6$	$3.06 \times 10^4$
Np-237	$6.71 \times 10^2$	$9.65 \times 10^4$
Pu-239	$7.55 \times 10^3$	$2.95 \times 10^7$
Pu-240	$3.47 \times 10^3$	$4.61 \times 10^7$
Pu-242	$6.77 \times 10^2$	$1.66 \times 10^5$
Am-241	$7.41 \times 10^2$	$8.62 \times 10^7$
Am-243	$1.29 \times 10^2$	$1.51 \times 10^6$
Cm-245	1.28	$1.31 \times 10^4$
Cm-246	$1.52 \times 10^{-1}$	$2.61 \times 10^3$

products will dissolve immediately when water contacts the waste.<sup>40</sup> The rest is alteration-controlled. The release rate of curium, the only readily soluble actinide investigated, is lower when calculated as an alteration-controlled release rate than as a solubility-limited release rate. Curium is thus treated as alteration-controlled, but with no instant-release fraction.

Solubilities of uranium, neptunium, plutonium, and americium are obtained from experimental data<sup>38</sup> and listed in Table 2.3. Solubility is the rate-controlling mechanism for these actinides. Th-230 and Ra-226 are assumed to dissolve congruently

Table 2.3. Solubilities of Actinides in Spent Fuel

Species	Elemental Solubility (g/m <sup>3</sup> )
U-234	0.3
U-238	0.3
Np-237	$3.0 \times 10^{-4}$
Pu-239	$9.5 \times 10^{-4}$
Pu-240	$9.5 \times 10^{-4}$
Pu-242	$9.5 \times 10^{-4}$
Am-241	$3.8 \times 10^{-5}$
Am-243	$3.8 \times 10^{-5}$
Cm-245	not used
Cm-246	not used

with U-234, so their solubilities are not used in the release rate calculations.

### 2.2.2 Reprocessing Wastes

Thompson and Taylor<sup>28</sup> have specified the waste forms, waste packages, and radionuclide inventories in wastes from reprocessing one unit each of LWR and ALMR spent fuel. One unit is defined to be the amount of spent fuel generated by the production of  $10^{11}$  kWh of electricity. For a PWR, this corresponds to 420.9 Mg of initial uranium; for an ALMR, it corresponds to 51 Mg of initial actinides (fuel assemblies only). The waste packages have been modified by Wilems and Danna,<sup>41</sup> and a few are further revised here. Waste stream constituents are given<sup>28</sup> for process step transuranic recoveries of 99% and 99.9%; for this study we choose the higher recovery. In this section we describe the waste streams and waste packages, calculate the number of packages in the repository from each stream, and calculate the per-package and repository inventories.

Figures 2.1 and 2.2 show the steps involved in the LWR and ALMR pyroprocesses.

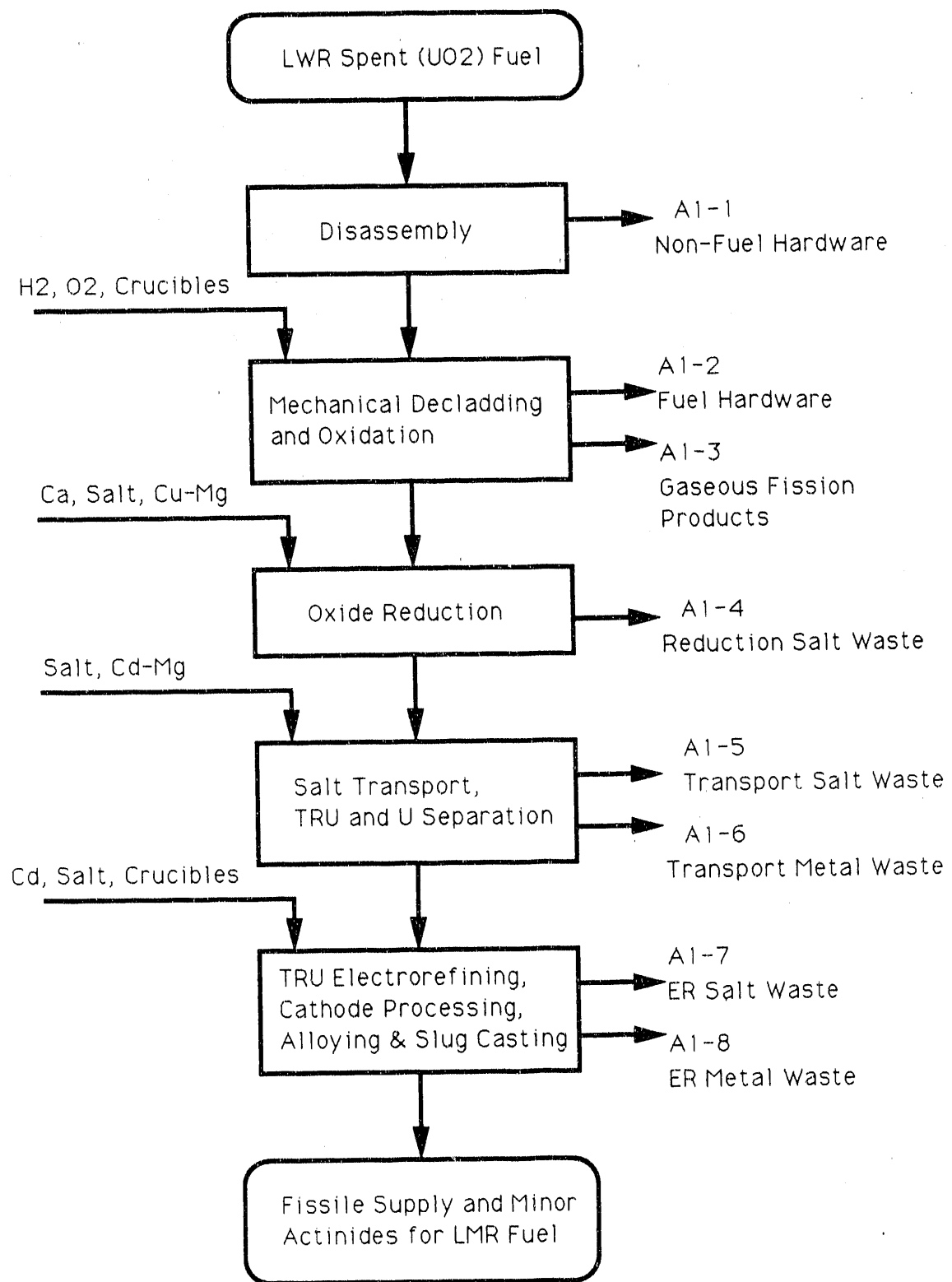


Figure 2.1. LWR Spent Fuel Pyroprocess Flowsheet, from Ref. 28

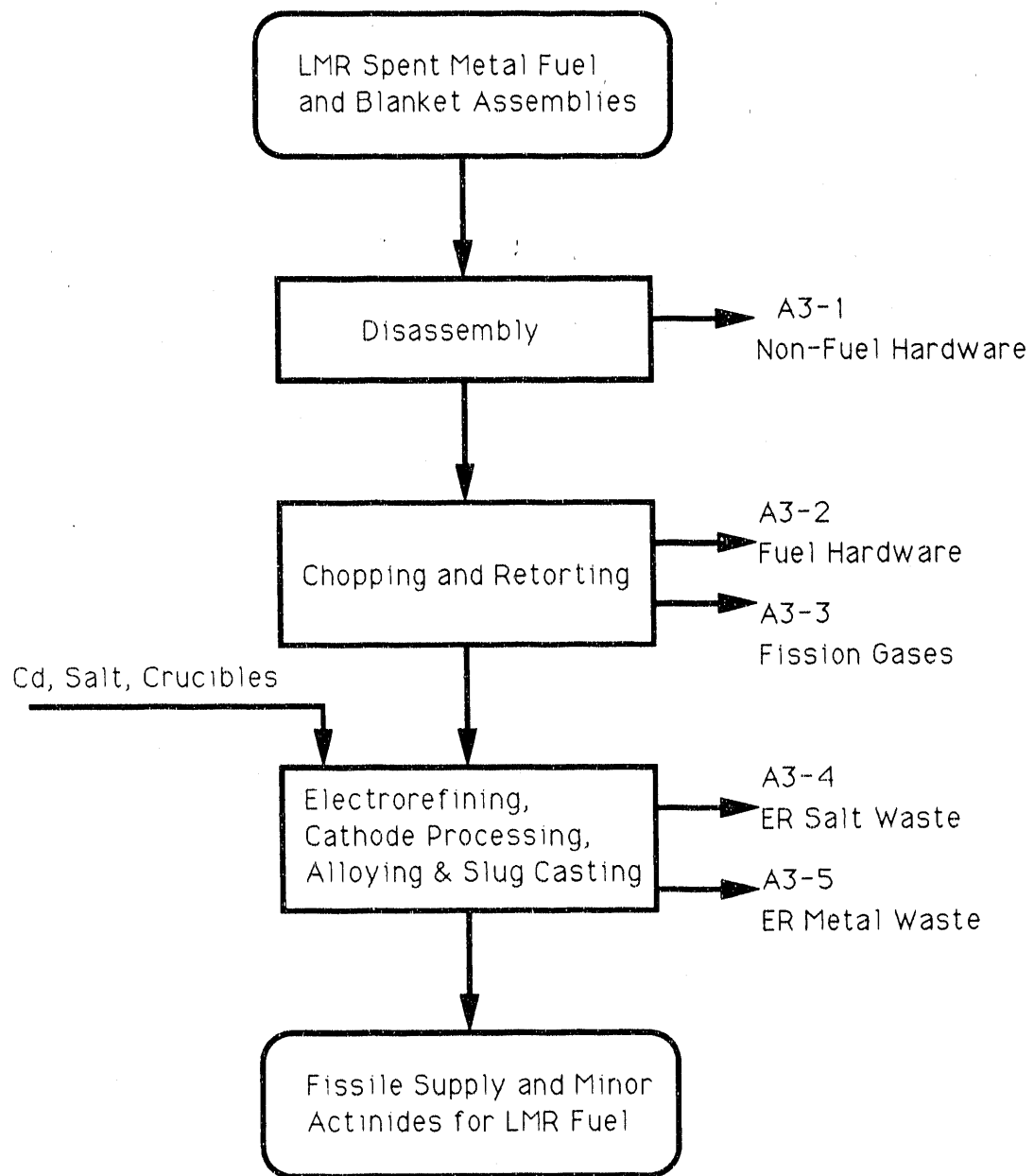


Figure 2.2. ALMR Spent Fuel Pyroprocess Flowsheet, from Ref. 28

The LWR pyroprocess is called A1 and produces eight waste streams, A1-1 to A1-8. The ALMR pyroprocess is called A3 and produces five waste streams, A3-1 to A3-5. For each process for one unit, the waste volume, waste form, wattage, and radionuclide inventories in each waste stream are given.<sup>28</sup> Not all of the waste streams are placed in the repository and not all of them contain nuclides that are included in this study.

The first step in the LWR pyroprocess consists of mechanical disassembly (separating the grid spacers and end fittings from the spent fuel assemblies). The resulting waste is labeled A1-1, non-fuel hardware waste. This stream is assumed to contain no radionuclides. The second process step separates the UO<sub>2</sub> fuel from the cladding. This produces two waste streams, fuel hardware (A1-2) and gaseous fission products (A1-3). The fuel hardware contains Tc-99 and actinides. During the second step, 0.1% of the actinides are lost to the waste; thus stream A1-2 contains 0.1% of the actinides in LWR spent fuel. Streams A1-1 and A1-2 are combined into one stream, A1-1,2 (non-fuel and fuel hardware).<sup>41</sup> The contents of this stream are to be placed directly into waste packages with no immobilization matrix.

The gaseous fission products (A1-3) are mainly H-3, I-129, C-14, krypton, and xenon. The Kr-85 (half-life 10.7 yrs) and Xe-131m (half-life 12 days) are collected cryogenically and packaged in high pressure cylinders. Wilems and Danna assigned these to the repository due to their high pressure inside the waste package. We assume they can instead be packaged into more containers at low pressures and stored in low-level facilities. Thus these wastes are not placed in the repository in the reprocessing scheme.

The H-3 is collected as tritiated water absorbed in a molecular sieve, the I-129 is collected as AgI on silver-impregnated zeolite, and C-14 is precipitated as calcium carbonate. Wilems and Danna package all three together and assign the packages to the repository. We assume the tritium can be packaged separately and stored at a low-level site since its half-life is only 12 years. We also assume that the CaCO<sub>3</sub>

can be packaged separately, and that the iodine can be separated from the zeolite and packaged as AgI, chosen for its low solubility.<sup>42</sup> Both wastes contain long-lived species and must be placed in the repository.

The third step in the LWR pyroprocess, termed oxide reduction, converts the UO<sub>2</sub> fuel fragments into metal, by combining them with a calcium salt. This produces waste stream A1-4, reduction salt waste. The salt is combined with a zeolite ceramic to immobilize the fission products. The only radionuclide included in this study that appears in this waste stream is Cs-135.

The fourth step in the LWR pyroprocess separates the Np, Pu, Am, and Cm from the noble metal fission products and the excess uranium metal. This produces two waste streams, transport salt waste (A1-5) and transport metal waste (A1-6). The transport salt does not contain any radionuclides included in this study. However, since it contains Sm-151 (half-life 90 years) we assume it will be placed in the repository. Therefore we take into account its heat generation rate when determining the amounts of waste to be placed in the repository, but do not otherwise deal with it in this study. The transport metal waste contains Tc-99 and uranium immobilized in a copper matrix. The portion of uranium lost to the wastes in this step is 1.4%.

The final step in the LWR pyroprocess further purifies the actinides by removing most of the rare earth elements. Two waste streams are produced: electrorefining salt (A1-7) and electrorefining metal (A1-8). The electrorefining salt is immobilized in zeolite. The only radionuclide included in this study that appears in this stream is Cs-135. The electrorefining metal contains Tc-99 and actinides. During this step, 0.1% of the actinides are lost to the waste; thus stream A1-8 contains 0.1% of the actinides in LWR spent fuel. The LWR reprocessing wastes will thus contain 0.2% of the transuranics, 1.6% of the uranium, and all of the fission products (since no fission products are recovered).

The first step of the ALMR pyroprocess is mechanical disassembly, which produces

non-fuel hardware waste (A3-1). This is designated by Wilems and Danna as appropriate for disposal in a low-level waste facility and is not assigned to the repository. The second step of the ALMR pyroprocess is fuel chopping and bond sodium recovery. This produces the fuel hardware (A3-2) and fission gases (A3-3) waste streams. The fuel hardware contains Tc-99 and 0.1% of the actinides. The fission gases are tritium, krypton, and xenon. We assume they can be processed as in A1-3 and stored in a low-level facility.

The final step of the ALMR pyroprocess is electrorefining, cathode processing, and alloying and slug casting. Two waste streams are produced: electrorefining salt (A3-4) and electrorefining metal (A3-5). The electrorefining salt contains I-129 and Cs-135 and is immobilized in zeolite. The electrorefining metal, which contains Tc-99 and 0.1% of the actinides, is combined with the fuel hardware to form waste stream A3-2,5. Both A3-4 and A3-2,5 wastes are assigned to the repository. The ALMR reprocessing wastes thus contain 0.2% of the actinides and all of the fission products from ALMR spent fuel.

Next we calculate the number of packages from each waste stream in the repository, with and without strontium and cesium separation. In both cases 84,000 Mg (200 units) of LWR spent fuel are reprocessed. The heat generation rates of the resulting wastes are summed and subtracted from the repository wattage limit of  $1.1 \times 10^8$  watts to obtain the maximum wattage allowed for ALMR reprocessing wastes. Table 2.4 gives the total wattages of each reprocessing waste stream, with and without Sr and Cs separation. Without Sr/Cs separation, the total thermal power of LWR wastes is  $7.65 \times 10^7$  watts, so  $3.35 \times 10^7$  watts of ALMR waste can be placed in the repository. This corresponds to about 167 units of ALMR waste without Sr/Cs separation.

With Sr/Cs separation, strontium and cesium are removed from both the LWR and ALMR reprocessing wastes and are stored above ground until the Sr-90 and Cs-137 have decayed. Their short-lived daughters Y-90 and Ba-137m are also removed in

Table 2.4. Waste Stream Heat Generation Rates at 10 Years

Waste Stream	Without Sr/Cs Separation		With Sr/Cs Separation	
	W/unit <sup>a</sup>	W in repository	W/unit <sup>a</sup>	W in repository
A1-1,2	$1.60 \times 10^4$	$3.20 \times 10^6$	$1.60 \times 10^4$	$3.20 \times 10^6$
A1-3 (C-14)	$8.38 \times 10^{-2}$	$1.68 \times 10^1$	$8.38 \times 10^{-2}$	$1.68 \times 10^1$
A1-3 (I-129)	$6.34 \times 10^{-4}$	1.27	$6.34 \times 10^{-4}$	1.27
A1-4	$3.41 \times 10^5$	$6.82 \times 10^7$	$1.87 \times 10^4$	$3.74 \times 10^6$
A1-5	$1.12 \times 10^3$	$2.24 \times 10^5$	$1.12 \times 10^3$	$2.24 \times 10^5$
A1-6	$3.09 \times 10^3$	$6.18 \times 10^5$	$3.09 \times 10^3$	$6.18 \times 10^5$
A1-7	$3.45 \times 10^3$	$6.90 \times 10^5$	$1.89 \times 10^2$	$3.78 \times 10^4$
A1-8	$1.77 \times 10^4$	$3.54 \times 10^6$	$1.77 \times 10^4$	$3.54 \times 10^6$
Total LWR	$3.82 \times 10^5$	$7.65 \times 10^7$	$5.68 \times 10^4$	$1.13 \times 10^7$
A3-4	$1.88 \times 10^5$	$3.14 \times 10^7$	$8.62 \times 10^3$	$3.97 \times 10^7$
A3-2,5	$1.28 \times 10^4$	$2.14 \times 10^6$	$1.28 \times 10^4$	$5.90 \times 10^7$
Total ALMR	$2.01 \times 10^5$	$3.35 \times 10^7$	$2.14 \times 10^4$	$9.87 \times 10^7$

<sup>a</sup> One unit of waste is defined to be the amount of waste obtained from reprocessing one unit of spent fuel, which is the amount of spent fuel generated by the production of  $10^{11}$  kWh of electricity.

this process. The remaining Cs-135 is then placed in the repository. The only waste streams that contain strontium and cesium are A1-4, A1-7, and A3-4; only for these streams are the waste heat generation rates different with and without Sr/Cs separation. With removal of Sr-90 and Cs-137, the total thermal power of LWR wastes is  $1.13 \times 10^7$  watts. Thus a total of  $9.87 \times 10^7$  watts, or 4610 units, of ALMR waste can be placed in the repository.

With one unit of ALMR waste resulting from the production of  $10^{11}$  kWh of electricity, the total electrical production of ALMRs without and with Sr/Cs separation is  $1.9 \times 10^6$  MWe-yr and  $5.2 \times 10^7$  MWe-yr, respectively. Since one 40-

year ALMR operated at 80% capacity produces a total of  $4.46 \times 10^4$  MWe-yr, the number of ALMRs used in the two cases is 43 and 1166. Since Sr-90, Y-90, Cs-137 and Ba-137m together account for about 95% of the heat generation of the waste streams in which they occur, their removal makes it possible to place a substantially higher amount of ALMR waste in the repository.

The way in which the reprocessed LWR spent fuel is used in the reactors depends on the type(s) of ALMR chosen. As an example, we consider an ALMR with capacity factor 0.8 and breeding ratio 0.76, without Sr/Cs separation. The LWR transuranics would be depleted after operation of 22 ALMRs. Wastes from 21 additional ALMRs can be placed in the repository; however, these reactors will need makeup transuranics which must be obtained either from the fuel cycle inventories of retired reactors or from additional breeders whose wastes would be placed in a second repository. The leftover inventory from a retired ALMR is taken to be the inventory in the reactor and fuel cycle, given in Table 1.2. Twenty-two ALMRs with breeding ratio 0.76 would produce a total of  $6.07 \times 10^5$  kg of leftover transuranics, which can fuel 16 more ALMRs, which in turn can fuel 12 more.

Waste packages for the reprocessing schemes are specified by Wilems and Danna<sup>41</sup> and are limited to a heat generation rate of 2.5 kW per package. All packages consist of a partially-filled waste container placed inside an outer canister. With the exception of waste stream A1-3, we use Wilems and Danna package types 5 and 6. Packages for the C-14 in waste stream A1-3 and for waste stream A1-5 are not specified since these isotopes are not being considered. Table 2.5 gives the waste package characteristics. Package type 6a is specified here for use with waste stream A1-3, as described below. The BG packages are used for the borosilicate glass option, described in section 2.4. The number of packages needed for one unit of waste is simply the waste volume divided by the volume available in one waste package, accounting for a void volume of typically 15% of the inner container volume. Table 2.6 gives the waste volumes, and number and type of waste packages for each waste stream, for one unit of waste and for the whole repository. The

volume of radionuclides removed from the wastes in the Sr/Cs separation scheme is negligible.

Table 2.5. Reprocessing Waste Package Characteristics

Package Type	5	6	6a	BG
Inner height (m)	5.0	5.0	5.0	3.0
Inner radius (m)	0.2	.295	.295	.305
Inner cross-sec. area (m <sup>2</sup> )	.126	.273	.273	.292
Waste volume (%)	85	85	83	85
Waste volume (m <sup>3</sup> )	.534	1.16	1.13	.745
Outer height (m)	5.22	5.22	5.22	3.28
Outer radius (m)	.235	.33	.33	.33
Outer cross-sec. area (m <sup>2</sup> )	.173	.342	.342	.342
Total void volume (m <sup>3</sup> )	.371	.624	.656	.377
Volumetric flow rate (m <sup>3</sup> /yr)	$8.65 \times 10^{-5}$	$1.71 \times 10^{-4}$	$1.71 \times 10^{-4}$	$1.71 \times 10^{-4}$
Time to fill container (year)	4290	3650	3890	2200

We formulate our own waste packages for the I-129 in stream A1-3. One unit of this waste contains 13.3 Ci of I-129, so the whole repository will contain  $2.66 \times 10^3$  Ci, or  $1.51 \times 10^7$  g. However, stable iodine will also be present. The weight ratio of I-127 to I-129 produced in a PWR is 0.167,<sup>43</sup> so the repository will contain  $2.53 \times 10^6$  g of I-127, and a total of  $1.76 \times 10^7$  g of iodine. All of this iodine will be packaged as AgI. Using the molecular weights of I-127, I-129, and AgI, we calculate a total of  $3.21 \times 10^7$  g of AgI to emplace in the repository.

The AgI  $\alpha$ -phase density is  $5.683$  g/ $10^{-6}$  m<sup>3</sup>, giving a total waste volume of  $5.65$  m<sup>3</sup>. This can be distributed equally in five type-6 packages if each package has a slightly smaller waste volume of  $1.13$  m<sup>3</sup> (83% of the inner container volume instead of 85%). Each package will thus contain  $6.42 \times 10^6$  g of AgI, of which  $3.02 \times 10^6$  g =

Table 2.6. Reprocessing Waste Packages

Waste Stream	Package Type	Unit Volume (m <sup>3</sup> )	No. Pkgs per Unit	No. Pkgs in Rep. (Without Sr/Cs Sep.)	No. Pkgs in Rep. (With Sr/Cs Sep.)
A1-1,2	6	32.0	28	5600	5600
A1-3	6a	*	*	5	5
A1-4	5	88.0	165	33,000	33,000
A1-6	6	18.2	16	3200	3200
A1-7	6	13.2	11	2200	2200
A1-8	5	5.5	10	2000	2000
A3-4	6	114.7	99	16,533	456,390
A3-2,5	6	40.1	35	5845	161,350

\* Not calculated separately.

532 Ci is I-129. We call this package type 6a. The container void volume is .656 m<sup>3</sup>.

Radionuclide per-package and repository inventories are calculated using data in Appendix B of Thompson and Taylor.<sup>28</sup> Tables 2.7 through 2.11 list these inventories for each waste stream. Except for Th-230 and Ra-226, the 1000-year inventories do not account for any radionuclide growth. The repository inventories for each stream are summed to obtain the total repository inventories in Table 2.12.

A comparison of the radionuclide inventories in the LWR reprocessing wastes and in 84,000 Mg of unprocessed LWR spent fuel provides a direct verification of the actinide recovery rate for the LWR spent fuel pyroprocess. Table 2.13 lists these inventories, along with the calculated inventory reduction factors. As expected, the reduction factors for the fission products are all unity, because no fission products are recovered during reprocessing. The reduction factors for the transuranics are all near 500, since 0.2% of the transuranics are lost to the wastes. Reduction factors

Table 2.7. 1000-Year Inventories: Waste Stream A1-1,2

Species	Package Inventory (g/pkg)	Repository Inventory (Ci)
Tc-99	$8.40 \times 10^{-1}$	$7.97 \times 10^1$
Ra-226	$3.22 \times 10^{-5}$	$1.78 \times 10^{-1}$
Th-230	$8.04 \times 10^{-3}$	$9.49 \times 10^{-1}$
U-234	2.86	$9.991 \times 10^1$
U-238	$1.43 \times 10^4$	$2.69 \times 10^1$
Np-237	6.82	$2.69 \times 10^1$
Pu-239	$7.35 \times 10^1$	$2.56 \times 10^4$
Pu-240	$3.11 \times 10^1$	$3.97 \times 10^4$
Pu-242	6.84	$1.46 \times 10^2$
Am-241	1.56	$3.00 \times 10^4$
Am-243	1.17	$1.31 \times 10^3$
Cm-245	$1.21 \times 10^{-2}$	$1.16 \times 10^1$
Cm-246	$1.27 \times 10^{-3}$	2.18

Table 2.8. 1000-Year Inventories: Iodine and Cesium Waste Streams

Waste Stream	Species	Package Inventory (g/pkg)	Repository Inventory (Ci)	
			Without Sr/Cs Sep.	With Sr/Cs Sep.
A1-3	I-129	$3.02 \times 10^6$	$2.66 \times 10^3$	$2.66 \times 10^3$
A1-4	Cs-135	$7.57 \times 10^2$	$2.88 \times 10^4$	$2.88 \times 10^4$
A1-7	Cs-135	$1.18 \times 10^2$	$3.00 \times 10^2$	$3.00 \times 10^2$
A3-4	I-129	$8.07 \times 10^2$	$2.35 \times 10^3$	$6.50 \times 10^4$
A3-4	Cs-135	$4.49 \times 10^3$	$8.55 \times 10^4$	$2.36 \times 10^6$

for uranium are near 500 if the losses in waste stream A1-6 are excluded; the overall

Table 2.9. 1000-Year Inventories: Waste Stream A1-6

Species	Package Inventory (g/pkg)	Repository Inventory (Ci)
Tc-99	$2.00 \times 10^4$	$1.08 \times 10^6$
Ra-226	$1.29 \times 10^{-3}$	4.09
Th-230	$3.23 \times 10^{-1}$	$2.18 \times 10^1$
U-234	$1.15 \times 10^2$	$2.29 \times 10^3$
U-238	$5.75 \times 10^5$	$6.19 \times 10^2$

Table 2.10. 1000-Year Inventories: Waste Stream A1-8

Species	Package Inventory (g/pkg)	Repository Inventory (Ci)
Tc-99	$3.23 \times 10^2$	$1.09 \times 10^4$
Ra-226	$9.01 \times 10^{-5}$	$1.78 \times 10^{-1}$
Th-230	$2.25 \times 10^{-2}$	$9.49 \times 10^{-1}$
U-234	7.99	$9.99 \times 10^1$
U-238	$4.01 \times 10^4$	$2.69 \times 10^1$
Np-237	$1.91 \times 10^1$	$2.69 \times 10^1$
Pu-239	$2.06 \times 10^2$	$2.56 \times 10^4$
Pu-240	$8.71 \times 10^1$	$3.97 \times 10^4$
Pu-242	$1.91 \times 10^1$	$1.46 \times 10^2$
Am-241	4.37	$3.00 \times 10^4$
Am-243	3.28	$1.31 \times 10^3$
Cm-245	$3.38 \times 10^{-2}$	$1.16 \times 10^1$
Cm-246	$3.55 \times 10^{-3}$	2.18

uranium reduction factors are near 40.

Table 2.11. 1000-Year Inventories: Waste Stream A3-2,5

Species	Package Inventory (g/pkg)	Repository Inventory (Ci)	
		Without Sr/Cs Sep.	With Sr/Cs Sep.
Tc-99	$7.05 \times 10^3$	$6.99 \times 10^5$	$1.93 \times 10^7$
Ra-226	$5.25 \times 10^{-5}$	$3.03 \times 10^{-1}$	8.38
Th-230	$1.31 \times 10^{-2}$	1.62	$4.46 \times 10^1$
U-234	4.66	$1.70 \times 10^2$	$4.70 \times 10^3$
U-238	$5.40 \times 10^3$	$1.06 \times 10^1$	$2.93 \times 10^2$
Np-237	9.72	$4.01 \times 10^1$	$1.11 \times 10^3$
Pu-239	$6.30 \times 10^2$	$2.29 \times 10^5$	$6.32 \times 10^6$
Pu-240	$2.03 \times 10^2$	$2.71 \times 10^5$	$7.46 \times 10^6$
Pu-242	$2.60 \times 10^1$	$5.80 \times 10^2$	$1.60 \times 10^4$
Am-241	5.33	$1.07 \times 10^5$	$2.95 \times 10^6$
Am-243	8.27	$9.63 \times 10^3$	$2.66 \times 10^5$
Cm-245	$5.18 \times 10^{-1}$	$5.20 \times 10^2$	$1.43 \times 10^4$
Cm-246	$9.14 \times 10^{-2}$	$1.64 \times 10^2$	$4.53 \times 10^3$

The reprocessing waste forms and radionuclide release mechanisms are summarized in Tables 2.14 and 2.15. In all cases where the actinides are solubility-limited, the solubilities for spent fuel are used. In stream A1-1,2, all of the technetium and curium are assumed to dissolve instantly because there is no waste matrix. The other actinides are solubility-limited. In stream A1-3, release of I-129 is controlled by the dissolution of silver iodide. The solubility of AgI is  $9.1 \times 10^{-9}$  moles/liter, or  $2.13 \times 10^{-3}$  g/m<sup>3</sup>. The salt/zeolite waste form of streams A1-4, A1-7, and A3-4 is expected to be highly soluble;<sup>44</sup> therefore it is assumed that all of the I-129 and Cs-135 dissolves instantly when water enters the waste container.

Wastes from streams A1-6, A1-8, and A3-2,5 are immobilized in copper. Release

Table 2.12. Repository Inventories at 1000 Years, Reprocessing Schemes

Species	Without Sr/Cs Sep. (Ci)	With Sr/Cs Sep. (Ci)
Tc-99	$1.79 \times 10^6$	$2.04 \times 10^7$
I-129	$5.01 \times 10^3$	$6.77 \times 10^4$
Cs-135	$1.15 \times 10^5$	$2.39 \times 10^6$
Ra-226	4.75	$1.28 \times 10^1$
Th-230	$2.53 \times 10^1$	$6.83 \times 10^1$
U-234	$2.66 \times 10^3$	$7.19 \times 10^3$
U-238	$6.83 \times 10^2$	$9.66 \times 10^2$
Np-237	$9.39 \times 10^1$	$1.16 \times 10^3$
Pu-239	$2.80 \times 10^5$	$6.37 \times 10^6$
Pu-240	$3.50 \times 10^5$	$7.54 \times 10^6$
Pu-242	$8.72 \times 10^2$	$1.63 \times 10^4$
Am-241	$1.67 \times 10^5$	$3.01 \times 10^6$
Am-243	$1.22 \times 10^4$	$2.69 \times 10^5$
Cm-245	$5.43 \times 10^2$	$1.43 \times 10^4$
Cm-246	$1.68 \times 10^2$	$4.53 \times 10^3$

of Tc-99 and curium is assumed to be alteration controlled, and the actinides are solubility-limited. To estimate the fractional alteration rate of the copper matrix waste form, we use data from experiments<sup>45</sup> in which a 99.9% copper alloy was immersed in Gatun Lake for 16 years. The metal was found to corrode at a rate of approximately  $5 \text{ g}/(\text{m}^2\text{-yr})$ .

The copper content in one package for waste streams A1-6 and A1-8 is calculated to be  $9.57 \times 10^6 \text{ g}$  and  $1.65 \times 10^6 \text{ g}$ , respectively. We assume that the waste is packaged so as to leave the entire void volume at the top of the container, so that the area of waste in contact with water is constant and equal to the cross-sectional area of the

Table 2.13. Reduction Factors of Reprocessed LWR Spent Fuel at 10 Years

Species	Spent Fuel Inventory (Ci/84,000 Mg)	LWR Reprocessing Waste Inventory (Ci/84,000 Mg)	Reduction Factor
Tc-99	$1.1 \times 10^6$	$1.1 \times 10^6$	1
I-129	$2.65 \times 10^3$	$2.66 \times 10^3$	1
Cs-135	$2.90 \times 10^4$	$2.91 \times 10^4$	1
U-234	$9.99 \times 10^4$	$2.50 \times 10^3$	40.0
U-238	$2.66 \times 10^4$	$6.72 \times 10^2$	39.6
Np-237	$2.65 \times 10^4$	$5.38 \times 10^1$	493
Pu-239	$2.63 \times 10^7$	$5.26 \times 10^4$	500
Pu-240	$4.80 \times 10^7$	$8.82 \times 10^4$	544
Pu-242	$1.44 \times 10^5$	$2.93 \times 10^2$	491
Am-241	$1.48 \times 10^8$	$2.97 \times 10^5$	498
Am-243	$1.44 \times 10^6$	$2.87 \times 10^3$	502
Cm-245	$1.23 \times 10^4$	$2.52 \times 10^1$	488
Cm-246	$2.62 \times 10^3$	5.05	519

inner container. We assume the total reaction surface area, due to internal cracks, is ten times the waste surface area. We thus calculate copper matrix alteration rates for waste streams A1-6 and A1-8 of  $1.4 \times 10^{-6}$  and  $3.8 \times 10^{-6}$  per year. Stream A3-2,5 consists of stream A3-2, which has no matrix, and stream A3-5, which has a copper matrix. We assume the streams are combined as is, with no extra copper added beyond what is specified for the A3-5 stream. The A3-2,5 package thus contains  $1.79 \times 10^6$  g of copper, leading to a fractional alteration rate of  $7.6 \times 10^{-6}$  per year.

Table 2.14. Reprocessing Waste Forms

Waste Stream	Species	Description	Waste Matrix
A1-1,2	Tc-99, actinides	Non-fuel and fuel hardware	none
A1-3	I-129	Gases	silver iodide
A1-4	Cs-135	Reduction salt	zeolite
A1-6	Tc-99, U	Transport metal	copper
A1-7	Cs-135	Electrorefining salt	zeolite
A1-8	Tc-99, actinides	Electrorefining metal	copper
A3-4	I-129, Cs-135	Electrorefining salt	zeolite
A3-2,5	Tc-99, actinides	Fuel hardware and electrorefining metal	copper

Table 2.15. Reprocessing Waste Release Mechanisms

Waste Stream	Species	Release Mechanism	Alteration Rate ( $\text{yr}^{-1}$ )
A1-1,2	Tc-99, Cm actinides	instant dissolution solubility-limited	
A1-3	I-129	solubility-limited	
A1-4	Cs-135	instant dissolution	
A1-6	Tc-99 U	alteration-controlled solubility-limited	$1.4 \times 10^{-6}$
A1-7	Cs-135	instant dissolution	
A1-8	Tc-99, Cm actinides	alteration-controlled solubility-limited	$3.8 \times 10^{-6}$
A3-4	I-129, Cs-135	instant dissolution	
A3-2,5	Tc-99, Cm actinides	alteration-controlled solubility-limited	$7.6 \times 10^{-6}$

## 2.3 Radionuclide Release Rates

Radionuclide release rates from individual packages and for the whole repository are calculated for both spent fuel and reprocessing wastes. In all cases, release rates are calculated for the first  $10^5$  years. The repository release rates in the two disposal schemes are compared with each other and with the NRC maximum allowable release rates.

### 2.3.1 Normalized Per-Package Release Rates

Radionuclide release rates from individual spent fuel packages, normalized to their 1000-year package inventories, have been calculated by Sadeghi *et. al.*<sup>40</sup> for all of the species included here except curium. They are shown, along with the normalized release rates of curium, in Figures 2.3 through 2.6. Since water contact is assumed to begin at 1000 years and it takes 8650 years to fill the container, all releases from spent fuel packages begin at 9650 years.

Release rates for alteration-controlled species are shown in Figure 2.3. Alteration of spent fuel ends well before the container overflows. Because we have assumed that the water in the container is always well mixed, the release rates of alteration-controlled species are the same as if they were instantly dissolved. The normalized release rates of curium are lower than those of the fission products because curium decays much more rapidly than the fission products.

Release rates of the solubility-limited species are shown in Figures 2.4 through 2.6. The solubilities of all the species investigated here are so low that their elemental release rates are constant beyond  $10^5$  years. The release rate of an individual isotope is determined by its time-dependent fraction in the waste. For example, as Pu-240 decays, the fractions of Pu-239 and Pu-242 in the waste increase. This increases the release rate of Pu-239 until about 60,000 years, when its own decay is sufficient to cause its release rate to decrease. The release rate of Pu-242, the longest-lived isotope, always increases as long as plutonium is solubility-limited.

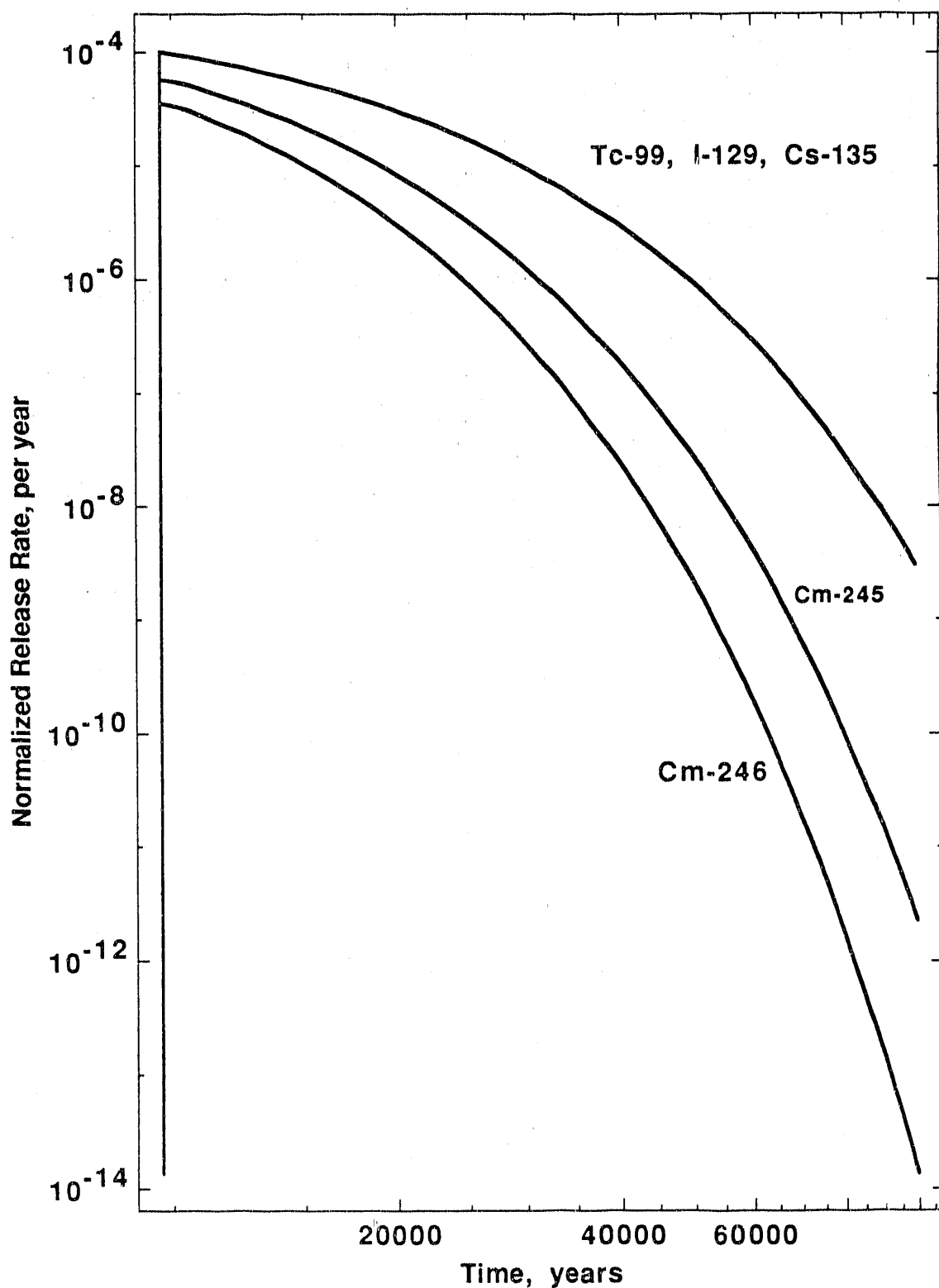


Figure 2.3. Normalized Release Rates of Alteration-Controlled Species from Spent Fuel

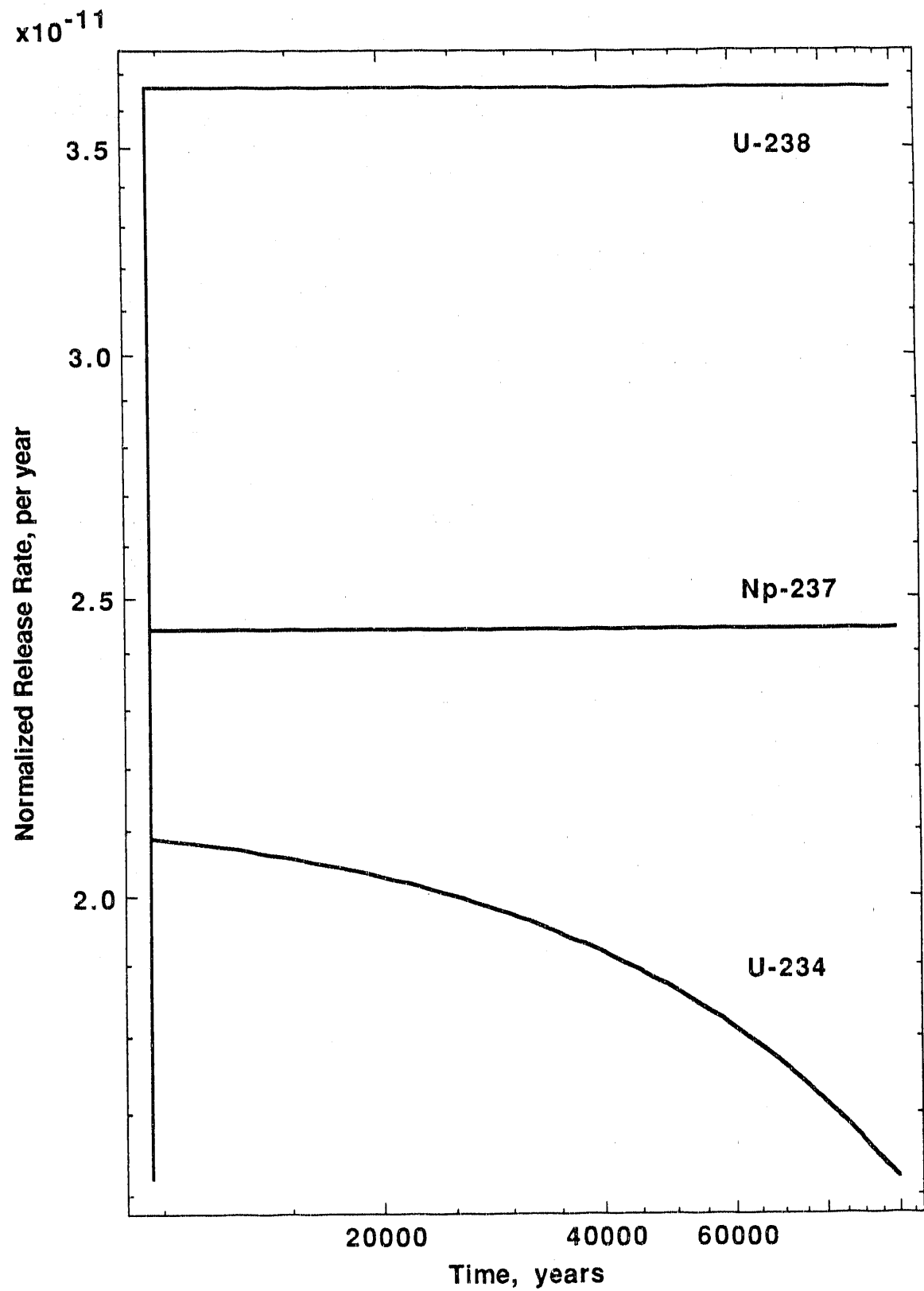


Figure 2.4. Normalized Release Rates of Uranium and Np-237 from Spent Fuel

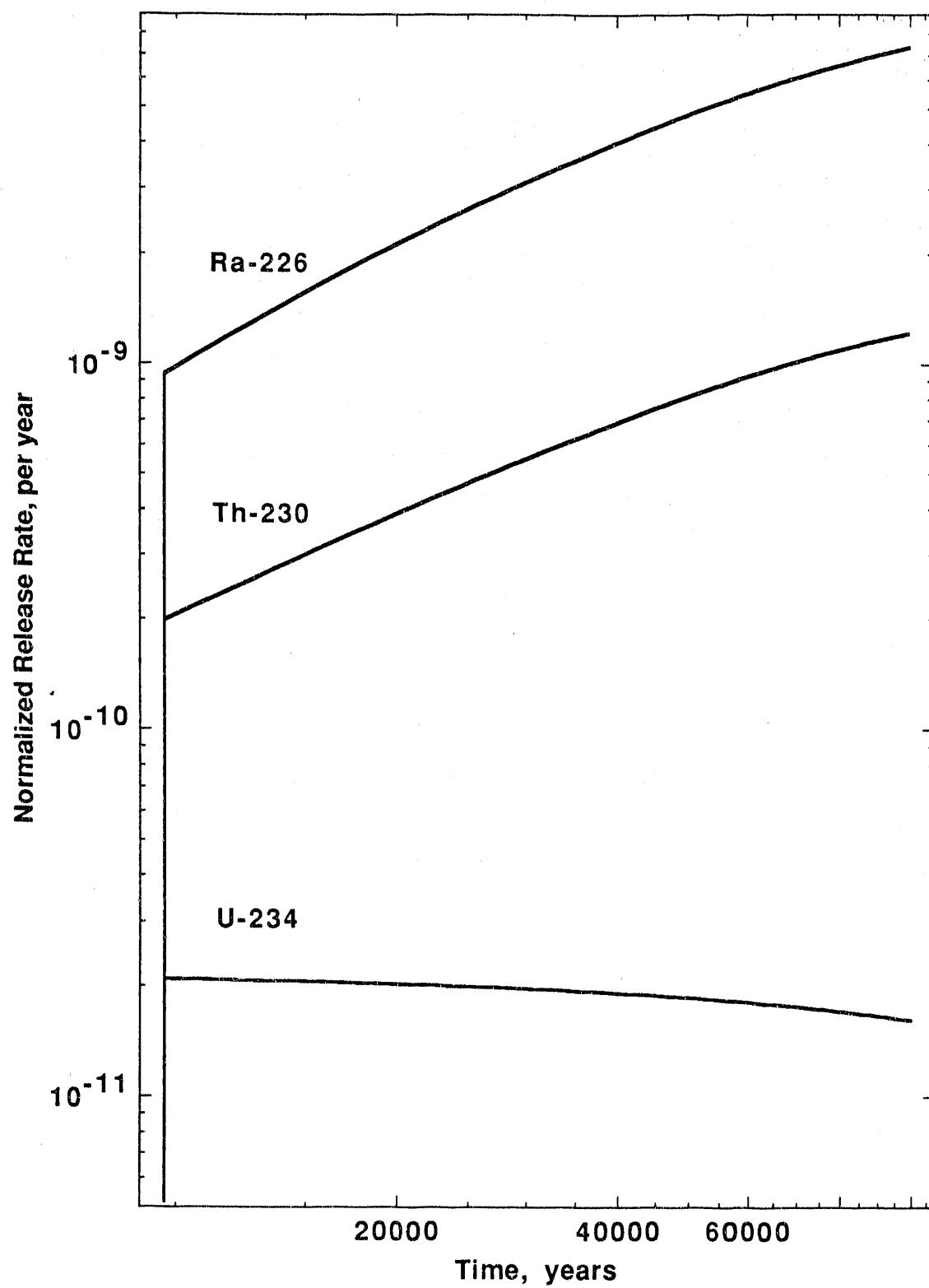


Figure 2.5. Normalized Release Rates of U-234 and Daughters from Spent Fuel

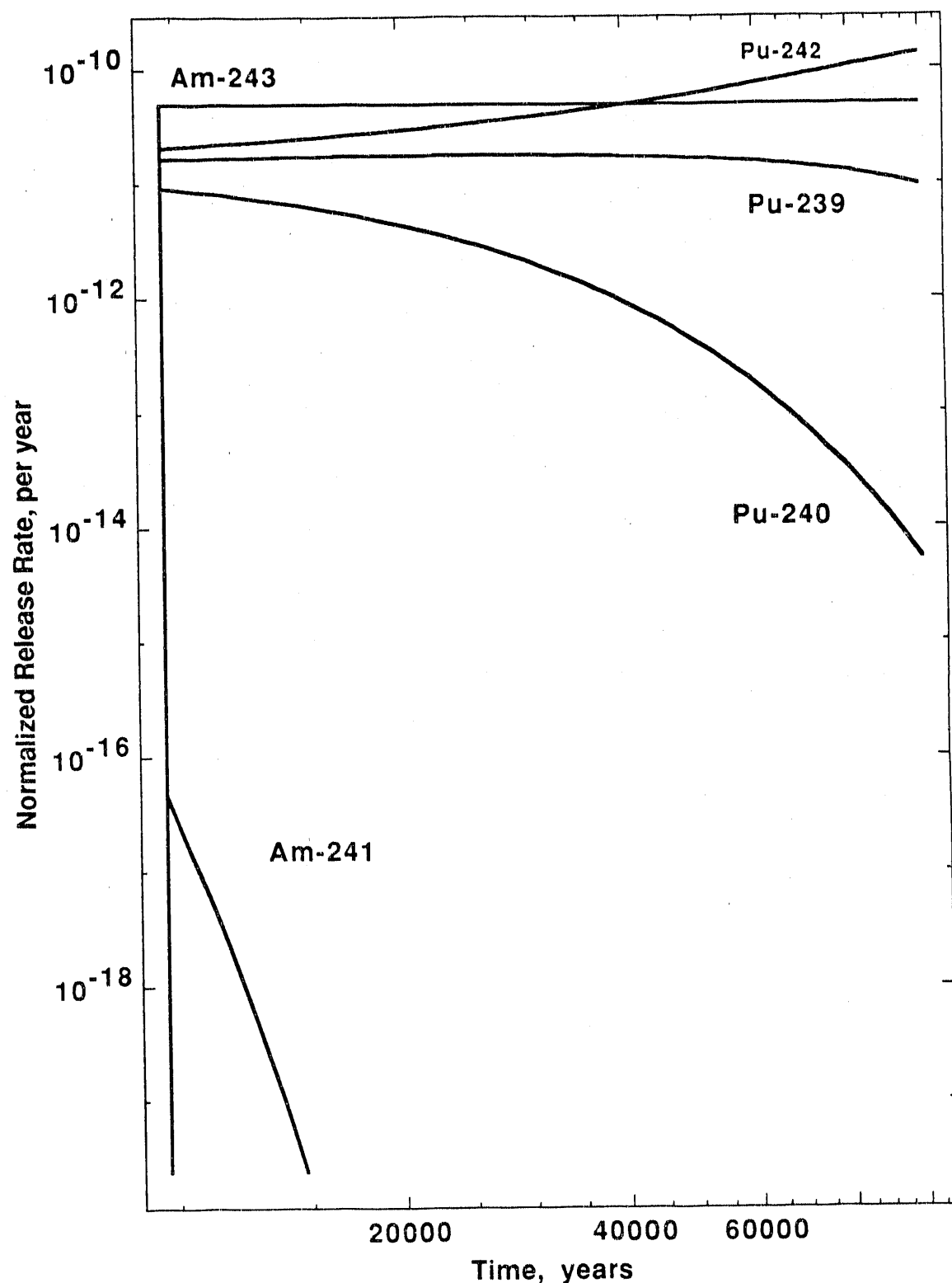


Figure 2.6. Normalized Release Rates of Plutonium and Americium from Spent Fuel

Uranium and americium display the same behavior. As U-234 decays, the release rate of U-238 increases. However, since the initial mass of U-238 in each package is over 1000 times greater than the initial U-234 mass, this increase is negligible. Similarly, because Am-241 decays significantly before release begins, its release rate is much lower than that of Am-243. Np-237 is the only neptunium isotope, so its release rate is constant.

Release rates from individual reprocessing waste packages, normalized to their 1000-year package inventories, are shown in Figures 2.7 through 2.14. Releases from type-5 packages begin at 5290 years, releases from type-6 packages begin at 4650 years, and releases from type-6a packages begin at 3890 years.

Tc-99 in waste stream A1-1,2 is instantly dissolved. Tc-99 release from streams A1-6, A1-8, and A3-2,5 is alteration-controlled. Alteration of the copper matrix continues beyond  $10^5$  years in all three streams.

Iodine and cesium in waste streams A1-4, A1-7, and A3-4 are instantly dissolved upon water contact with the waste. As in spent fuel, in waste streams A1-7 and A3-4 the normalized release rates of these two species are nearly equal. Container overflow in stream A1-4 occurs 640 years later than in the other two streams, so the release rate curve is shifted later in time. Release of I-129 in stream A1-3 is limited by the relatively low solubility of silver iodide, so the release rate is constant until all of the silver iodide is dissolved, which occurs much later than  $10^5$  years.

As in spent fuel, curium in reprocessing wastes behaves similarly to technetium, but its normalized release rates are lower due to its faster decay. The other actinides in reprocessing wastes are solubility-limited. Their release rates in reprocessing waste packages are all qualitatively similar to those in spent fuel. Because we assumed the same solubilities as for spent fuel, elemental release rates from type-6 packages are the same as those from spent fuel packages, because they have the same volumetric flow rate. Only the starting times are different, because the void volumes in the packages are different. This is illustrated in Figure 2.15, which

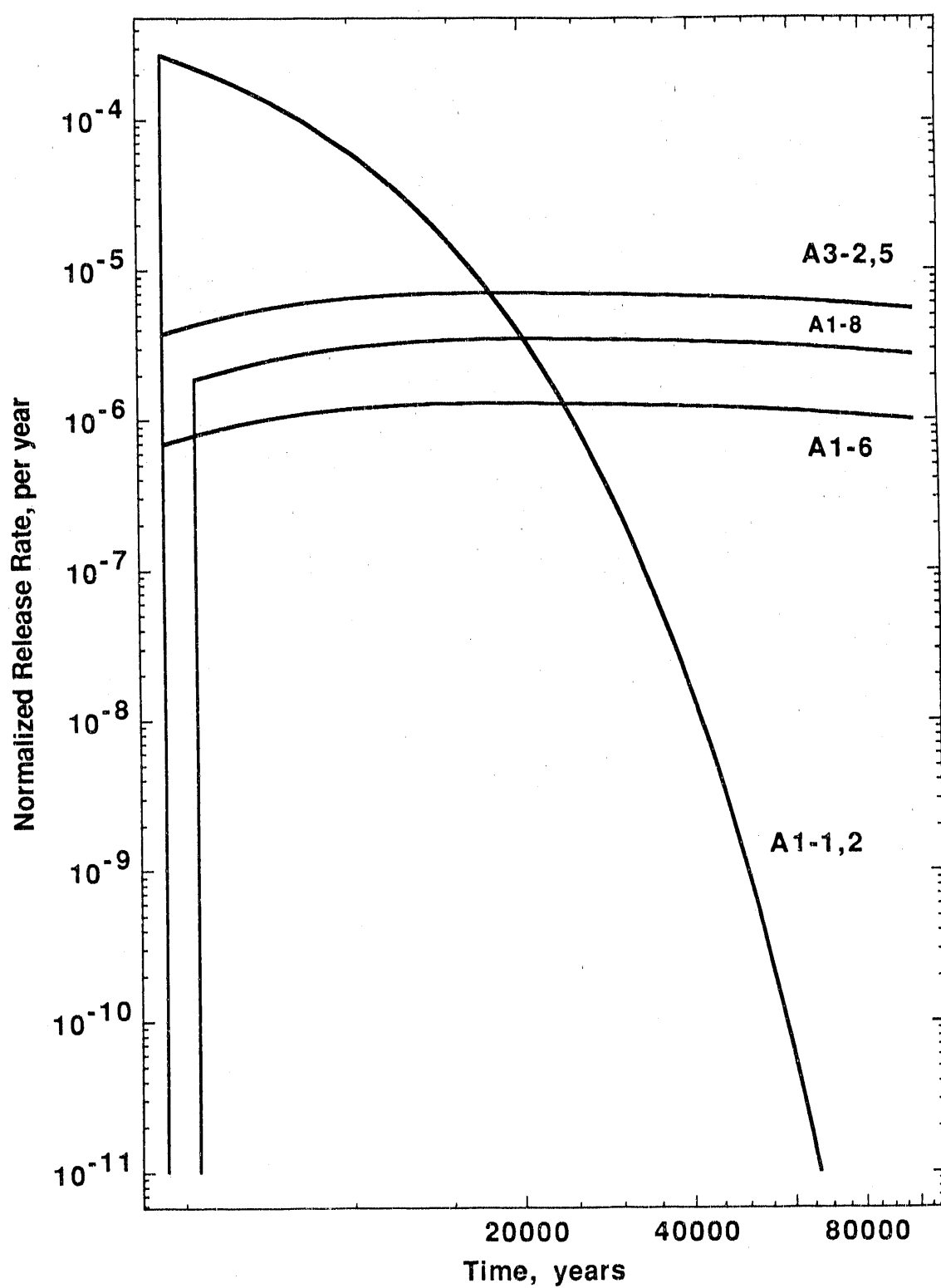


Figure 2.7. Normalized Release Rates of Tc-99 from Reprocessing Wastes

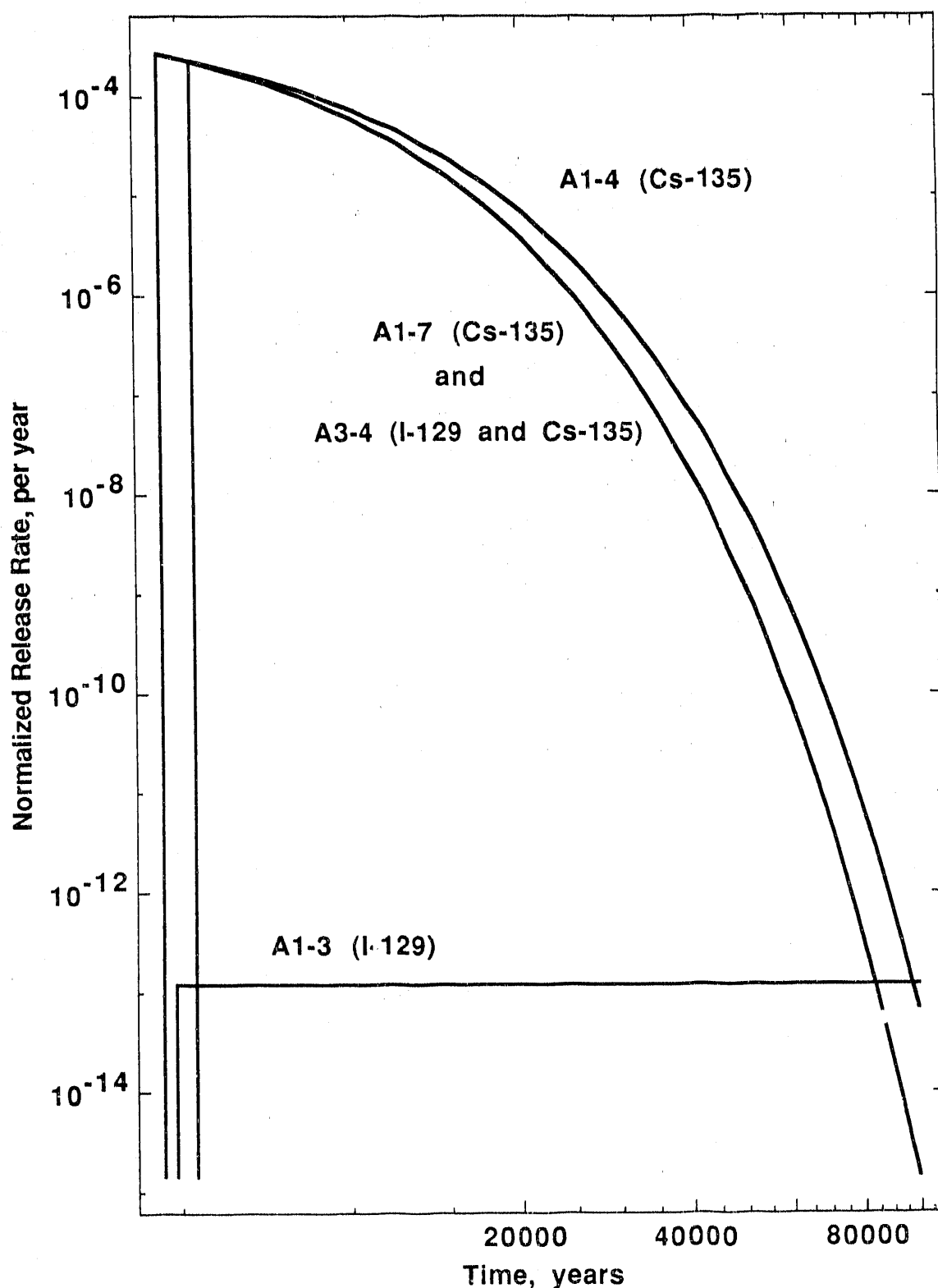


Figure 2.8. Normalized Release Rates of I-129 and Cs-135 from Reprocessing Wastes

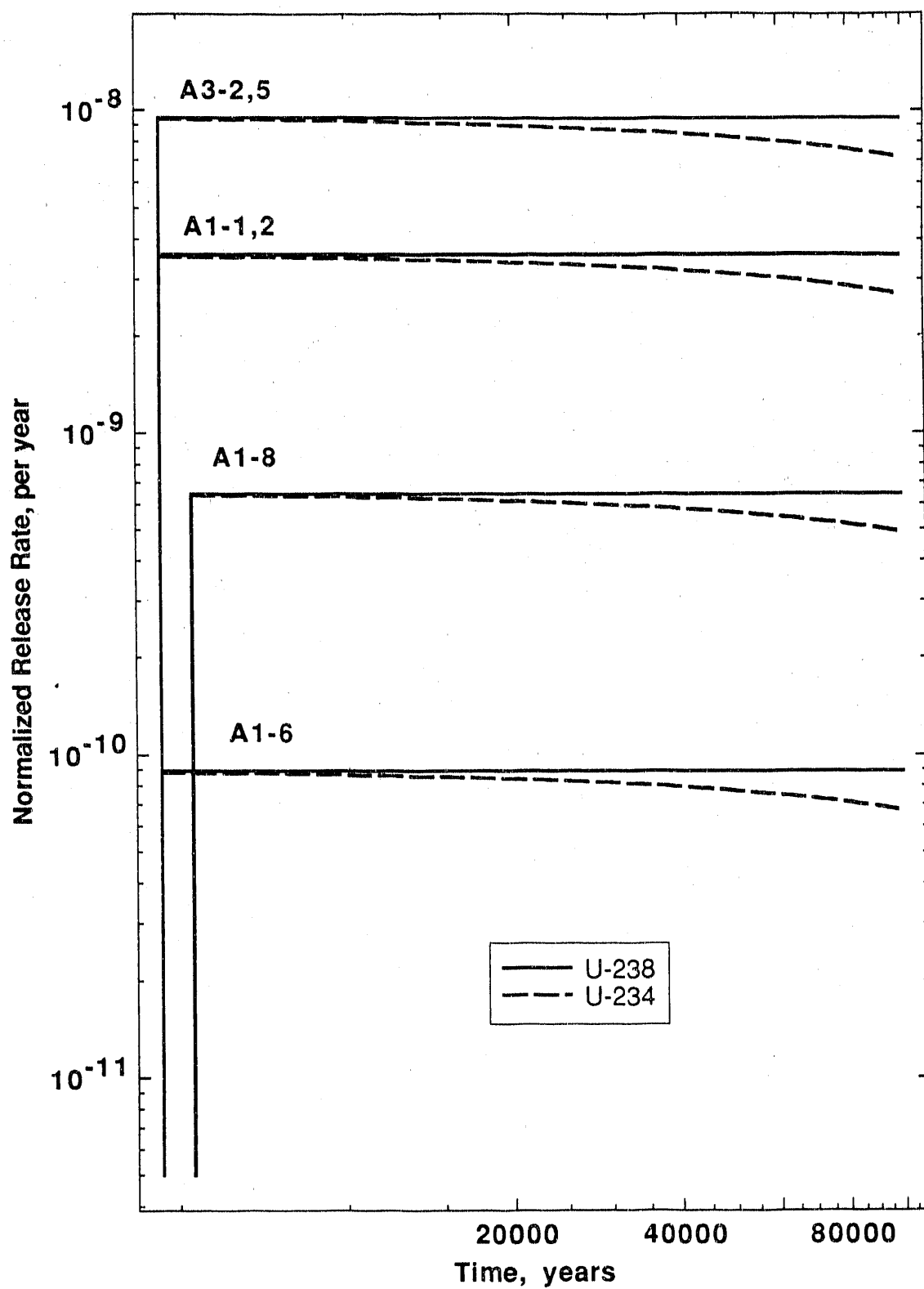


Figure 2.9. Normalized Release Rates of Uranium from Reprocessing Wastes

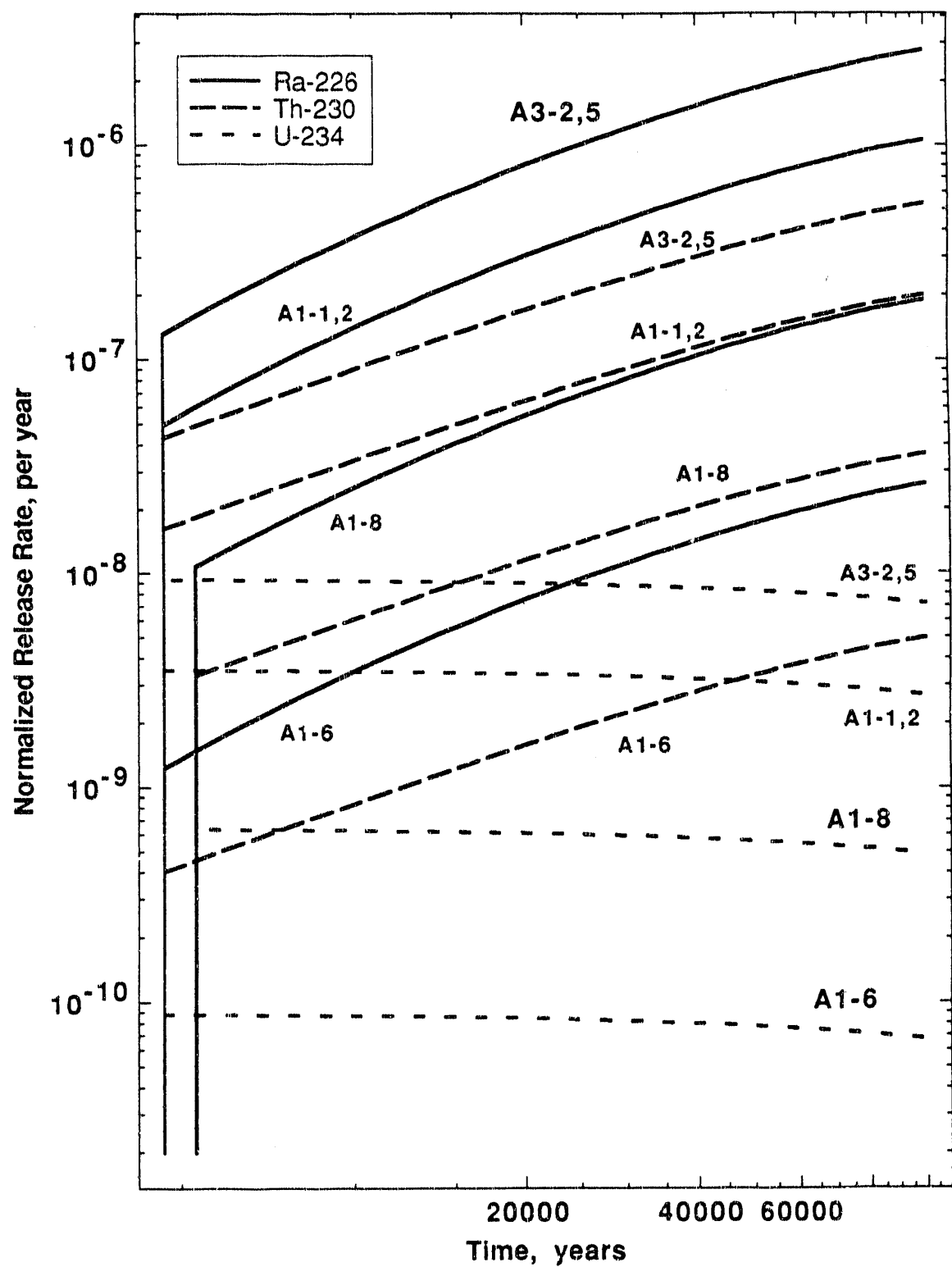


Figure 2.10. Normalized Release Rates of U-234 and Daughters from Reprocessing Wastes

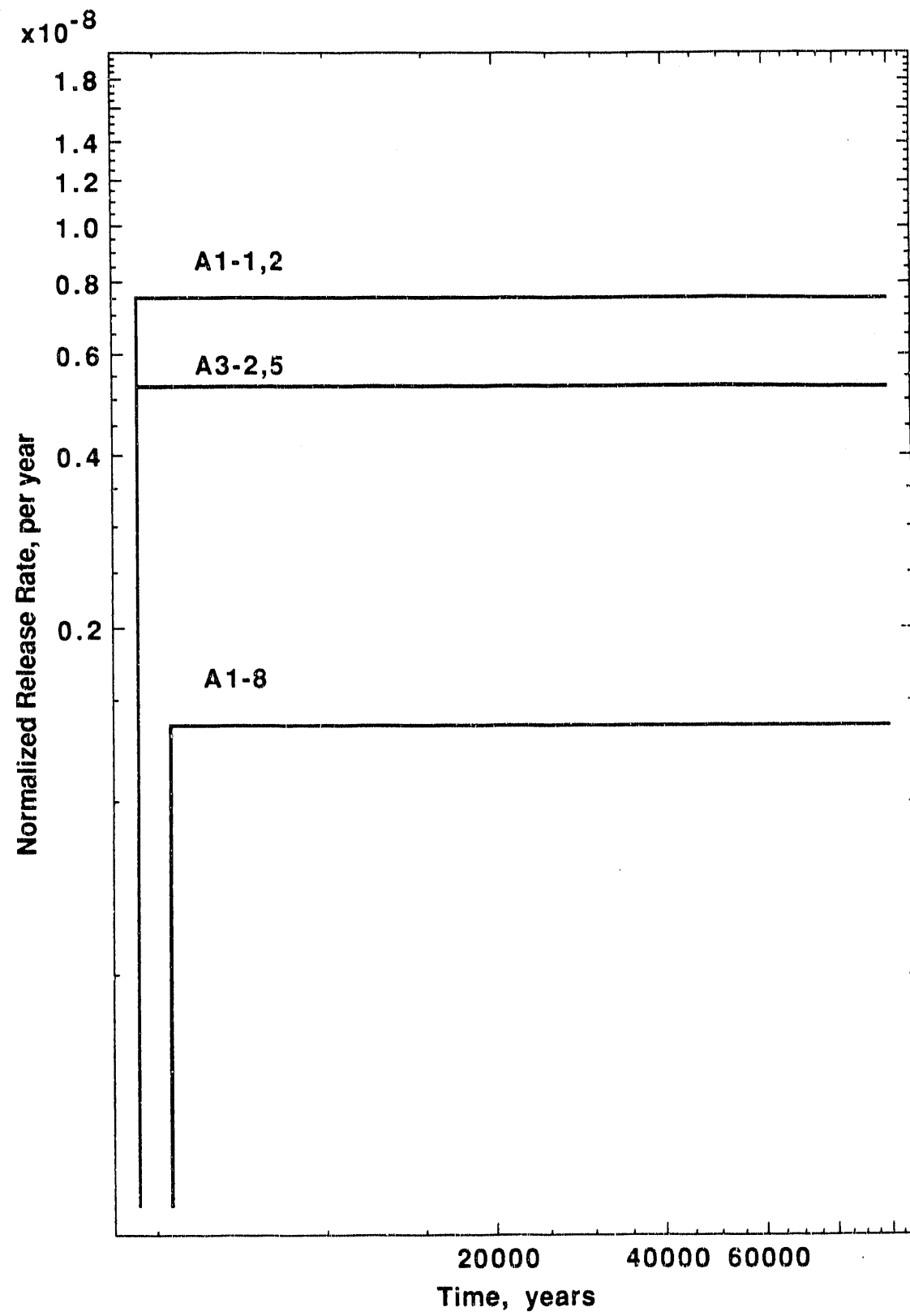


Figure 2.11. Normalized Release Rates of Np-237 from Reprocessing Wastes

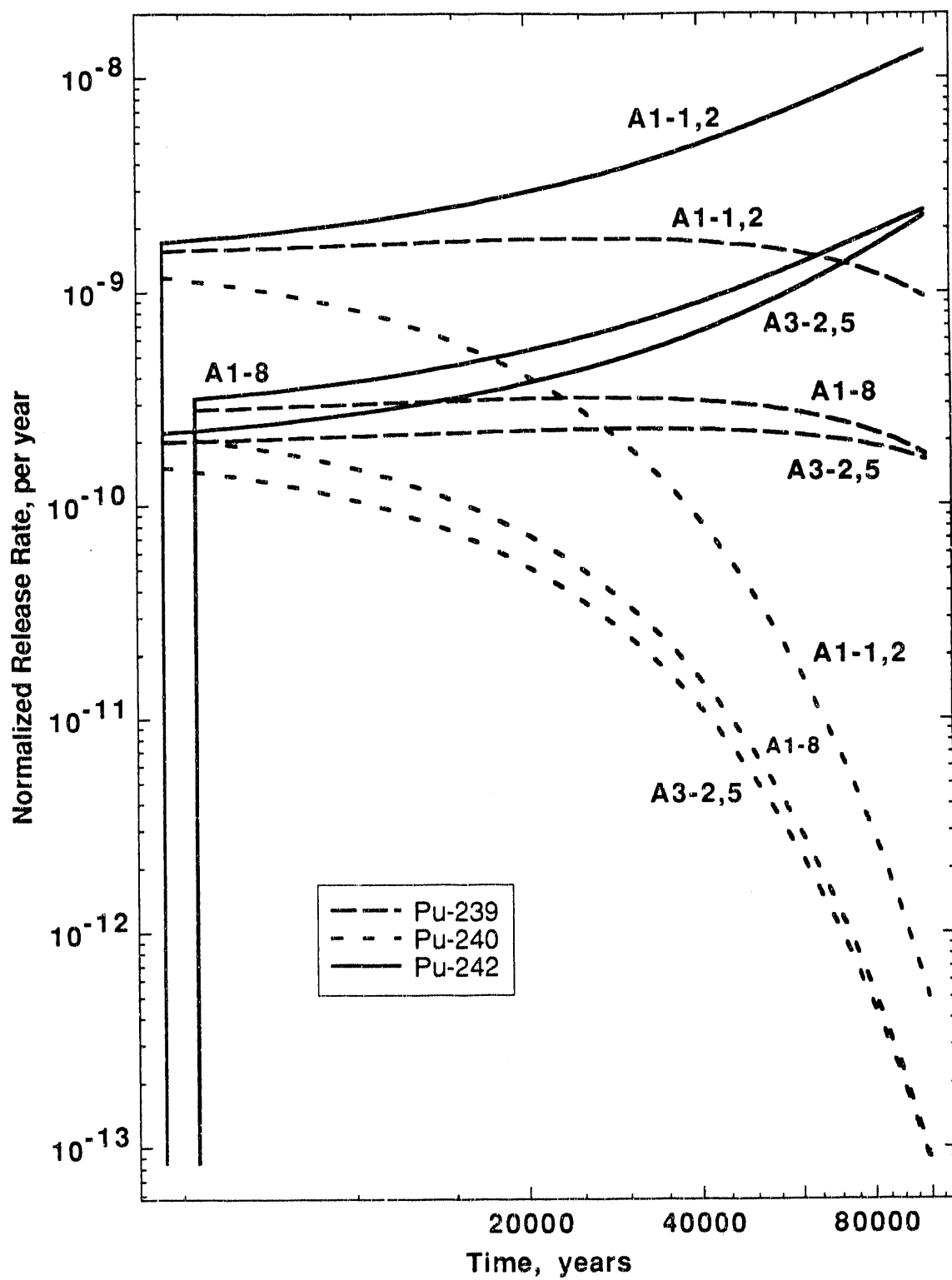


Figure 2.12. Normalized Release Rates of Plutonium from Reprocessing Wastes

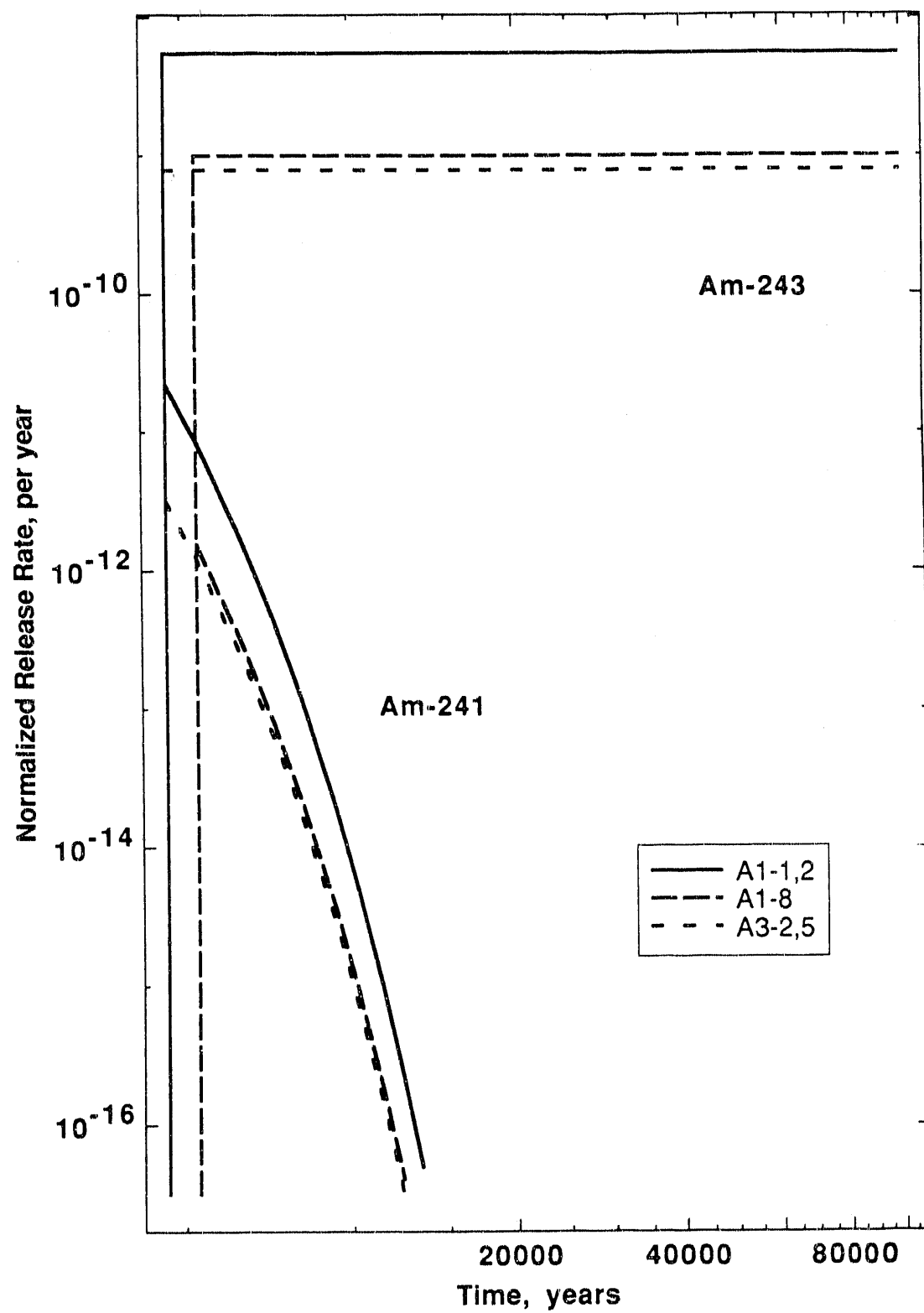


Figure 2.13. Normalized Release Rates of Americium from Reprocessing Wastes

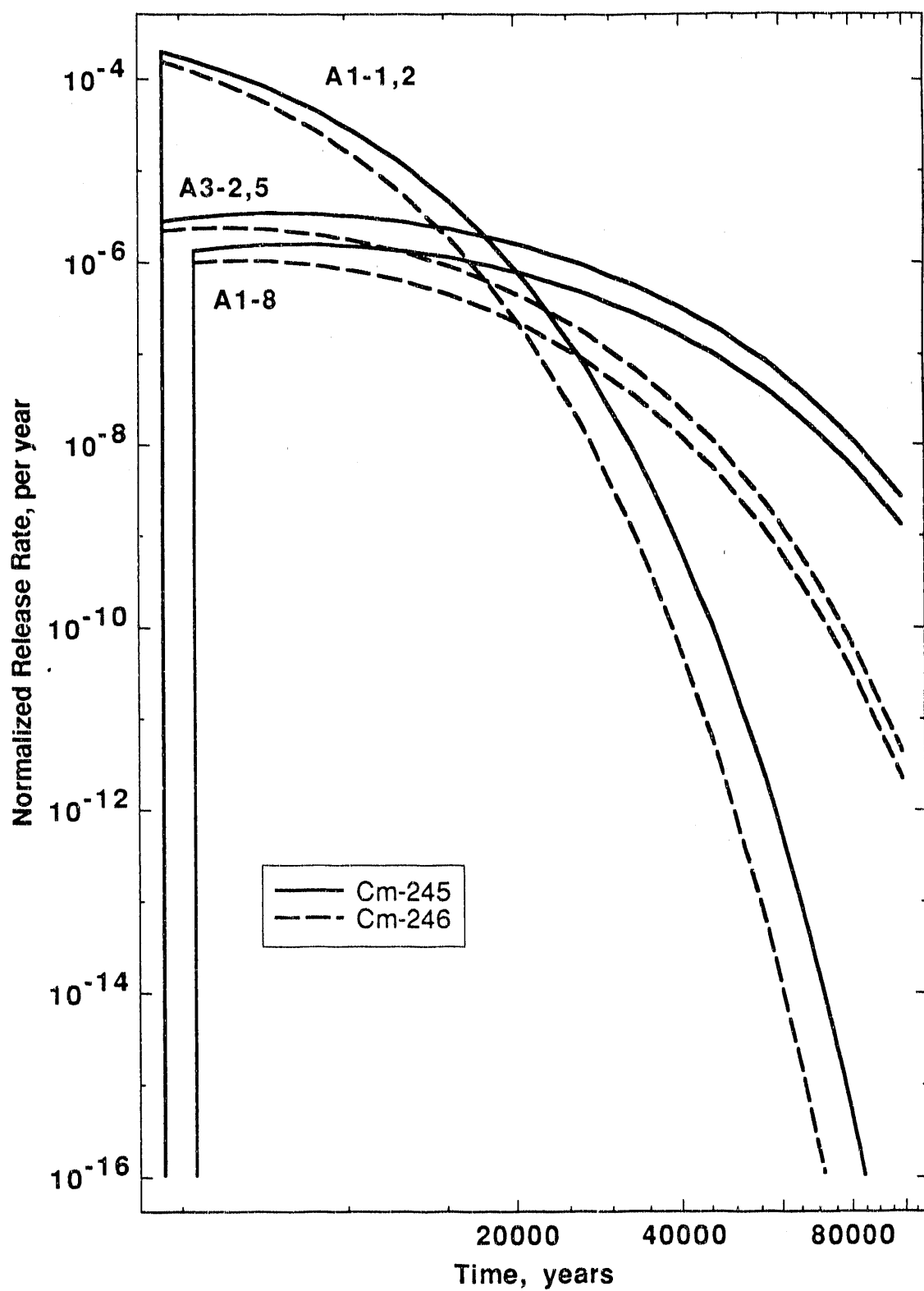


Figure 2.14. Normalized Release Rates of Curium from Reprocessing Wastes

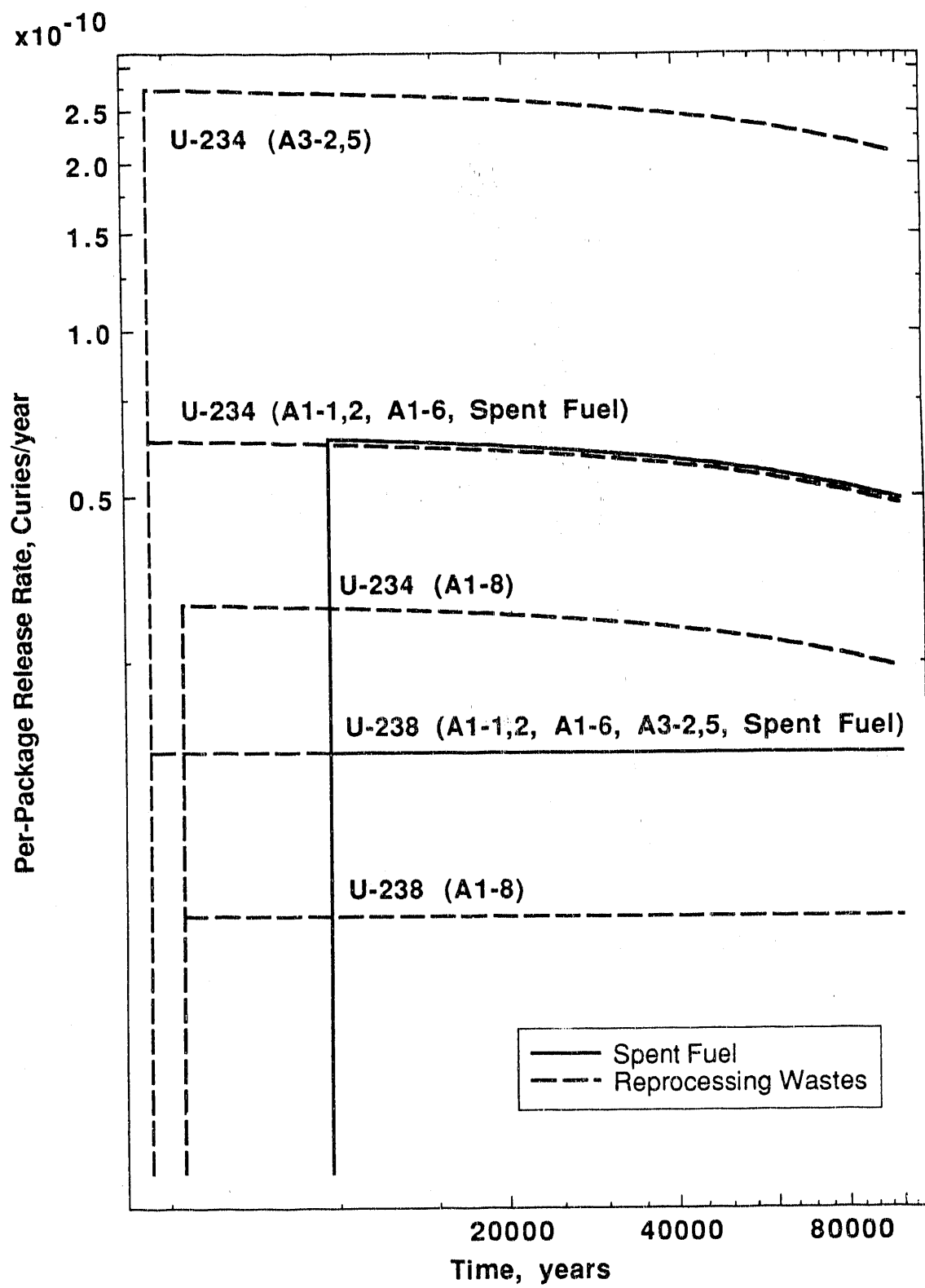


Figure 2.15. Per-Package Release Rates of Uranium from Spent Fuel and Reprocessing Wastes

shows the per-package release rates of uranium for both spent fuel and reprocessing wastes. Spent fuel packages and packages for streams A1-1,2, A1-6, and A3-2,5 all have the same volumetric flow rate, and the release rate of U-238 is the same in all of them. The release rate of U-234 from A3-2,5 packages is higher than that from spent fuel, A1-1,2, and A1-6 packages because the fraction of U-234 in ALMR waste is higher than that in LWR waste. However, the mass of U-234 in each package is still much less than the mass of U-238, so the change in the U-238 release rate is negligible.

### **2.3.2 Repository Release Rates**

Repository release rates for reprocessing wastes in the disposal scheme without Sr/Cs separation are compared with those for spent fuel in Figures 2.16 through 2.22. For spent fuel, the per-package release rates are multiplied by the number of packages to obtain the total repository release rates. Thus, as stated in Chapter 1, as long as the same 1.5 Mg packages are used, the repository release rates will be proportional to the number of Mg placed in the repository. This approach is conservative; a more realistic method of obtaining the repository release rates would be by convolution with the time-distributed water-contact time.<sup>46</sup>

For reprocessing wastes, per-package release rates are multiplied by the number of packages in each waste stream to obtain the total release rate for that stream. The totals are then summed to obtain the entire release rate for the repository. Release rates from reprocessing wastes all increase sharply at 5290 years, when releases from the type-5 packages begin. Repository release rates for the strontium/cesium separation case are shown only for neptunium, as an illustrative example. Repository release rates are always much higher in the Sr/Cs separation case because the repository contains many more ALMR reprocessing waste containers.

Although the repository inventory of fission products is higher in the reprocessing scheme than in the spent fuel scheme, the total release rate of Tc-99 is lower in the reprocessing scheme. The Tc-99 inventory in stream A1-1,2, the stream with the

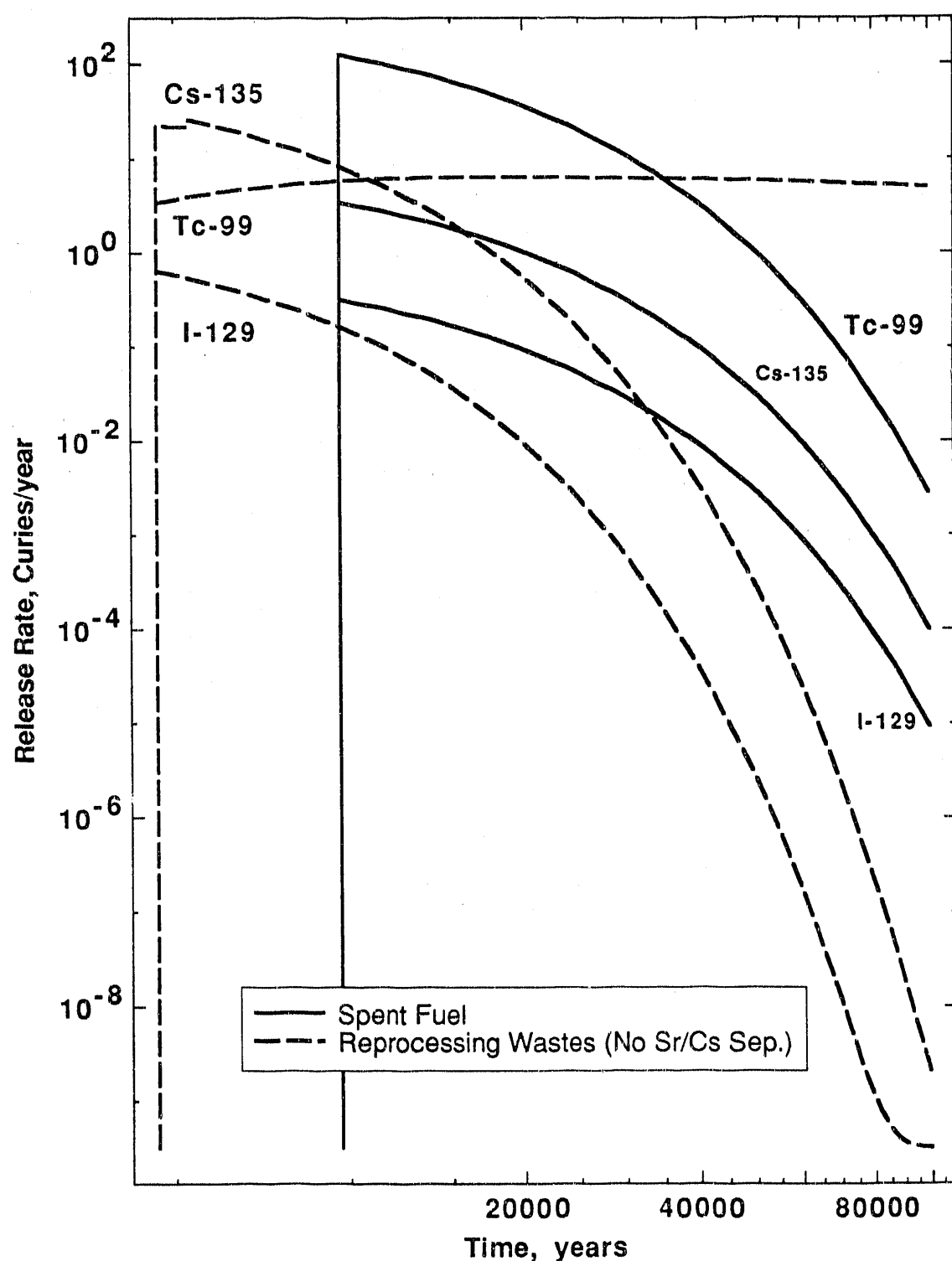


Figure 2.16. Repository Release Rates of Fission Products from Spent Fuel and Reprocessing Wastes

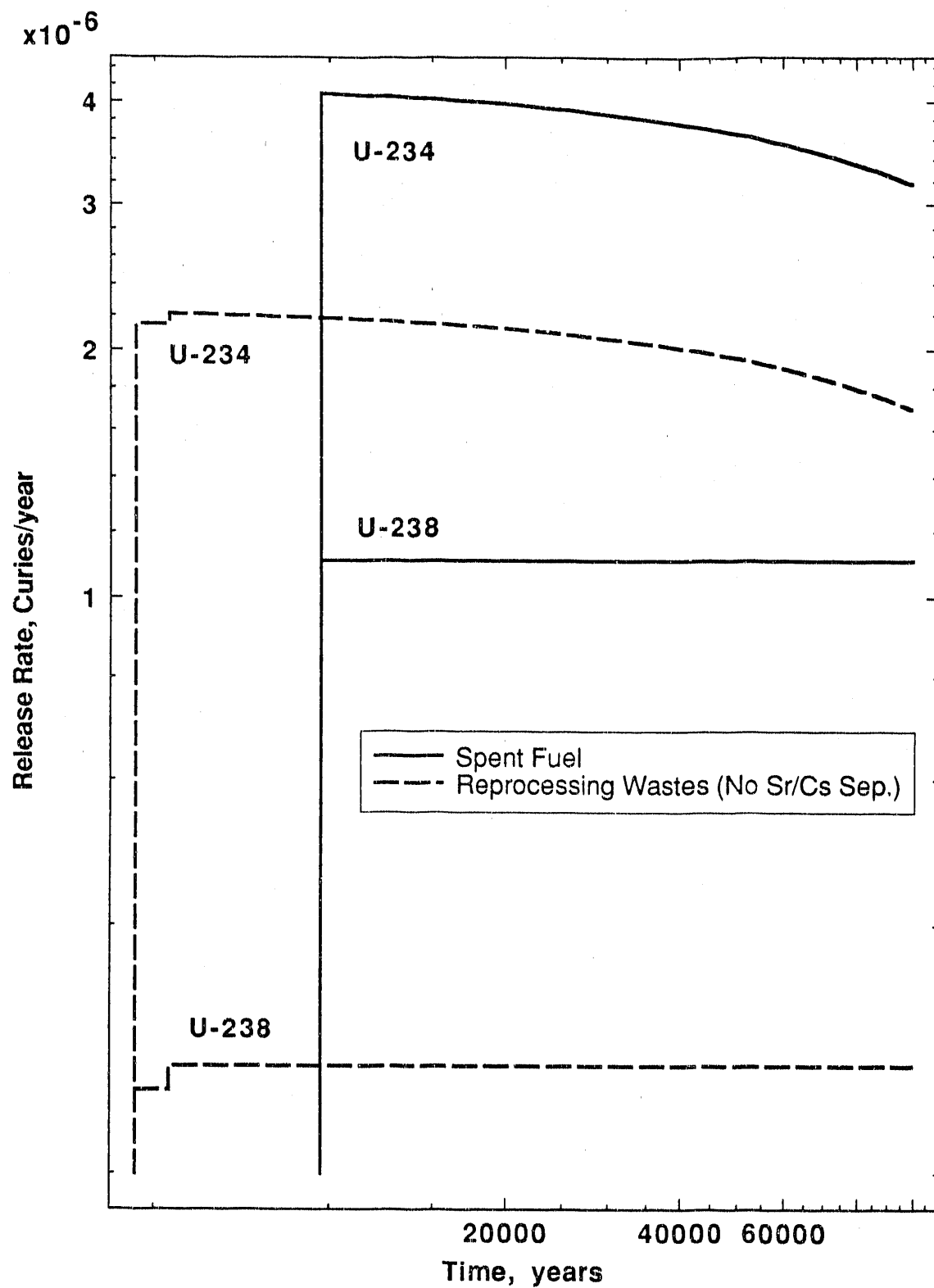


Figure 2.17. Repository Release Rates of Uranium from Spent Fuel and Reprocessing Wastes

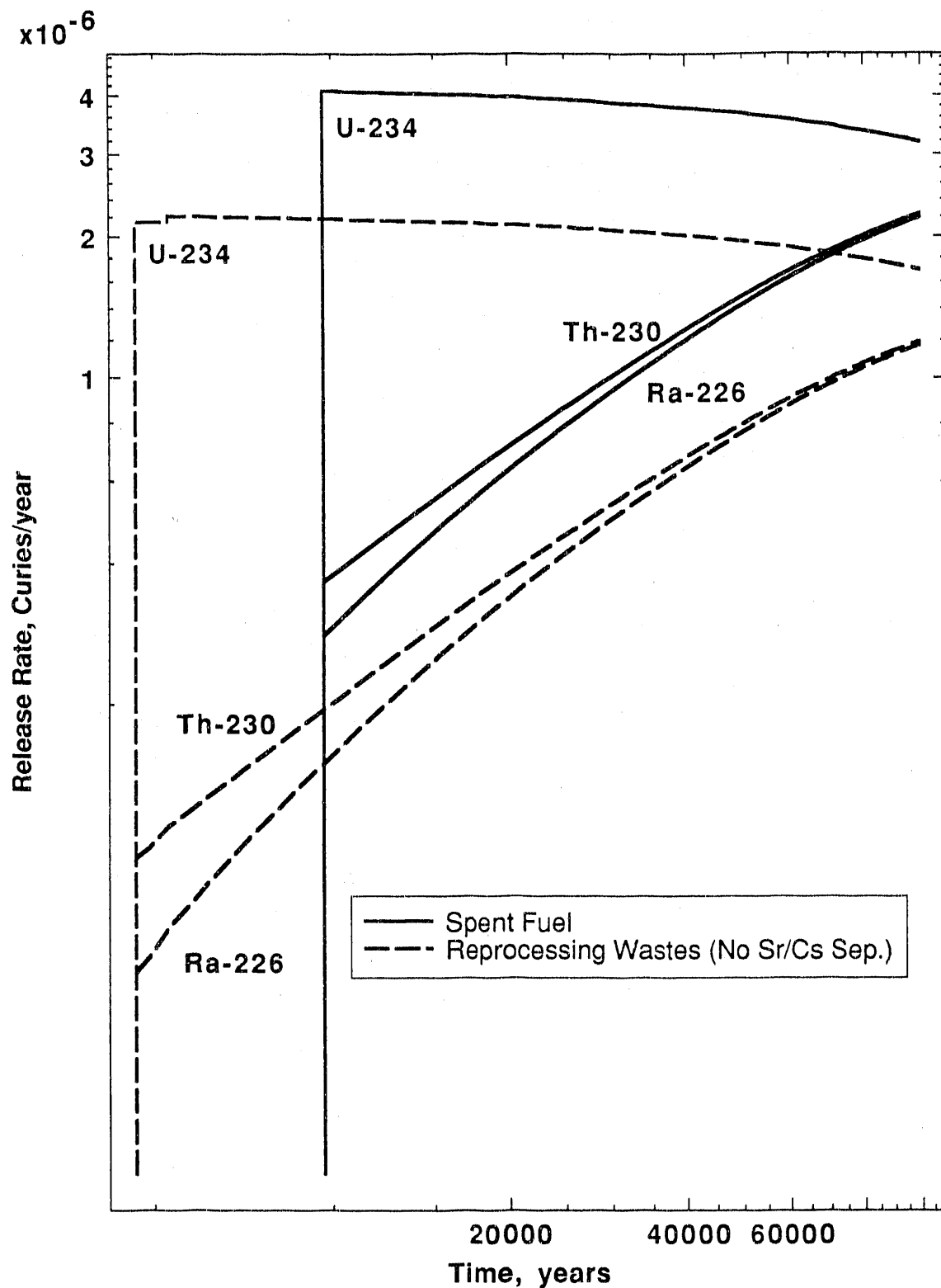


Figure 2.18. Repository Release Rates of U-234 and Daughters from Spent Fuel and Reprocessing Wastes

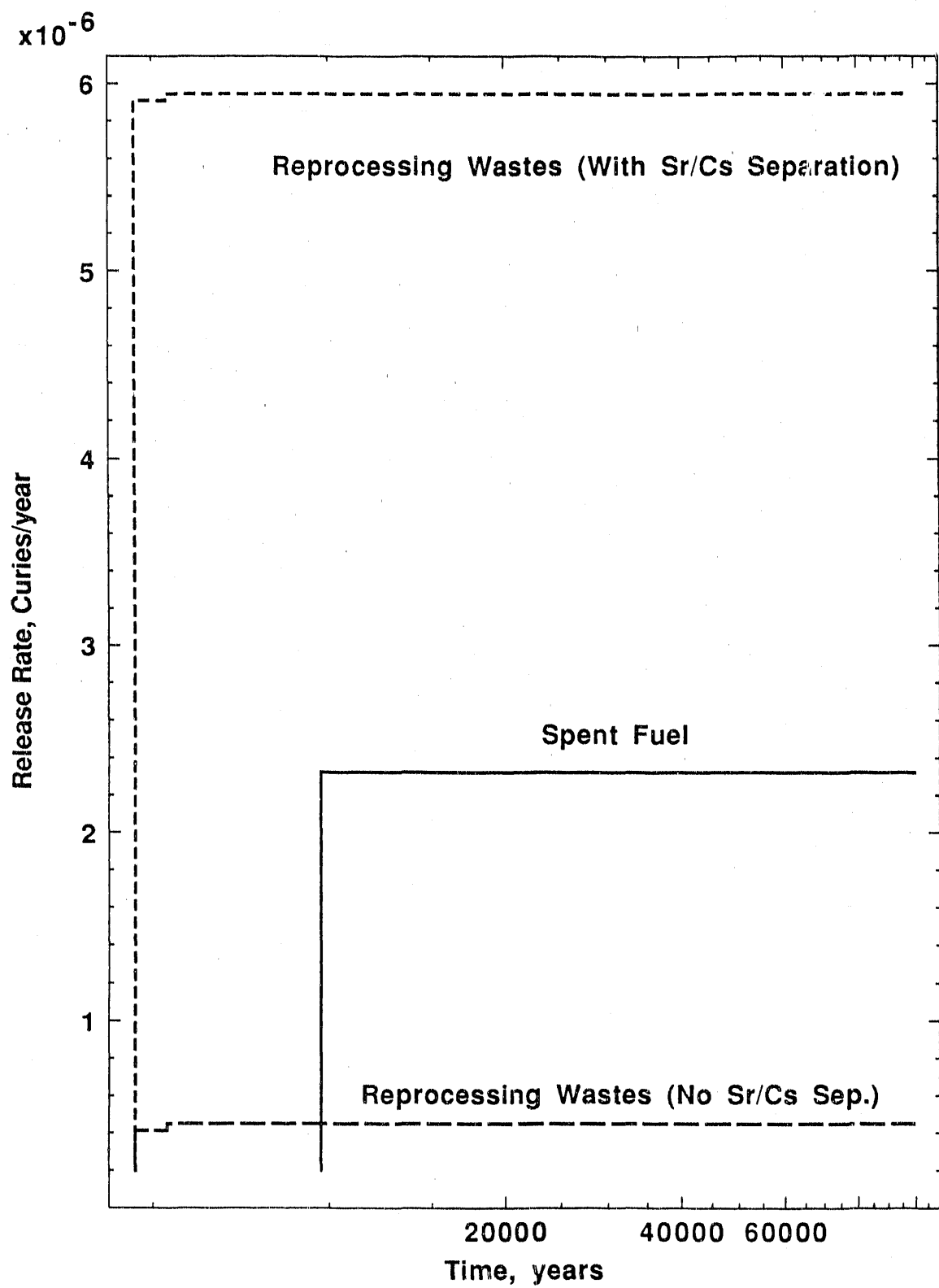


Figure 2.19. Repository Release Rates of Np-237 from Spent Fuel and Reprocessing Wastes

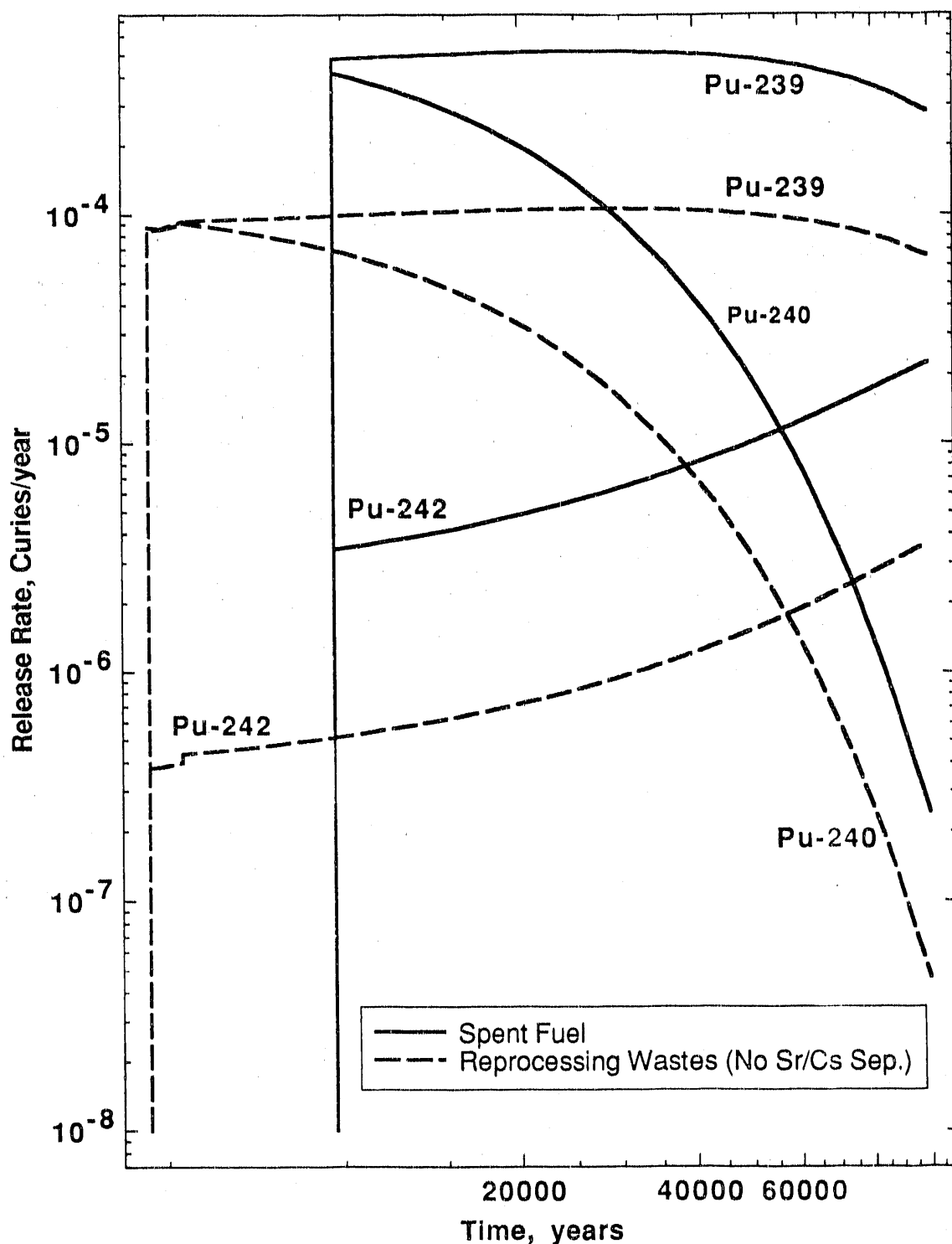


Figure 2.20. Repository Release Rates of Plutonium from Spent Fuel and Reprocessing Wastes

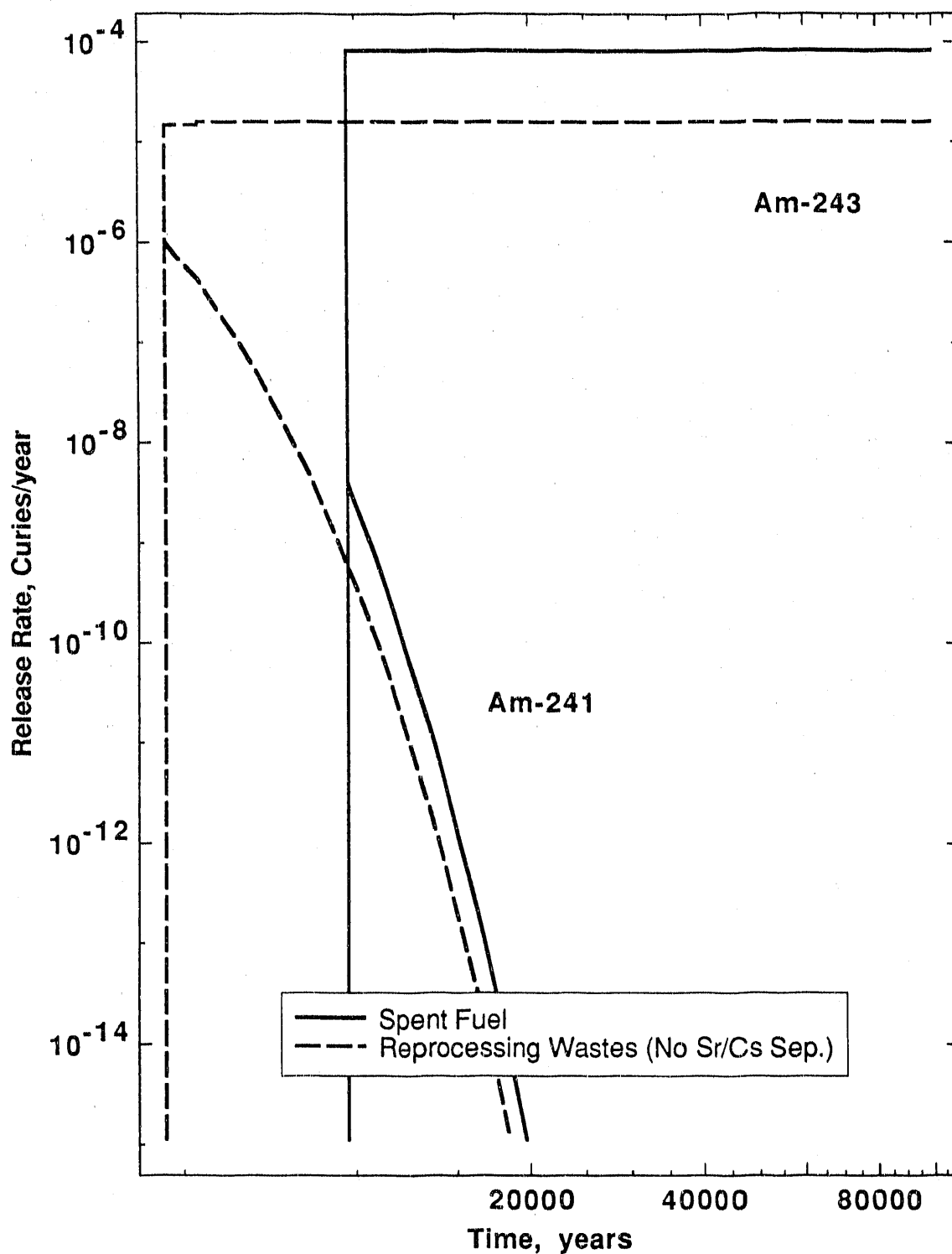


Figure 2.21. Repository Release Rates of Americium from Spent Fuel and Reprocessing Wastes

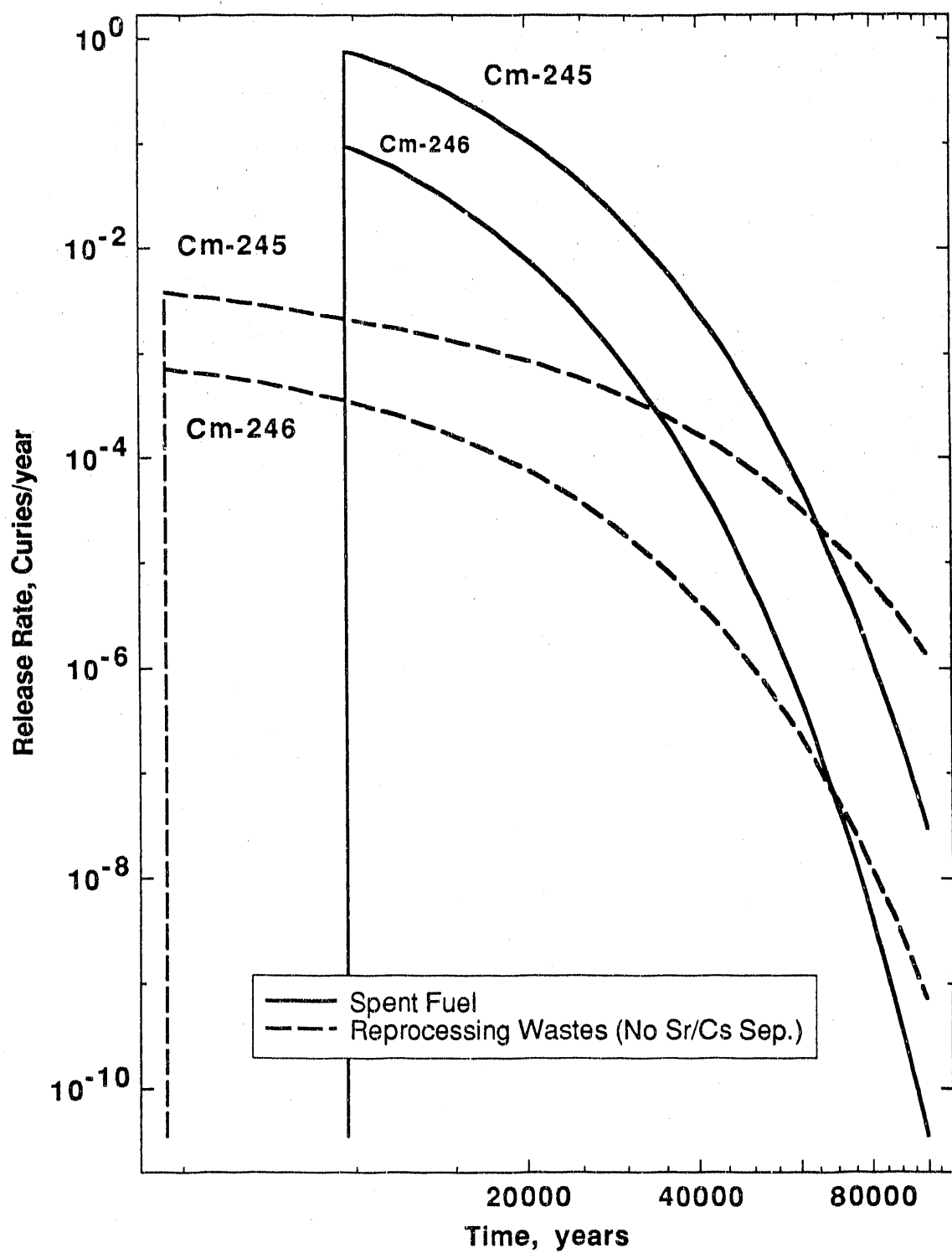


Figure 2.22. Repository Release Rates of Curium from Spent Fuel and Reprocessing Wastes

highest normalized release rate, is very small compared to the inventory in the other streams, so it does not contribute appreciably to the repository release rate. Release of most of the Tc-99 in the reprocessing scheme is limited by the expected slow alteration rate of the copper matrix in the other streams.

The release rate of Cs-135 at early time is higher in the reprocessing scheme than in the spent fuel scheme, because its inventory in the reprocessing scheme is higher. At later time when most of the Cs-135 in reprocessing wastes has been released, the spent fuel release rate is higher. Although the I-129 inventory is also higher in the reprocessing scheme, about half of it is contained in A1-3 packages and released very slowly. For the first  $10^5$  years, the release rate of I-129 in the reprocessing scheme is due mainly to the instantly dissolved I-129 in A3-4 packages. Shortly before  $10^5$  years, the I-129 release rate levels off due to the contribution from the A1-3 packages.

The inventories of the solubility-limited actinides do not affect their release rates; however, their release rates in the reprocessing scheme without Sr/Cs separation are all lower than in the spent fuel scheme. Because the per-package elemental release rate of a solubility-limited species in the wet-drip water-contact mode is proportional to the top area of the package, the total repository elemental release rate is proportional to the combined top area of all the packages containing the element. Table 2.16 lists the total top areas of waste packages containing solubility-limited species. Without Sr/Cs separation, the reprocessing waste total areas are about four to five times lower than the spent fuel total area, and the elemental release rates are correspondingly lower. However, with Sr/Cs separation, the reprocessing waste total areas are over twice the spent fuel total areas, due to the larger number of ALMR waste packages in the repository. As a result, the release rate of Np-237 in the Sr/Cs separation scheme is over twice that in the spent fuel scheme, and about ten times that in the reprocessing scheme without Sr/Cs separation. Although not explicitly shown, elemental release rates of the other solubility-limited species are also highest in the Sr/Cs separation scheme. Relative release rates of

Table 2.16. Total Top Areas of Waste Packages Containing Solubility-Limited Species

Disposal Scheme	Species	Total Top Area (m <sup>2</sup> )
Spent Fuel	all	$2.20 \times 10^4$
Reprocessing Wastes (No Sr/Cs Separation)	U,Th,Ra	$5.35 \times 10^3$
	Np,Pu,Am	$4.26 \times 10^3$
Reprocessing Wastes (Sr/Cs Separation)	U,Th,Ra	$5.85 \times 10^4$
	Np,Pu,Am	$5.74 \times 10^4$

individual isotopes differ due to their different fractions in the wastes.

Curium release rates in the reprocessing scheme are lower than in the spent fuel scheme due to both its lower inventory and its immobilization in copper. The masses of curium in streams A1-1,2 and A1-8 are nearly equal. At early time the repository release rate in the reprocessing scheme is dominated by the relatively high A1-1,2 release rate; at later time it is due mainly to releases from the other streams.

Table 2.17 lists for spent fuel the peak repository release rates and NRC maximum allowable release rates.<sup>3</sup> For low-inventory species, those which constitute less than 0.1 percent of the total curie inventory at 1000 years, the allowable annual release is  $10^{-8}$  of the total curie inventory in the repository at 1000 years. For PWR fuel of 33,000 MWd/Mg burnup, the total 1000-year inventory is  $1.74 \times 10^3$  Ci/Mg, so the maximum allowable release rate for low-inventory species is 1.68 Ci/yr. For high-inventory species, the maximum allowable release rate is  $10^{-5}$  per year of the 1000-year inventory of that species.

Only Tc-99 and Cs-135 exceed their NRC release rate limits. The release rate of Cs-135 drops below its NRC limit at about 16,000 years, and the Tc-99 release rate does so at about 29,000 years. Release rates of the solubility-limited species are all well

Table 2.17. Peak Release Rates from Spent Fuel in  $10^5$  Years

Species	Peak Repository Release Rate (Ci/yr)	NRC Allowable Release Rate (Ci/yr)
Tc-99	$1.26 \times 10^2$	$1.25 \times 10^1$
I-129	$3.14 \times 10^{-1}$	1.6
Cs-135	3.43	1.68
Ra-226	$2.20 \times 10^{-6}$	1.68
Th-230	$2.24 \times 10^{-6}$	1.68
U-234	$4.10 \times 10^{-6}$	1.96
U-238	$1.11 \times 10^{-6}$	1.68
Np-237	$2.33 \times 10^{-6}$	1.68
Pu-239	$5.21 \times 10^{-4}$	$2.95 \times 10^2$
Pu-240	$4.17 \times 10^{-4}$	$4.61 \times 10^2$
Pu-242	$2.26 \times 10^{-5}$	1.68
Am-241	$3.98 \times 10^{-9}$	$8.62 \times 10^2$
Am-243	$8.33 \times 10^{-5}$	$1.51 \times 10^1$
Cm-245	$7.55 \times 10^{-1}$	1.68
Cm-246	$9.35 \times 10^{-2}$	1.68

below their NRC limits for the first  $10^5$  years. Although the release rate of Pu-242 is still increasing at that time, it can never exceed  $4 \times 10^{-5}$  Ci/yr, the solubility-limited release rate of plutonium. Release rates of Ra-226 and Th-230 are also increasing at  $10^5$  years; however, they also cannot exceed their solubility limits. Solubilities of Ra-226 and Th-230, given in the Yucca Mountain *Site Characterization Plan*<sup>34</sup> (SCP), are  $6.8 \times 10^{-2}$  g/m<sup>3</sup> and  $2.3 \times 10^{-4}$  g/m<sup>3</sup>, respectively. These values lead to maximum repository release rates of 0.74 and  $5.34 \times 10^{-5}$  Ci/yr, both of which are below NRC limits.

Table 2.18 lists for the reprocessing scheme without Sr/Cs separation the peak repository release rates and NRC maximum allowable release rates. The total 1000-year inventory in this scheme is  $4.24 \times 10^7$  curies, so the maximum allowable release rate for low-inventory species is  $4.24 \times 10^{-1}$  Ci/yr. A few radionuclides have different status in this reprocessing scheme: Cs-135 is a high-inventory species, and U-234 and Am-243 are low-inventory species.

Table 2.18. Peak Release Rates from Reprocessing Wastes  
in  $10^5$  Years, Without Sr/Cs Separation

Species	Peak Repository Release Rate (Ci/yr)	NRC Allowable Release Rate (Ci/yr)
Tc-99	6.42	$1.79 \times 10^1$
I-129	$6.4 \times 10^{-1}$	$4.24 \times 10^{-1}$
Cs-135	$2.64 \times 10^1$	1.15
Ra-226	$1.17 \times 10^{-6}$	$4.24 \times 10^{-1}$
Th-230	$1.19 \times 10^{-6}$	$4.24 \times 10^{-1}$
U-234	$2.22 \times 10^{-6}$	$4.24 \times 10^{-1}$
U-238	$2.70 \times 10^{-7}$	$4.24 \times 10^{-1}$
Np-237	$4.51 \times 10^{-7}$	$4.24 \times 10^{-1}$
Pu-239	$1.06 \times 10^{-4}$	2.80
Pu-240	$9.20 \times 10^{-5}$	3.50
Pu-242	$3.65 \times 10^{-6}$	$4.24 \times 10^{-1}$
Am-241	$1.02 \times 10^{-6}$	1.67
Am-243	$1.61 \times 10^{-5}$	$4.24 \times 10^{-1}$
Cm-245	$3.84 \times 10^{-3}$	$4.24 \times 10^{-1}$
Cm-246	$7.17 \times 10^{-4}$	$4.24 \times 10^{-1}$

In the reprocessing scheme, I-129 and Cs-135 exceed their NRC limits. I-129 ex-

ceeds its limit only very briefly at the beginning of release. The Cs-135 release rate exceeds its limit for about 17,000 years. However, we have conservatively assumed these species to be instantly dissolved in all waste packages, leading to very high initial release rates. In reality, the waste form will present some mass transfer resistance, and they may not exceed their limits. Release rates of the actinides are again well below their NRC limits.

The cumulative mass release  $M$  in the first  $T$  years after emplacement is defined as

$$M(T) = \int_0^T \dot{M}(t)dt \quad (2.1)$$

where  $\dot{M}(t)$  is the time dependent release rate at the repository (M/t). Table 2.19 lists the cumulative releases from spent fuel and reprocessing wastes in the first  $10^5$  years. Only for Cs-135 and Am-241 are the cumulative releases greater in the reprocessing scheme. In both schemes, essentially all of the Cs-135 is released by  $10^5$  years. The cumulative release of Cs-135 is thus higher in the reprocessing scheme due to its higher inventory. However, the Am-241 inventory is 500 times smaller in the reprocessing scheme than in the spent fuel scheme. Its cumulative release is higher in the reprocessing scheme because release begins much earlier. At 5290 years after emplacement, release from all reprocessing waste packages has begun. By 9650 years, when release from spent fuel packages begins, almost all of the Am-241 has already decayed.

## 2.4 The Borosilicate Glass Option

We have assumed that the salt/zeolite waste form used in the reprocessing scheme is so highly soluble that the iodine and cesium in these wastes are completely dissolved upon water contact. As a result, their release rates are very high soon after release begins. In the reprocessing scheme without Sr/Cs separation, the I-129 and Cs-135 peak release rates are 1.5 and 23 times higher, respectively, than their NRC limits. However, the instant-dissolution assumption is very conservative and may not accurately represent radionuclide behavior in this type of waste. It has

Table 2.19. Cumulative Releases from Spent Fuel and Reprocessing Wastes  
Without Sr/Cs Separation, in  $10^5$  Years

Species	Spent Fuel Cumulative Release (Ci)	Reprocessing Wastes Cumulative Release (Ci)
Tc-99	$1.06 \times 10^6$	$5.41 \times 10^5$
I-129	$2.73 \times 10^3$	$2.35 \times 10^3$
Cs-135	$2.97 \times 10^4$	$1.14 \times 10^5$
Ra-226	.129	$6.90 \times 10^{-2}$
Th-230	.134	$7.20 \times 10^{-2}$
U-234	.326	$1.84 \times 10^{-1}$
U-238	$9.98 \times 10^{-2}$	$2.55 \times 10^{-2}$
Np-237	.209	$4.26 \times 10^{-2}$
Pu-239	$3.96 \times 10^1$	8.83
Pu-240	5.68	1.35
Pu-242	1.06	$1.66 \times 10^{-1}$
Am-241	$3.12 \times 10^{-6}$	$7.77 \times 10^{-4}$
Am-243	7.50	1.53
Cm-245	$4.22 \times 10^3$	$3.93 \times 10^1$
Cm-246	$4.11 \times 10^2$	5.01

been suggested<sup>41</sup> that the salt/zeolite wastes be converted to a more stable waste form such as borosilicate glass. In this section, we investigate the effects of immobilizing the radionuclides in waste streams A1-4, A1-7, and A3-4 in borosilicate glass instead of zeolite. Release rates of I-129 and Cs-135 from borosilicate glass packages are calculated and compared to their release rates in the salt/zeolite packages. Repository release rates are calculated for the reprocessing scheme without Sr/Cs separation. The analysis of the borosilicate glass option ends here; discharge rates at the water table and concentrations at the accessible environment are not

calculated for borosilicate glass packages.

We assume that all the radionuclides can be separated from the salt and placed into borosilicate glass instead of zeolite. In formulating the borosilicate glass waste packages, we adopt a thermal limit of 2.5 kW per package.<sup>41</sup> The standard defense waste package,<sup>27,34</sup> referred to here as type BG, contains 1660 kg glass. The container characteristics are listed in Table 2.6. Release of I-129 and Cs-135 from borosilicate glass is alteration-controlled, and the fractional alteration rate is  $2 \times 10^{-5}$  per year.<sup>40,47</sup>

We assume that radionuclides from each waste stream are packaged separately. Table 2.20 lists, along with the I-129 and Cs-135 per-package inventories, the number of packages needed for each stream in order to achieve heat generation rates of at most 2.5 kW per package. In all packages the radionuclide volume is a small fraction of the glass volume.

Table 2.20. Borosilicate Glass Per-Package Inventories at 1000 Years,  
Without Sr/Cs Separation

Waste Stream	No. Pkgs in Rep.	I-129 Inv. (Ci)	Cs-135 Inv. (Ci)
A1-4	27,280	0	1.05
A1-7	276	0	1.09
A3-4	12,560	$1.87 \times 10^{-1}$	6.81

The normalized release rates of I-129 and Cs-135 from borosilicate glass and salt/zeolite wastes are compared in Figure 2.23. Alteration of glass begins at 1000 years and continues for  $5 \times 10^4$  years. Release begins at 4890 years and drops off rapidly after alteration ends. Because the half-lives of I-129 and Cs-135 are both much longer than the alteration time, their normalized release rates are essentially the same. The alteration-controlled release rates are lower than the instant-dissolution release rates only for about the first 20,000 years. None is as low as the release

rate from silver iodide (A1-3), in which I-129 is solubility-limited. Figure 2.24 shows the repository release rates for borosilicate glass and salt/zeolite wastes in the reprocessing scheme without Sr/Cs separation.

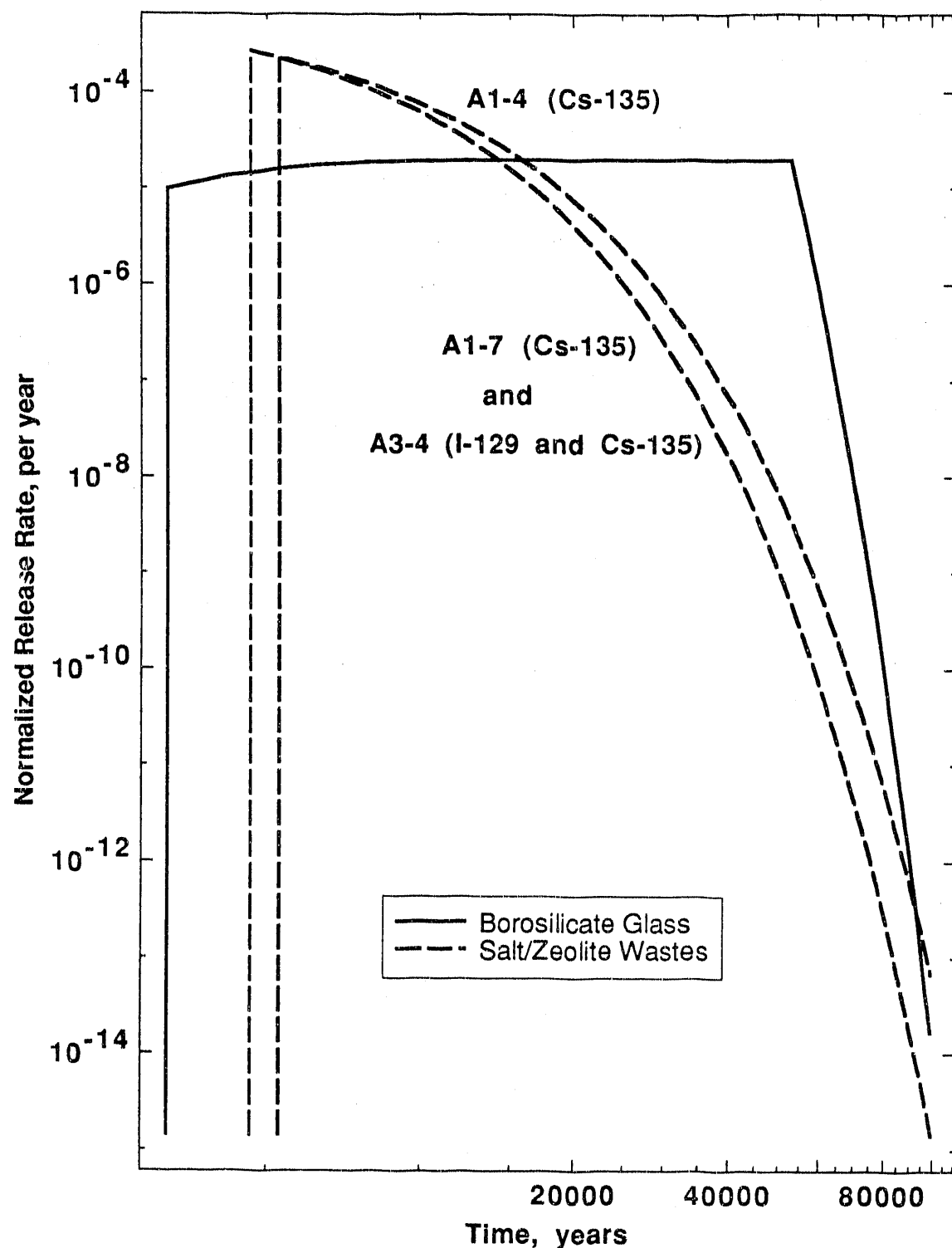


Figure 2.23. Normalized Release Rates of I-129 and Cs-135 in Borosilicate Glass and Salt/Zeolite Wastes

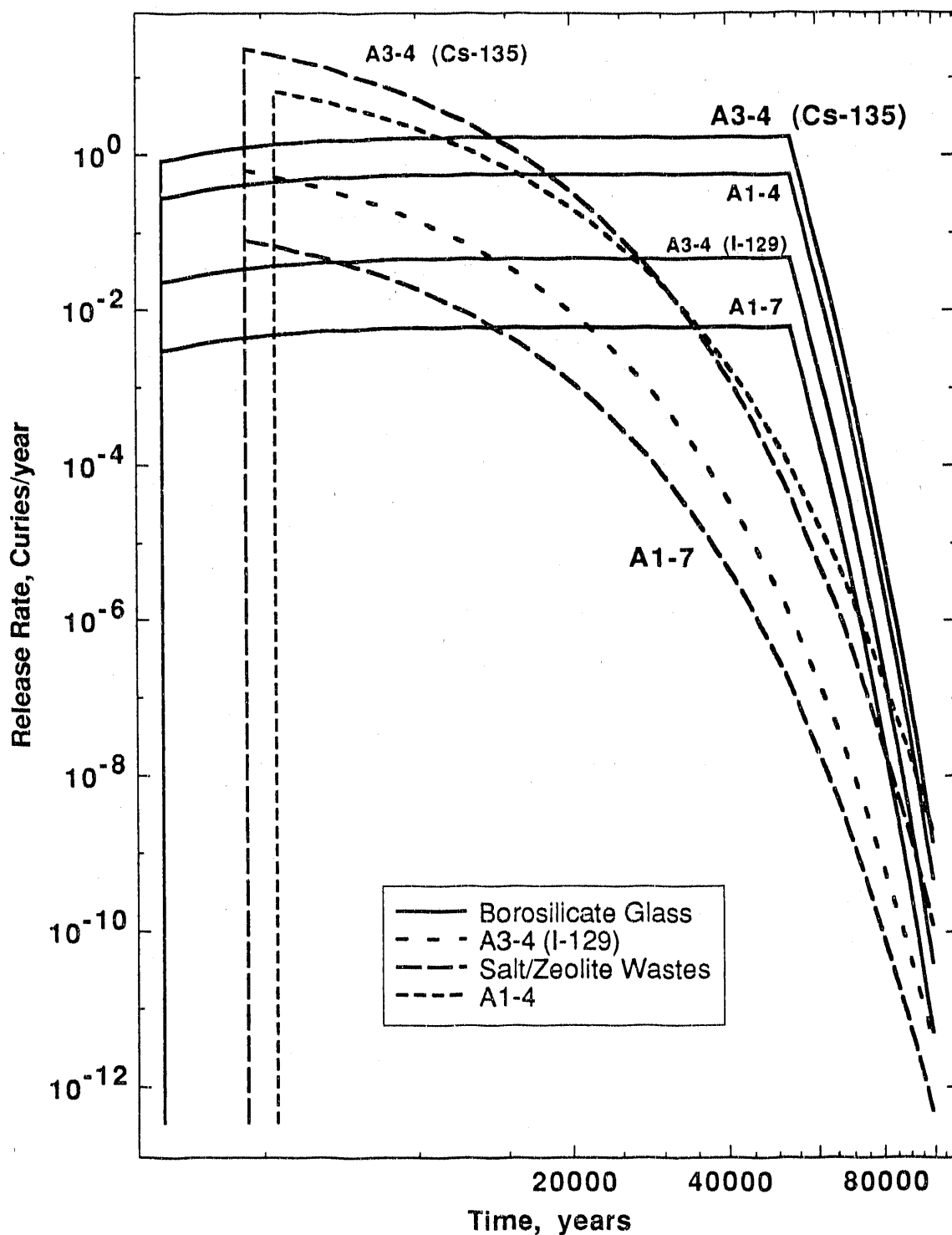


Figure 2.24. Repository Release Rates of I-129 and Cs-135 in Borosilicate Glass and Salt/Zeolite Wastes, Without Sr/Cs Separation

## Chapter 3

### Transport in the Unsaturated Zone

In this chapter, radionuclide release rates from the repository are used to calculate mass discharge rates at the water table. Discharge rates resulting from repository releases during the first  $10^5$  years after emplacement are calculated. Discharge rates are calculated for spent fuel and for the reprocessing scheme without Sr/Cs separation. The Sr/Cs separation scheme and the borosilicate glass option are not further investigated.

#### 3.1 Transport Model

At Yucca Mountain, a small fraction of the local precipitation infiltrates through the ground surface and into the unsaturated zone. Groundwater is expected to percolate downward past the repository horizon and eventually reach the water table. Radionuclides which escape from the waste containers are carried downward with the groundwater until they reach the saturated zone, where they are transported horizontally along with the faster moving water. In the unsaturated zone, water flow is expected to occur mainly in the rock matrix.<sup>34</sup>

Radionuclide transport from the repository to the water table is analyzed using a one-dimensional model in which the repository is represented as an infinite plane source at the emplacement horizon, and radionuclides migrate by diffusion and advection to the water table. The mass release rate, specified as the repository release rate calculated in Chapter 2, is assumed to be uniformly distributed across the plane source. Because the repository area is much greater than the distance to the water table, the repository is well approximated by an infinite plane. The unsaturated zone is considered a uniform porous medium without differentiation of layers. Figure 3.1 illustrates the transport model.

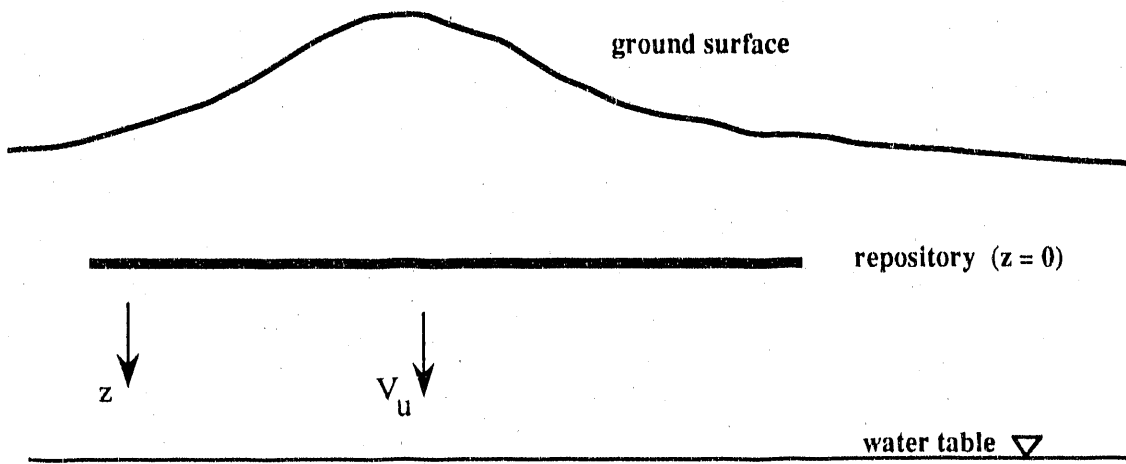


Figure 3.1. Unsaturated Zone Radionuclide Transport Model

For radionuclides without precursors, the governing equation for one-dimensional transport is

$$D \frac{\partial^2 N(z, t)}{\partial z^2} - V_u \frac{\partial N(z, t)}{\partial z} - K \frac{\partial N(z, t)}{\partial t} = \lambda K N(z, t) - \frac{\dot{M}(t) \delta(z)}{\epsilon \psi A} \quad (3.1)$$

$$t > 0, \quad -\infty < z < \infty$$

where

$N(z, t)$  is the radionuclide concentration ( $M/L^3$ ),

$z$  is the distance from the repository ( $L$ ),

$\lambda$  is the radionuclide decay constant ( $1/t$ ),

$D$  is the diffusion/dispersion coefficient ( $L^2/t$ ),

$K$  is the retardation coefficient,

$V_u$  is the pore velocity in the unsaturated zone ( $L/t$ ),

$\epsilon$  is the porosity,

$\psi$  is the saturation,

$A$  is the repository area ( $L^2$ ),

$\dot{M}(t)$  is the time dependent release rate at the repository ( $M/t$ ).

We assume an infinite domain with the concentration equal to zero initially and at  $z$  equal to infinity for all time. This assumption does not allow for a boundary condition at the water table. In reality, fast-moving water at the water table will quickly carry radionuclides away from the area directly beneath the repository. Thus the discharge rates may be greater than predicted here due to an increased concentration gradient at the water table.

The governing equation may be rewritten as

$$\left( \frac{\partial}{\partial t} + \lambda \right) N(z, t) + V_K \frac{\partial N(z, t)}{\partial z} - D_K \frac{\partial^2 N(z, t)}{\partial z^2} = \frac{\dot{M}(t) \delta(z)}{\epsilon \psi A K} \quad (3.2)$$

$t > 0, \quad -\infty < z < \infty$

with

$$D_K = \frac{D}{K} \quad (3.3)$$

$$V_K = \frac{V_u}{K}$$

The solution to this equation, subject to the initial and boundary conditions

$$N(z, 0) = 0 \quad (3.4)$$

$$N(\pm\infty, t) = 0$$

is

$$N(z, t) = \int_0^t \frac{\dot{M}(\tau) e^{-\lambda(t-\tau)}}{\epsilon \psi A K} G(z - V_K(t - \tau), t - \tau) d\tau \quad (3.5)$$

$$G(z, t) = \frac{e^{-z^2/4D_K t}}{\sqrt{4\pi D_K t}}$$

For an impulse release,

$$\dot{M}(t) = I_p \delta(t - t_p) \quad (3.6)$$

where  $t_p$  is the time of the impulse release,  $I_p = I_o e^{-\lambda t_p}$  is the inventory at  $t_p$  (the amount released during the pulse), and  $I_o$  is the inventory at emplacement ( $t = 0$ ).

Thus the solution simplifies to

$$N(z, t) = \frac{I_p e^{-\lambda(t-t_p)}}{\epsilon \psi A K} G(z - V_K(t - t_p), t - t_p) \quad (3.7)$$

The flux  $\phi(z, t)$  is calculated as the sum of an advective and a diffusive term:

$$\begin{aligned} \phi(z, t) &= \epsilon \psi K V_K N(z, t) - \epsilon \psi K D_K \frac{\partial N(z, t)}{\partial z} \\ &= \frac{I_p e^{-\lambda(t-t_p)}}{A} G(z - V_K(t - t_p), t - t_p) \left( \frac{z + V_K(t - t_p)}{2(t - t_p)} \right) \quad (3.8) \end{aligned}$$

The discharge rate  $\dot{M}_D(z, t)$  is simply the flux multiplied by the area:

$$\dot{M}_D(z, t) = I_p e^{-\lambda(t-t_p)} G(z - V_K(t - t_p), t - t_p) \left( \frac{z + V_K(t - t_p)}{2(t - t_p)} \right) \quad (3.9)$$

Equation 3.9 is used to calculate the discharge rates at the water table for all radionuclides without precursors. For each species, the time-dependent repository release rate calculated in Chapter 2 is estimated as a series of impulse releases occurring at 1000-year time intervals. The contribution to the discharge rate from release between times  $t_i$  and  $t_{i+1}$  is given by (3.9) with

$$\begin{aligned} I_p &= I_i \\ t_p &= \frac{1}{2} (t_{i+1} + t_i) \quad (3.10) \end{aligned}$$

where  $I_i$  is the amount released between  $t_i$  and  $t_{i+1}$ . For each output time  $t$ , the contributions to the discharge rate from all impulse releases  $I_p(t_p)$ ,  $t_p < t$ , are summed to obtain the total discharge rate.

The governing equation for the one-dimensional transport of a radionuclide decay chain through isotropic porous media is derived and solved by Harada *et. al.*<sup>48</sup> Solutions of the equation for a variety of radionuclide release modes have been implemented in the widely used computer code UCB-NE-10.4 (originally called

MIGRATO3).<sup>48,49</sup> Here a modification of UCB-NE-10.4 is used to calculate discharge rates at the water table for the U-234→Th-230→Ra-226 chain.

The one-dimensional transport equation with an infinite plane source boundary condition is

$$D \frac{\partial^2 N_i(z, t)}{\partial z^2} - V_u \frac{\partial N_i(z, t)}{\partial z} - K_i \frac{\partial N_i(z, t)}{\partial t} = \lambda_i K_i N_i(z, t) - \lambda_{i-1} K_{i-1} N_{i-1}(z, t) - V_u N_i^*(t) \delta(z) \quad (3.11)$$

$t > 0, \quad -\infty < z < \infty$

where

$i = 1, 2, 3\dots$

$N_i(z, t)$  is the concentration of radionuclide  $i$  ( $M/L^3$ ),

$z$  is the distance from the repository ( $L$ ),

$\lambda_i$  is the decay constant of radionuclide  $i$  ( $1/t$ ),

$D$  is the diffusion/dispersion coefficient ( $L^2/t$ ),

$K_i$  is the retardation coefficient of radionuclide  $i$ ,

$V_u$  is the pore velocity in the unsaturated zone ( $L/t$ ),

$N_i^*(t) = N_i(0, t)$  is the concentration of radionuclide  $i$  at the repository ( $M/L^3$ ).

A "band release" from a waste form occurs when radionuclides dissolve uniformly for a finite time into the water flowing past the waste. If diffusional transport of dissolved radionuclides in the vicinity of the waste material is neglected, the concentration at the repository ( $z = 0$ ) is given by

$$N_i(0, t) = \frac{\dot{M}_i(t)}{Q} \quad (3.12)$$

where  $\dot{M}_i(t)$  is the rate of radionuclide dissolution ( $M/t$ ) and  $Q$  is the volumetric flow rate of water past the waste ( $L^3/t$ ). Here  $Q$  is the flow rate for the entire repository, equal to the product of the groundwater Darcy velocity and the repository area. If the entire radionuclide inventory in the waste is dissolved within a

leach time  $T$ , the initial concentration at this location is then

$$N_i(0, 0) = \frac{M_i^o}{QT} \quad (3.13)$$

where  $M_i^o$  is the initial inventory of radionuclide  $i$  in the waste (M). Using the Bateman equation for radioactive decay, the prescribed concentration at the source becomes

$$N_i^*(t) = \sum_{j=1}^3 B_{ij} e^{\lambda_j t} \quad (3.14)$$

where the Bateman coefficient  $B_{ij}$  is defined as

$$B_{ij} = \sum_{m=1}^j \frac{N_m^o \prod_{r=m}^i \lambda_r}{\lambda_i \prod_{l=m, l \neq j}^i (\lambda_l - \lambda_j)} \quad (3.15)$$

The solution to the transport equation for the band release mode, subject to the initial and boundary conditions

$$\begin{aligned} N_i(z, 0) &= 0 \\ N_i(\pm\infty, t) &= 0 \end{aligned} \quad (3.16)$$

is given by equations 5.29-5.35 in Harada *et. al.* and implemented in UCB-NE-10.4. We represent the time-dependent release rate from the repository as a series of band releases of duration  $T = 1000$  years. The initial amount present at the start of each band release is taken to be the entire amount released during the 1000-year interval. For each band, the flux and discharge rate are calculated as in (3.8) and (3.9). Again, the contributions to the discharge rate from each band release are summed to obtain the total discharge rate.

The source condition for the band release mode specifies a radionuclide concentration at the repository that changes, due to growth and decay, during the time of the band release. This rate of change will not correspond exactly with the actual release rate during that time interval. For example, the release rate of U-234 is

controlled by the decay rates of both itself and U-238. Decay of U-234 decreases its release rate, but decay of U-238 allows a larger portion of the uranium solubility limit to be taken up by U-234. However, because U-238 does not decay significantly during the first  $10^5$  years, the duration of release, the release rate of U-234 is close to an exponentially decaying release rate.

Approximating an exponentially decaying release rate with a series of short decaying band release rates also introduces error. Because we take the total amount released during each time interval to be the initial amount present at the start of each band release, the total amount released during the band will be less than the actual amount released during that interval, due to decay during the band release. However, this error is very small for U-234 since its half-life is much longer than 1000 years.

The boundary concentration of Th-230 and Ra-226 in the band release mode also does not correspond with the release rates given in Chapter 2. However, it will be shown later that all Th-230 and Ra-226 released from the repository completely decays before reaching the water table. Therefore, their discharge rates are due entirely to decay of U-234 during transport. Because the Th-230 and Ra-226 that leave the repository travel in the ground for some time before decaying, they affect the diffusive transport of the Th-230 and Ra-226 that are produced later. However, errors in the Th-230 and Ra-226 discharge rates introduced by the band series approximation should be small.

### 3.2 Discussion of Parameters

Data on the hydrologic and geologic conditions at Yucca Mountain are taken from the SCP. The Darcy velocity ( $V_D$ ) of 0.5 mm/year is taken as constant throughout the distance from the repository to the water table. The two main tuff units lying between the repository horizon and the water table, the Topopah Springs and Calico Hills units, are divided for site characterization purposes into six layers. Values of the saturation ( $\psi$ ), porosity ( $\epsilon$ ), and dry bulk density ( $\rho$ ) (mass of rock

divided by volume of rock and pores) are given in the SCP for each of these layers. Only about 32% of the top layer, denoted in the SCP as TSw2, is underneath the repository. Table 3.1 lists the properties of the tuff layers. The values of porosity, saturation, and density are weighted by the layer thicknesses to obtain the average values  $\epsilon\psi = 0.25$  and  $\rho = 1.76 \text{ g/cm}^3$ . This leads to a volumetric flow rate  $Q$  of  $4230 \text{ m}^3/\text{yr}$ . The pore velocity ( $V_p = V_D/\epsilon\psi$ ) is  $2 \times 10^{-3} \text{ m/yr}$ . The water travel time for the total distance of 218 m from the repository to the water table is  $1.09 \times 10^5$  years.

Table 3.1. Properties of Yucca Mountain Tuff Layers (Data from Ref. 34)

Tuff Layer *	Thickness (m)	Porosity	Saturation	Dry Bulk Density (g/cm <sup>3</sup> )
TSw2	42**	.12	.65	2.24
TSw3	18	.04	.65	2.29
CHn1v	126	.36	.90	1.50
CHn1z	together	.33	.91	1.61
CHn2z	16	.29	1.0	1.80
CHn3z	16	.36	1.0	1.54

\* SCP convention for naming Yucca Mountain tuff layers:

TS = Topopah Springs unit

CH = Calico Hills unit

w = welded tuff, n = non-welded tuff

v = vitric, z = zeolitic

\*\* Thickness under the repository horizon (32% of total thickness).

The diffusion coefficient of cesium in moisture present in intact tuff has been determined experimentally<sup>50</sup> to be  $9.5 \times 10^{-3} \text{ m}^2/\text{yr}$ . de Marsily<sup>51</sup> observes that compilations of published dispersivities have revealed average values of order one tenth the distance traveled. Recent analyses<sup>52</sup> of unsaturated zone transport at

Yucca Mountain considered transport separately for 20 tuff layers and assumed dispersivity values ( $\alpha$ ) of ten percent of the layer thickness. An average dispersivity of 10 m was obtained. Here we consider only one layer, so we take the dispersivity to be one tenth of the distance traveled, or 22 m. Both values are within the range of uncertainty for this parameter. An effective diffusion/dispersion coefficient is calculated using

$$D = D_m + \alpha V_u \quad (3.17)$$

where  $D_m$  is the coefficient of molecular diffusion and  $V_u$  is the groundwater pore velocity.<sup>51</sup> This gives  $D = 0.05 \text{ m}^2/\text{yr}$ .

Retardation coefficients for all radionuclides except iodine, thorium and curium are obtained from experimental sorption ratios in the SCP. Table 3.2 lists the sorption ratios for the two tuff units between the repository and the water table. Average sorption ratios for each unit are calculated and weighted by the thicknesses of the units to obtain the sorption ratios  $K_D$  used here. The thicknesses of the Topopah Springs and Calico Hills tuffs are 60m and 158m, respectively. The sorption ratio of iodine is assumed to be zero. Remaining sorption ratios are compiled by Sinnock *et. al.*<sup>53</sup>

Table 3.2. SCP Unsaturated Zone Sorption Experiment Data:  $K_D$  in ml/g

Tuff Unit	Tc	Cs	Ra	U	Np	Pu	Am
Topopah	.3	290	1500	1.8	7.0	64	1200
Spring	0	350		0	2.7	360	1100
	.03	430		0	5.0	290	1800
		855		2.5		120	180
Calico Hills	-	7800	-	0	2.7	66	1700
		63,300		20.0			

Assuming local chemical equilibrium between a species in the pore liquid and that

same species sorbed on the rock, the sorption retardation coefficient  $K$  is given by

$$K = 1 + \frac{\rho}{\epsilon\psi} K_D . \quad (3.18)$$

Table 3.3 lists the average sorption ratios  $K_D$  and the calculated retardation coefficients.

Table 3.3. Unsaturated Zone Retardation Parameters

Element	Sorption ratio (ml/g)	Retardation coefficient
Technetium	.11	1.8
Iodine	0	1
Cesium	25,900	182,000
Radium	1500	10,500
Thorium	580	4000
Uranium	7.6	54
Neptunium	3.3	24
Plutonium	106	740
Americium	1530	10,700
Curium	180	1200

### 3.3 Discharge Rates at the Water Table

Figures 3.2 through 3.5 show the discharge rates at the water table for Tc-99, I-129, U-234 and daughters, U-238, Np-237, and Pu-242. The remaining nuclides are so retarded during transport that they decay before reaching the water table. If there were no diffusional transport, the expected radionuclide travel time from the repository to the water table would be the water travel time multiplied by the retardation coefficient. The expected travel times are listed in Table 3.4. Nuclides that decay in this time do not arrive at the water table. The travel times for Ra-226 and Th-230 are longer than the times for them to decay, so their discharge rates result entirely from decay of U-234 during transport.

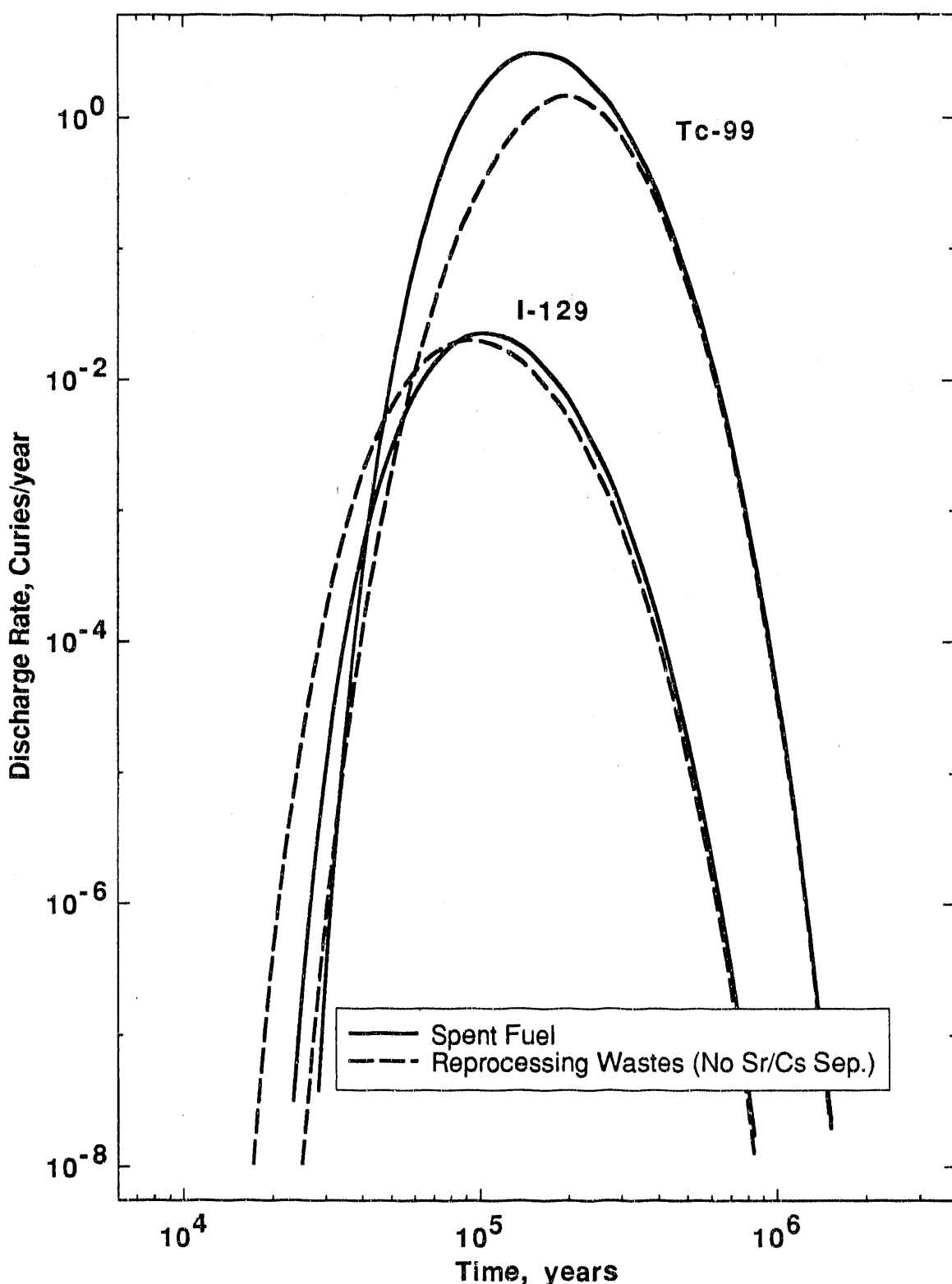


Figure 3.2. Tc-99 and I-129 Discharge Rates at the Water Table for Spent Fuel and Reprocessing Wastes

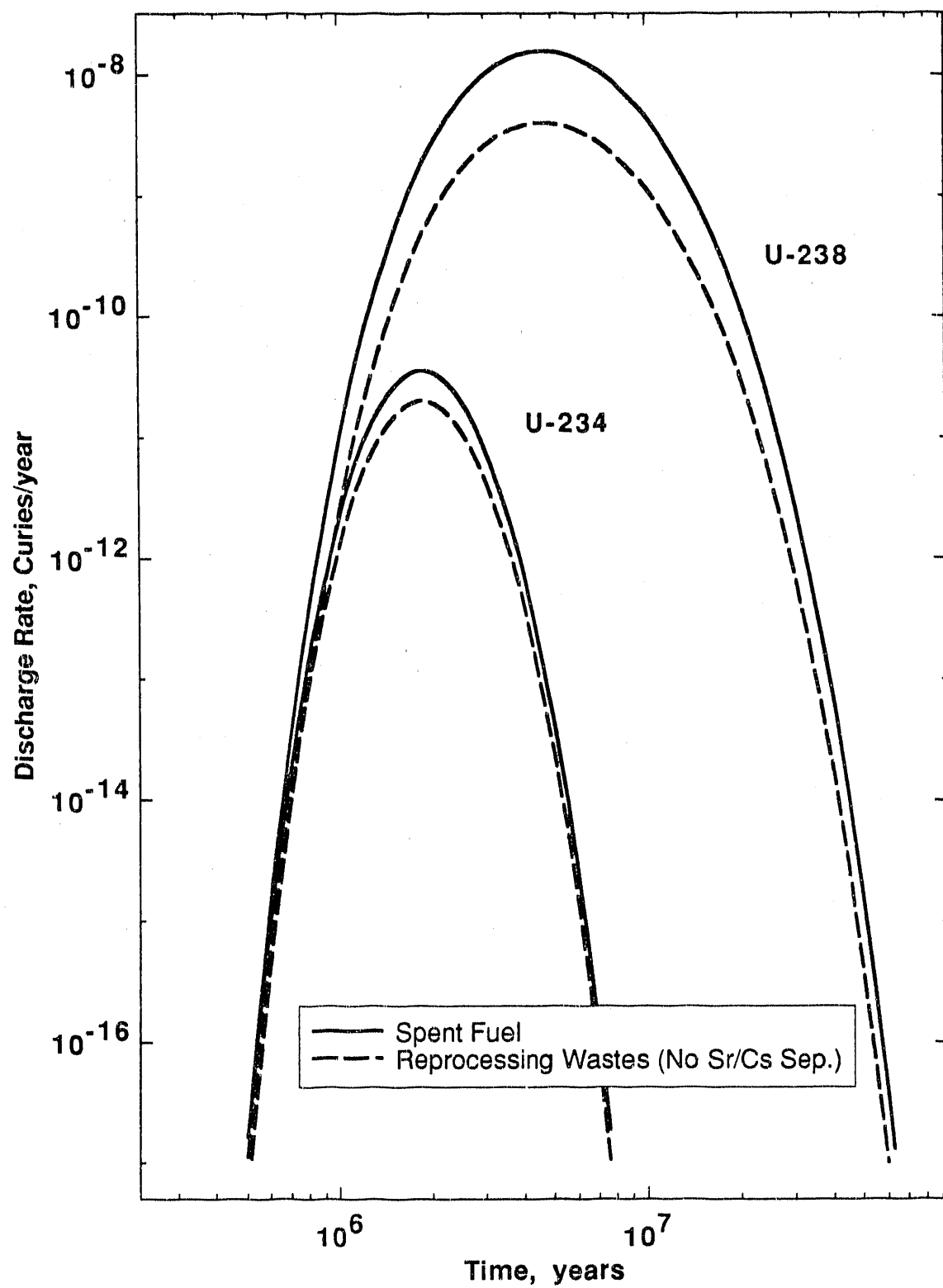


Figure 3.3. Uranium Discharge Rates at the Water Table for Spent Fuel and Reprocessing Wastes

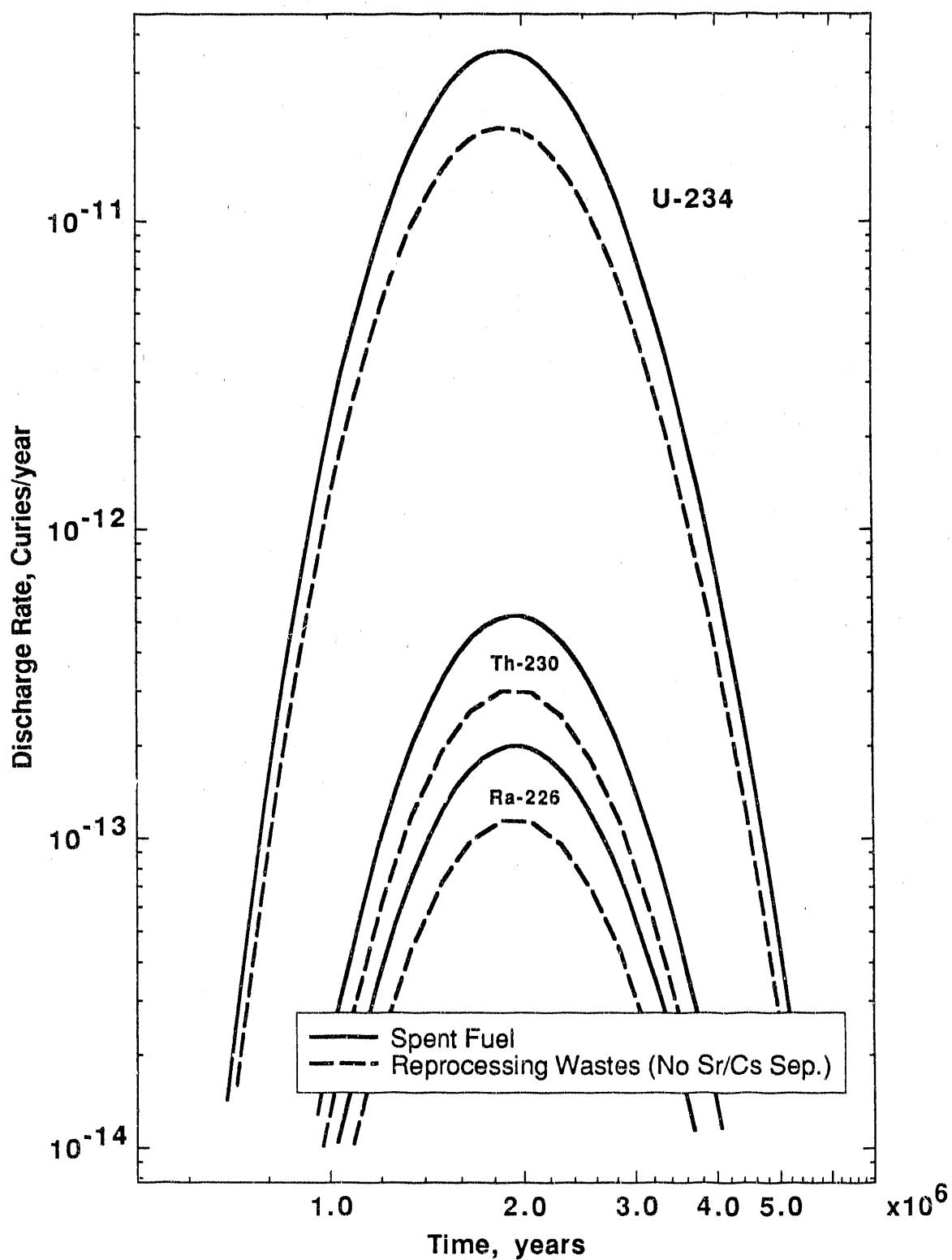


Figure 3.4. U-234 and Daughters Discharge Rates at the Water Table for Spent Fuel and Reprocessing Wastes

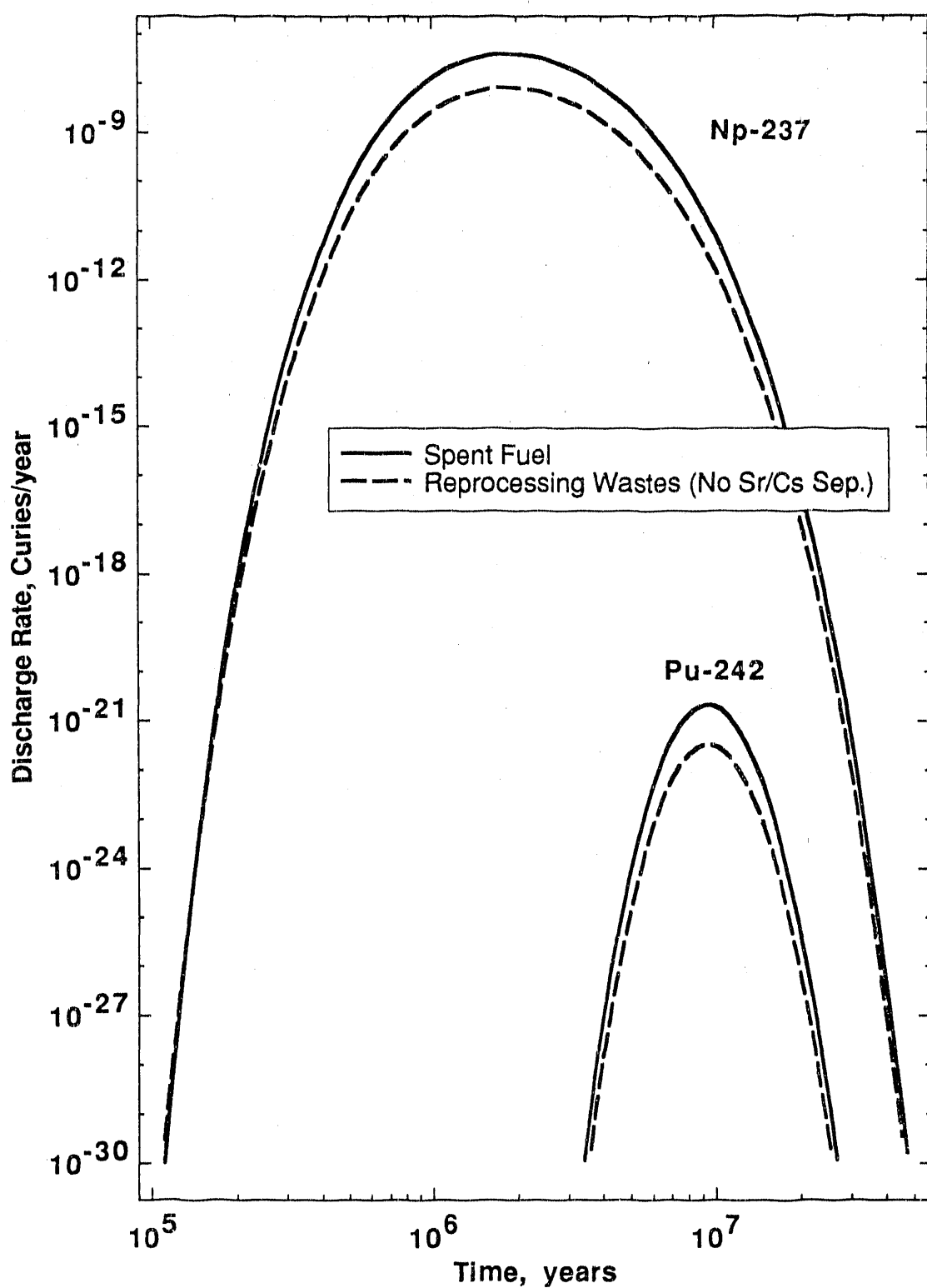


Figure 3.5. Np-237 and Pu-242 Discharge Rates at the Water Table for Spent Fuel and Reprocessing Wastes

Table 3.4. Radionuclide Travel Times to the Water Table

Species	Expected Travel Time (years)	Time to Decay to $10^{-10}$ of Original Amount (years)
Tc-99	$1.96 \times 10^5$	$7.08 \times 10^6$
I-129	$1.09 \times 10^5$	$5.22 \times 10^8$
Cs-135	$1.98 \times 10^{10}$	$1.00 \times 10^8$
Ra-226	$1.14 \times 10^9$	$5.32 \times 10^4$
Th-230	$4.36 \times 10^8$	$2.51 \times 10^6$
U-234	$5.89 \times 10^6$	$8.15 \times 10^6$
U-238	$5.89 \times 10^6$	$1.48 \times 10^{11}$
Np-237	$2.62 \times 10^6$	$7.11 \times 10^7$
Pu-239	$8.07 \times 10^7$	$8.01 \times 10^5$
Pu-240	$8.07 \times 10^7$	$2.18 \times 10^5$
Pu-242	$8.07 \times 10^7$	$1.25 \times 10^7$
Am-241	$1.17 \times 10^9$	$1.44 \times 10^4$
Am-243	$1.17 \times 10^9$	$2.45 \times 10^5$
Cm-245	$1.31 \times 10^8$	$2.84 \times 10^5$
Cm-246	$1.31 \times 10^8$	$1.58 \times 10^5$

Diffusion causes all radionuclides to arrive at the water table earlier than their expected times. For example, the discharge rate of Tc-99 from spent fuel has reached  $10^{-8}$  of its peak value at  $2.8 \times 10^4$  years. However, diffusion does not decrease the radionuclide travel times enough for any more nuclides to appear.

For each radionuclide that arrives at the water table, discharge from reprocessing wastes begins earlier than discharge from spent fuel, because release from the repository starts earlier for reprocessing wastes. However, some of the graphs do not show the discharge rates at times early enough for this to be apparent. For Tc-99, the spent fuel discharge rate is substantially higher only for early times, cor-

responding to its higher release rate from the repository. At later times when the Tc-99 spent fuel release rate rapidly decreases, its discharge rate approaches that of the reprocessing wastes. A comparison of the I-129 discharge rates from spent fuel and borosilicate glass would yield a similar relationship. Also corresponding to the repository release rates, the I-129 discharge rates are almost the same in both schemes. In the spent fuel scheme the peak discharge rate of Tc-99 is about twice that of the reprocessing scheme, and for I-129 it is about ten percent higher.

The discharge rates of uranium, Np-237, and Pu-242 also correspond closely to their release rates from the repository. For example, the Np-237 release rate (constant with time) and peak discharge rate are both about five times higher in the spent fuel scheme. Discharge rates of Th-230 and Ra-226 are higher in the spent fuel scheme because the release rate of U-234 is higher.

## Chapter 4

### Transport in the Saturated Zone

In this chapter, discharge rates at the water table are used to calculate time-dependent concentrations at the accessible environment. The concentrations are then converted to dose rates using dose conversion factors.

#### 4.1 Transport Model

At and below the water table, the saturation  $\psi$  is equal to unity, and groundwater is assumed to flow horizontally to the southeast.<sup>34</sup> Radionuclides which reach the water table are transported downstream toward a hypothetical well which is located at the accessible environment, defined by the EPA to be 5 km from the repository perimeter. Water from the saturated zone is extracted from the well and used by future humans for drinking and agriculture.

We assume that all radionuclides that reach the water table do so within an area directly beneath the repository. In reality, they will be spread beyond this area due to transverse diffusion and dispersion. The time-dependent discharge rate at the water table is represented as a time-dependent release from an array of point sources located at the water table, within an area directly beneath the repository. Radionuclides released from the point sources migrate by diffusion and advection toward the well. We assume that the well does not perturb the aquifer.

The time-dependent concentration at the point where the well drillhole intersects the water table is calculated using a three-dimensional transport model. Radionuclides emitted from the point sources diffuse and disperse horizontally and downward. We ignore any transport back up into the unsaturated zone. Figure 4.1 shows the transport model. Figure 4.2 shows the array of point sources chosen to represent the area of the repository, superimposed on a top view of the repository.

The concentration at the output point is the sum of the concentrations resulting from releases from all of the point sources.

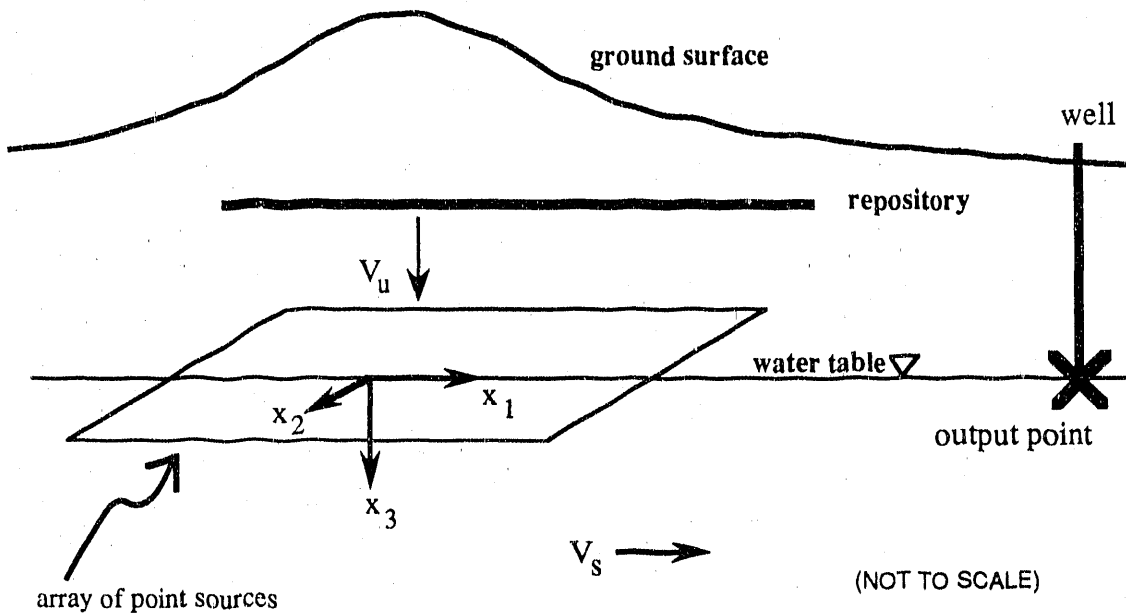


Figure 4.1. Saturated Zone Radionuclide Transport Model

Flow in the saturated zone is assumed to occur mainly in fractures.<sup>34</sup> However, for these calculations the saturated zone is treated as an isotropic porous medium with porosity given by the bulk effective fracture porosity. This is sufficient because the fractures at Yucca Mountain are extremely small compared to the distance over which flow is being analyzed. It is thus possible to represent the saturated zone as a porous medium without sacrificing much accuracy.

The governing equation for radionuclide transport from a point source in porous media is solved by Chambré *et. al.*<sup>54</sup> The governing equation for a radionuclide without precursors is

$$K \frac{\partial N}{\partial t} + V_1 \frac{\partial N}{\partial x_1} + V_2 \frac{\partial N}{\partial x_2} + V_3 \frac{\partial N}{\partial x_3} = D_1 \frac{\partial^2 N}{\partial x_1^2} + D_2 \frac{\partial^2 N}{\partial x_2^2} + D_3 \frac{\partial^2 N}{\partial x_3^2} - \lambda K N$$

$$t > 0, \quad -\infty < x_i < \infty, \quad i = 1, 2, 3 \quad (4.1)$$

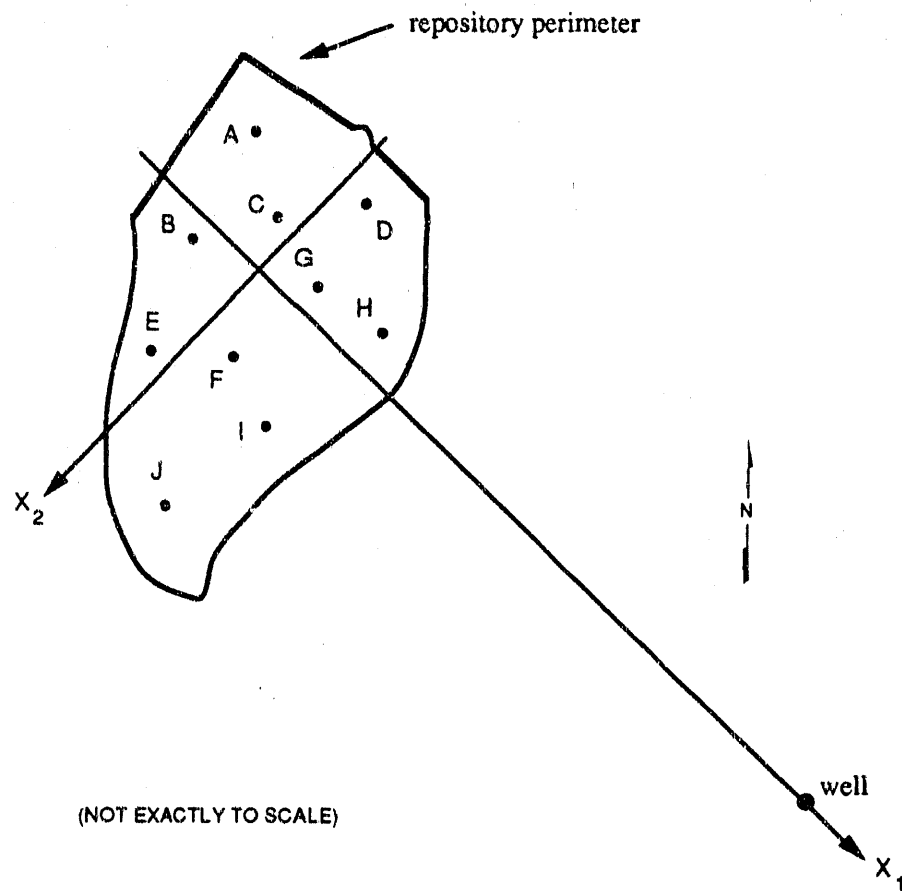


Figure 4.2. Source Point Locations for the Saturated Zone Transport Model

where

$N(x_1, x_2, x_3, t)$  is the radionuclide concentration ( $M/L^3$ ),

$x_1, x_2, x_3$  are the distances from the point source in each direction ( $L$ ),

$\lambda$  is the radionuclide decay constant ( $1/t$ ),

$D_1, D_2, D_3$  are the diffusion/dispersion coefficients in each direction ( $L^2/t$ ),

$K$  is the retardation coefficient,

$V_1, V_2, V_3$  are the pore velocities in the saturated zone ( $L/t$ ).

The solution to (4.1), subject to the initial and boundary conditions

$$\begin{aligned}
 N(x_1, x_2, x_3, 0) &= 0 \\
 N(\pm\infty, \pm\infty, \pm\infty, t) &= 0
 \end{aligned} \tag{4.2}$$

due to a point source  $j$  located at  $(x_1^o, x_2^o, x_3^o)$  and with a mass release rate  $M_j(\tau)$ ,

is

$$N(x_1, x_2, x_3, t) = \int_0^t \frac{\dot{M}_j(\tau)}{\epsilon K} e^{-\lambda(t-\tau)} \prod_{i=1}^3 C_i(x_i, t-\tau) d\tau \quad (4.3)$$

$$C_i(x_i, t-\tau) = \frac{1}{\sqrt{4\pi D_i(t-\tau)}} e^{-\frac{[(x_i - x_i^0) - V_i(t-\tau)]^2}{4D_i(t-\tau)}}$$

where  $\epsilon$  is the porosity of the medium.

We take  $\hat{x}_1$  to be the direction of water flow (horizontal). We take  $\hat{x}_2$  to be the horizontal direction perpendicular to water flow, and  $\hat{x}_3$  is the vertical downward direction. The velocity in the saturated zone is denoted  $V_s$ ; thus  $V_1 = V_s$ , and  $V_2 = V_3 = 0$ . We also assume the transverse dispersion coefficients are equal:  $D_2 = D_3$ .

Ten source points are chosen, located so as to approximate the area of the repository. The origin is located near the middle of the repository. The output point is located 5 km downstream from the repository edge, at (6250 m, 0, 0). The source points are listed in Table 4.1. With these source points and output point,  $x_3 = x_3^0 = 0$  always.

The solution to the transport equation allows for diffusion and dispersion both upward and downward. Using this solution, half of the radionuclides released from each point source will migrate above the plane of the array and half will migrate below. However, because radionuclides are continuously traveling down through the unsaturated zone, the high concentration of radionuclides above the water table will prevent much diffusive transport back up toward the repository. To adjust the solution so that all of the radionuclides emitted from each point source travel downward, we simply double  $\dot{M}_j(\tau)$  in the expression for the concentration. If the discharge rate to the water table is evenly distributed among the ten point sources, the mass release rate from each point source is  $\dot{M}_j(\tau) = \frac{1}{P} \dot{M}_D(\tau)$ , where  $P=10$  is the number of point sources. With these parameters the solution for the

Table 4.1. Source Points for the Saturated Zone Transport Model

Source Point	Location ( $x_1, x_2, x_3$ ) (Distances in Meters)
A	(-780,-860,0)
B	(-580,220,0)
C	(-110,-360,0)
D	(310,-910,0)
E	(-110,970,0)
F	(330,470,0)
G	(360,-220,0)
H	(910,-330,0)
I	(890,670,0)
J	(830,1600,0)

concentration arising from a point source at  $(x_1^o, x_2^o, 0)$  simplifies to

$$\begin{aligned}
 N(x_1, x_2, x_3, t) &= \frac{2}{10} \int_0^t \frac{\dot{M}_D(\tau)}{\epsilon K} e^{-\lambda(t-\tau)} \prod_{i=1}^3 C_i d\tau \\
 C_1(x_1, t - \tau) &= \frac{1}{\sqrt{4\pi D_1(t - \tau)}} e^{\frac{-[(x_1 - x_1^o) - V_s(t - \tau)]^2}{4D_1(t - \tau)}} \\
 C_2(x_2, t - \tau) &= \frac{1}{\sqrt{4\pi D_2(t - \tau)}} e^{\frac{-(x_2 - x_2^o)^2}{4D_2(t - \tau)}} \\
 C_3(x_3, t - \tau) &= \frac{1}{\sqrt{4\pi D_3(t - \tau)}} .
 \end{aligned} \tag{4.4}$$

For each radionuclide that reaches the water table, Equation 4.4 is used to calculate the concentration at the well due to release each point source. These contributions are summed to obtain the total time-dependent concentration. Because the water travel time from the area underneath the repository to the well is only about 100 years, it is reasonable to neglect growth of Th-230 and Ra-226 during transport in

the saturated zone.

#### 4.2 Discussion of Parameters

Data on the hydrogeologic conditions in the saturated zone are taken from the SCP. Because the layers of tuff under the repository are tilted with respect to the horizontal, water at the top of the saturated zone flows through both the Calico Hills and Topopah Spring Units. For 3000 meters downstream from the repository perimeter, the water table is in the Calico Hills unit; for the next 2000 meters it intersects the Topopah Springs unit. The porosity of the saturated zone is taken to be the average bulk effective fracture porosity in these two units. Saturated zone hydrologic parameters for these units are given in Table 4.2. The average fracture porosity is  $1.4 \times 10^{-3}$ , and the average pore velocity is 65 m/yr.

Table 4.2. Saturated Zone Hydrologic Parameters (Data from Ref. 34)

Parameter	Calico Hills Unit	Topopah Spring Unit
path length (m)	3000	2000
bulk effective fracture porosity	$4 \times 10^{-4}$	$2.8 \times 10^{-3}$
pore velocity (m/yr)	100	14

The longitudinal dispersion coefficient for the saturated zone is taken to be  $D_1 = 50 \text{ m}^2/\text{yr}$ .<sup>55</sup> Molecular diffusion is negligible compared to dispersion and is ignored. The transverse dispersion coefficients are estimated to be one tenth of the longitudinal dispersion coefficient:  $D_2 = D_3 = 5 \text{ m}^2/\text{yr}$ .

Retardation coefficients for all radionuclides except iodine and thorium are obtained from experimental sorption ratios in the SCP. Table 4.3 lists the sorption ratios for the three main tuff units that make up the saturated zone: the Prow Pass, Bullfrog, and Tram units. Their thicknesses are 145 m, 135 m, and 121 m, respectively.

Average sorption ratios for each unit are calculated and weighted by the thicknesses of the units to obtain the sorption ratios  $K_D$  used here. The sorption ratio of iodine is assumed to be zero. The sorption ratio of thorium is assumed to be the same as that in the unsaturated zone. Sorption ratios for radionuclides that do not reach the water table are not included.

Table 4.3. SCP Saturated Zone Sorption Experiment Data:  $K_D$  in ml/g

Tuff Unit	Tc	Ra	U	Np	Pu
Prow Pass	.15	-	-	6.4	77
	.21			9.0	230
Bullfrog	4.2	46,000	1.3	-	80
		540	2.2		110
Tram	-	-	4.6	24	400

Retardation coefficients for the saturated zone are calculated by taking into account its fracture characteristics. The retardation coefficient  $K$  in fractured media is given by

$$K = 1 + \frac{K_f}{b} \quad (4.5)$$

$$K_f = K_D S$$

where

$K_f$  is the the sorption distribution coefficient (L),

$b$  is the average fracture half-width (L),

$S$  is the mass per surface area of the medium ( $M/L^2$ ).

The value of the fracture half-width used here,  $10^{-5}$  m, is characteristic of reported values.<sup>56</sup> The mass per surface area is  $10^{-6}$  g/cm<sup>2</sup>.<sup>53</sup> Table 4.4 gives the average sorption ratios and the calculated retardation coefficients.

Dose conversion factors are used to convert the time-dependent concentrations at the well into dose rates to individuals. Charles and Smith<sup>57</sup> have calculated dose

Table 4.4. Saturated Zone Retardation Parameters

Element	$K_D$ (ml/g)	$K_f$ (cm)	$K$
Technetium	2.1	$2.1 \times 10^{-6}$	1.0
Iodine	0	0	1.0
Radium	23,200	$2.3 \times 10^{-2}$	24
Thorium	580	$5.8 \times 10^{-4}$	1.5
Uranium	3.1	$3.1 \times 10^{-6}$	1.0
Neptunium	15	$1.5 \times 10^{-5}$	1.0
Plutonium	210	$2.1 \times 10^{-4}$	1.2

conversion factors for a hypothetical well which supplies water for land irrigation, livestock feeding, and human consumption. The exposure pathways considered are external irradiation from contaminated irrigated land, inhalation of resuspended soil, and consumption of crops and livestock grown on the irrigated land. Conversion factors for the radionuclides that reach the accessible environment are listed in Table 4.5.

Table 4.5. Radionuclide Dose Conversion Factors (Data from Ref. 56)

Species	Dose Conversion Factor $\left( \frac{\text{rem/year}}{\text{Ci/m}^3} \right)$
Tc-99	$2.1 \times 10^3$
I-129	$3.9 \times 10^5$
Ra-226	$4.0 \times 10^6$
Th-230	$1.1 \times 10^6$
U-234	$3.7 \times 10^5$
U-238	$3.6 \times 10^5$
Np-237	$2.6 \times 10^6$
Pu-242	$3.5 \times 10^6$

### 4.3 Concentrations at the Accessible Environment

Concentrations and dose rates at the accessible environment, for both disposal schemes, are shown in Figures 4.3 through 4.10. The relative concentrations of individual species in the two disposal schemes closely parallel their relative discharge rates at the water table. Concentrations of the fission products Tc-99 and I-129 are both about  $10^6$  times higher than those of any of the actinides. This is a direct result of their correspondingly higher release rates from the repository, the reasons for which are explained in detail in Chapter 2. Dose conversion factors for all species except Tc-99 are within an order of magnitude of each other; thus, their relative dose rates also correspond roughly to their relative discharge rates. The dose conversion factor of Tc-99 is about 100 times lower than those of the other species. However, it is nowhere near low enough for the Tc-99 dose rate to be comparable to that of any of the actinides. These results are consistent with earlier studies<sup>55,58</sup> which found that doses from the fission products are among the most significant concerns about geologic disposal of nuclear waste.

For no species investigated is the peak dose rate at the accessible environment more than seven times lower in the reprocessing scheme than in the spent fuel scheme. Again, this is due to the relative release rates from the repository in these two schemes. The reasons for the closeness of the Tc-99 and I-129 dose rates in the two schemes thus lie mainly in their chosen packaging, as described in Chapter 2. The dominant factor in the determination of the dose rate of a solubility-limited actinide is not its repository inventory, but the number of waste packages among which this inventory is distributed. In the reprocessing scheme investigated here, inventory reduction is coupled with actinide distribution in a smaller number of packages than in the spent fuel scheme. The resulting actinide dose rates are thus lower, roughly in proportion to the lower total top area of the packages in the repository. Pigford<sup>59</sup> has anticipated this result by noting that risk from actinides is only proportional to inventory when the per-package inventory of actinides is reduced so much that their release is no longer solubility-limited but is instead

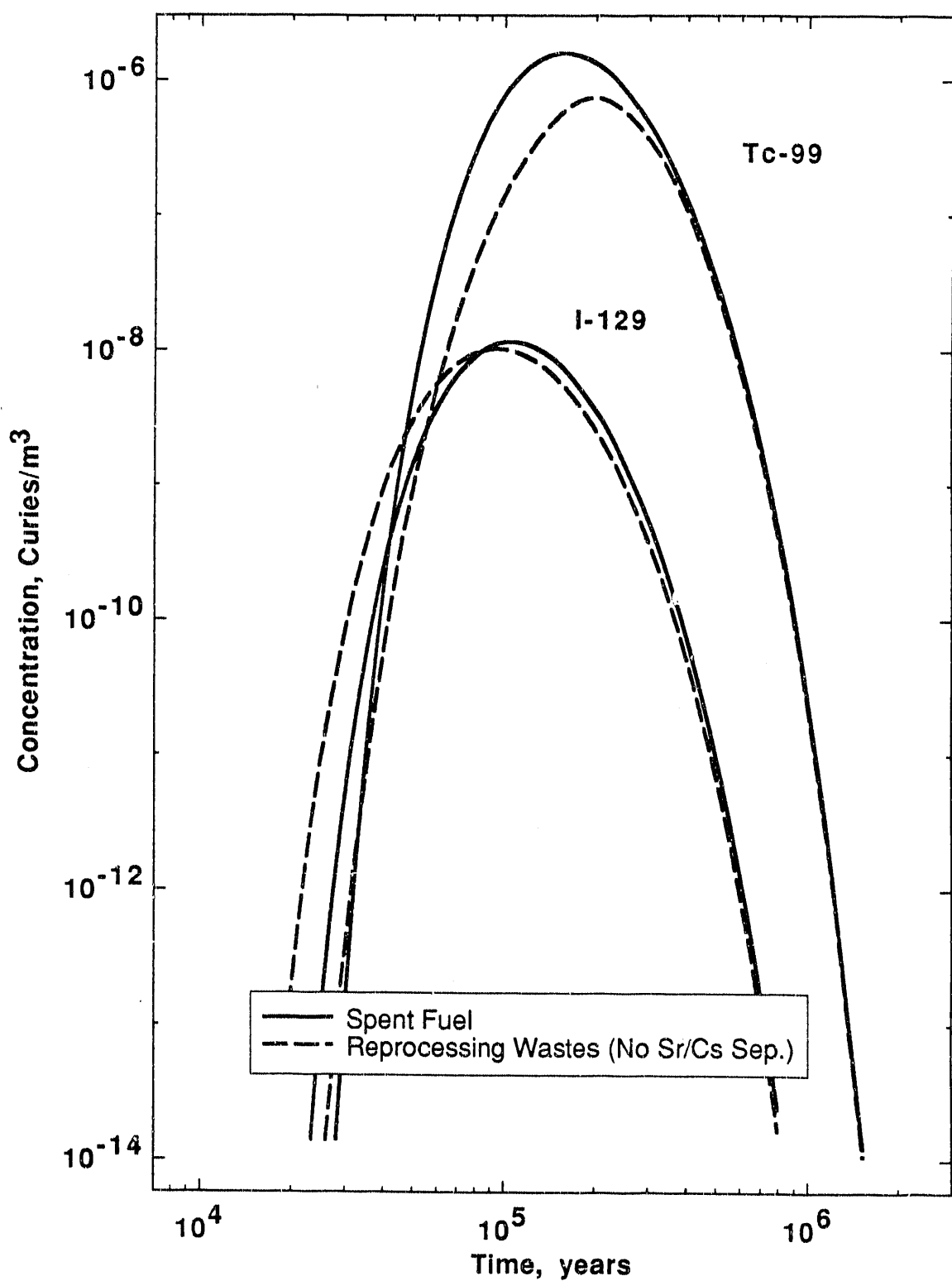


Figure 4.3. Tc-99 and I-129 Concentrations at the Accessible Environment for Spent Fuel and Reprocessing Wastes

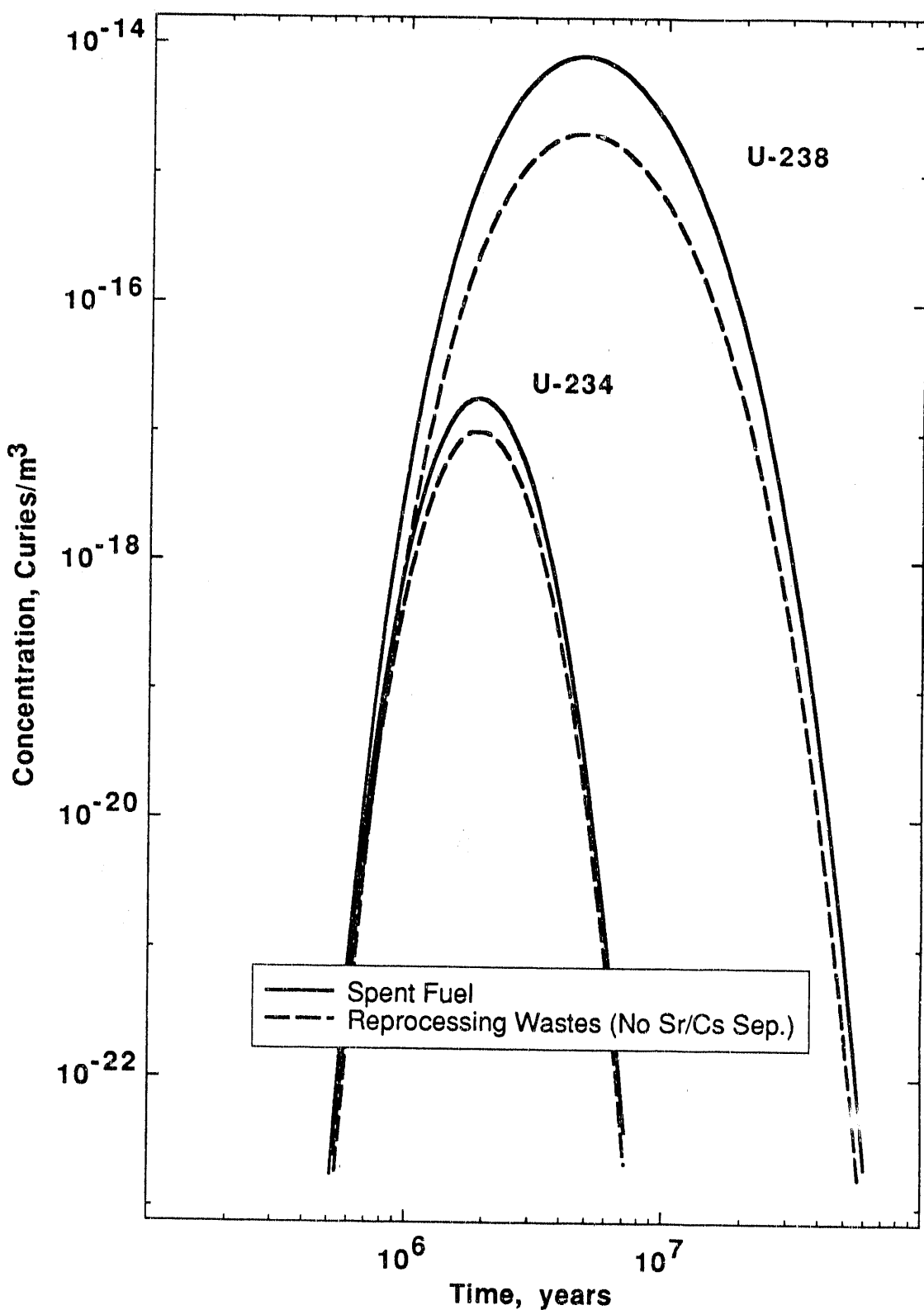


Figure 4.4. Uranium Concentrations at the Accessible Environment for Spent Fuel and Reprocessing Wastes

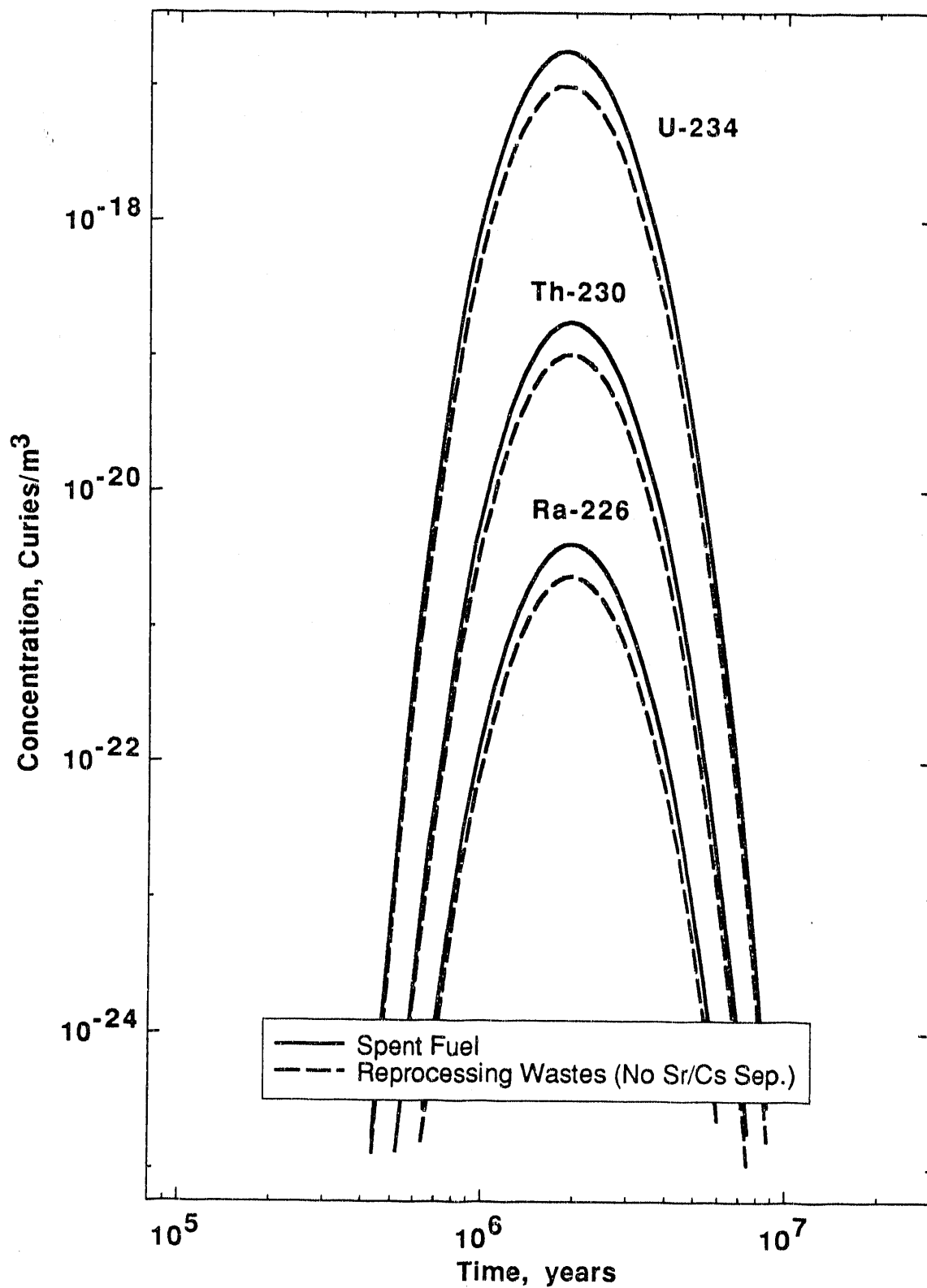


Figure 4.5. U-234 and Daughters Concentrations at the Accessible Environment for Spent Fuel and Reprocessing Wastes

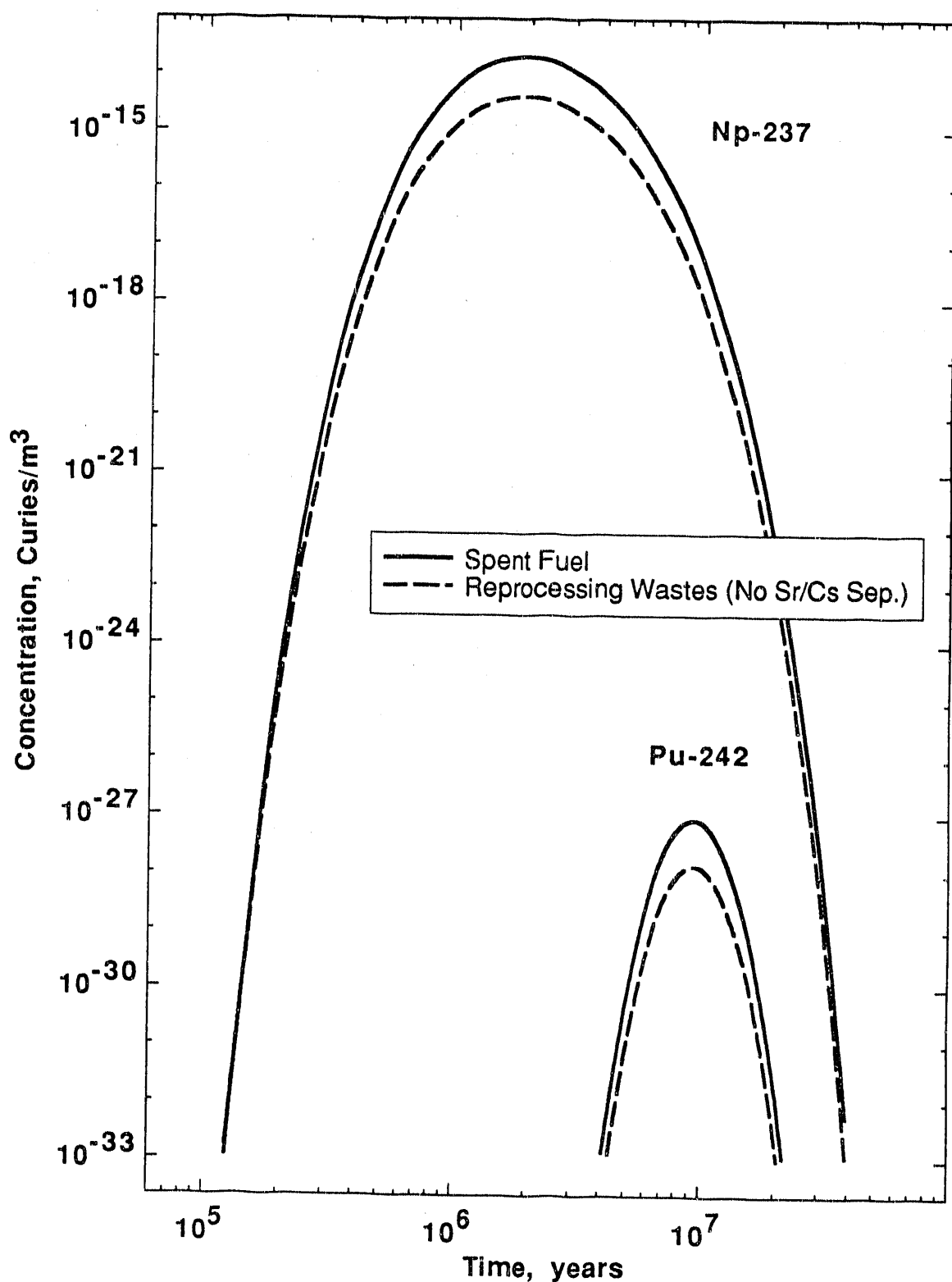


Figure 4.6. Np-237 and Pu-242 Concentrations at the Accessible Environment for Spent Fuel and Reprocessing Wastes

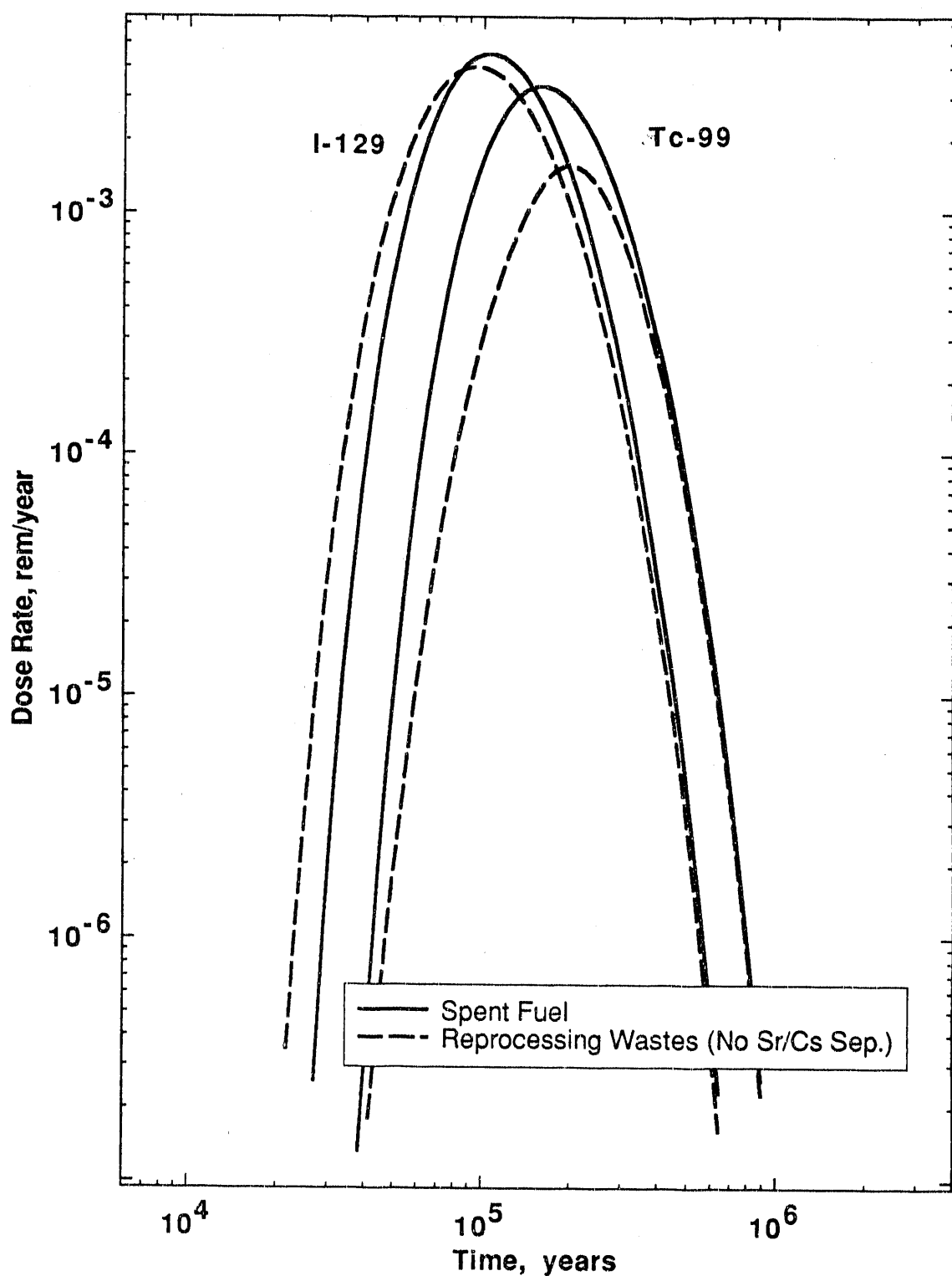


Figure 4.7. Tc-99 and I-129 Dose Rates at the Accessible Environment for Spent Fuel and Reprocessing Wastes

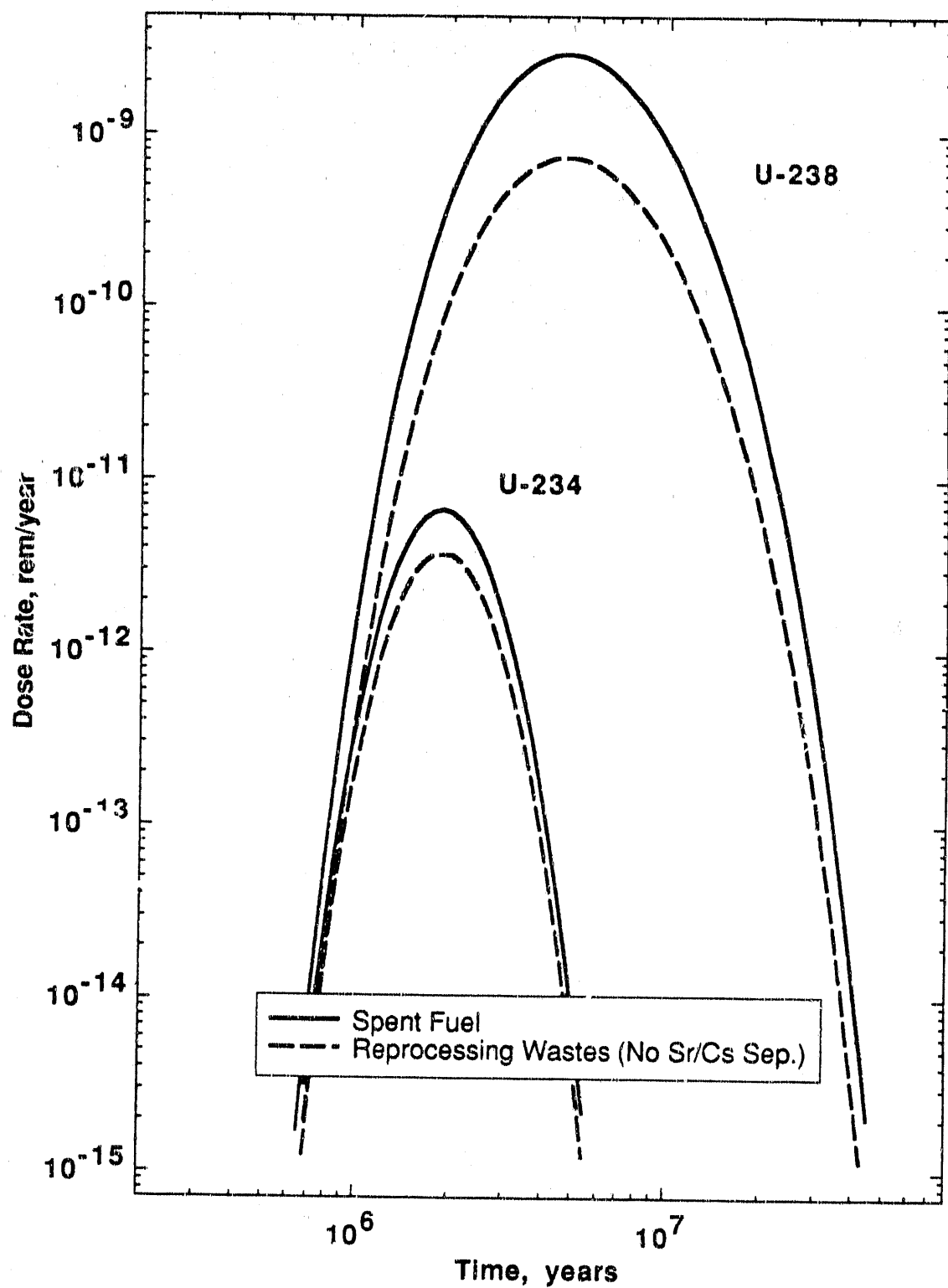


Figure 4.8. Uranium Dose Rates at the Accessible Environment for Spent Fuel and Reprocessing Wastes

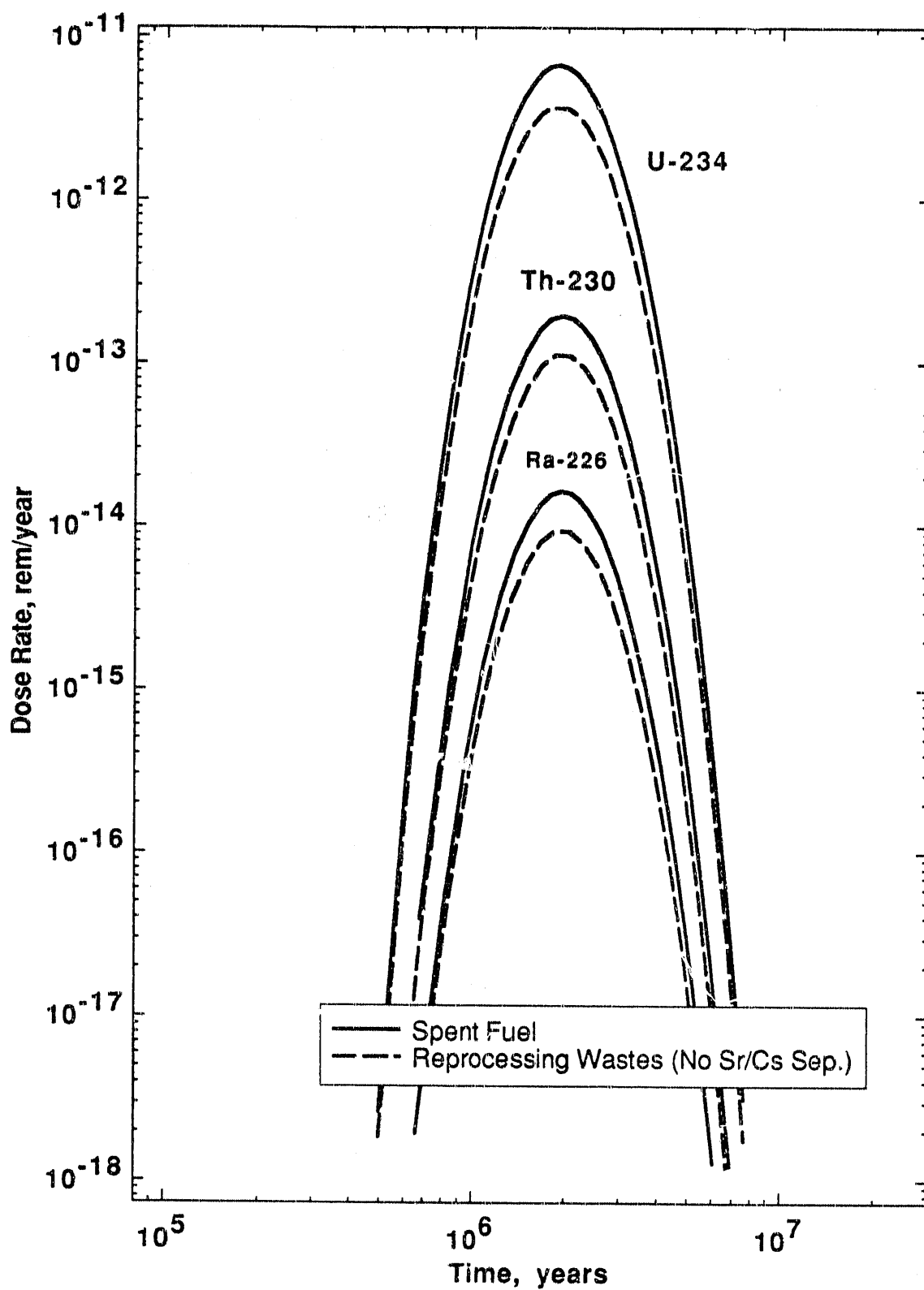


Figure 4.9. U-234 and Daughters Dose Rates at the Accessible Environment for Spent Fuel and Reprocessing Wastes

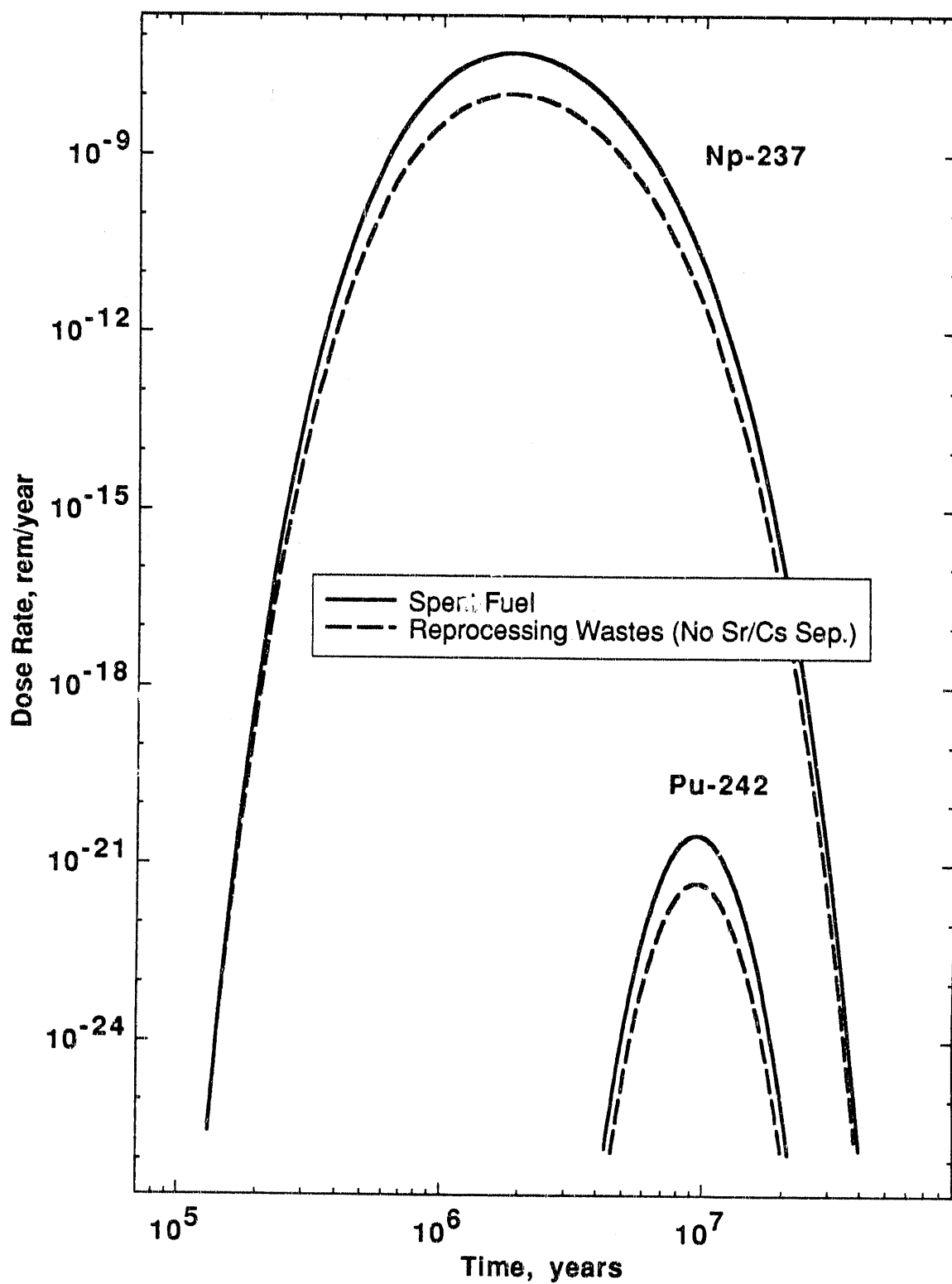


Figure 4.10. Np-237 and Pu-242 Dose Rates at the Accessible Environment for Spent Fuel and Reprocessing Wastes

congruent with the alteration of the waste form.

The EPA<sup>5</sup> has set limits on the allowable cumulative radionuclide releases at the accessible environment in the first 10,000 years. The criteria for determining these limits for various types of repositories result in different release limits for the spent fuel and reprocessing waste disposal schemes. However, with the parameters adopted for this study, no radionuclides from either scheme reach the accessible environment before that time.

Neither NRC or EPA has established an individual dose limit for a U. S. repository; however, the International Commission on Radiological Protection (ICRP) has recommended that individuals subject to prolonged exposure (more than 10 years) receive no more than 0.1 rem/year.<sup>60</sup> In this study, no radionuclides exceed this dose rate. The highest peak dose rate, that of I-129 in the spent fuel scheme, is about 25 times below this limit.

Although dose rate calculations were not carried out for the case of reprocessing with strontium and cesium separation, or for the borosilicate glass option, it is possible to predict qualitatively the dose rates for radionuclides in these disposal schemes by using knowledge of their release rates. Dose rates of the actinide elements in the Sr/Cs separation scheme will be about 2.6 times higher than those in the spent fuel scheme, since the total top area of all waste packages containing actinides in this scheme is about 2.6 times higher than in the spent fuel scheme. However, this number will differ for individual isotopes because in the Sr/Cs separation scheme the repository contains many extra ALMR packages, which contain wastes with a different isotopic composition than LWR spent fuel. The dose rate of Tc-99, which in the plain reprocessing scheme arises almost entirely from alteration-controlled release from  $1.1 \times 10^4$  packages, is expected to be roughly 15 times higher with the addition of almost  $1.6 \times 10^5$  extra packages in the Sr/Cs separation scheme. Similarly,  $4.4 \times 10^5$  extra packages containing instantly-dissolved I-129 will make this species' dose rate in the Sr/Cs separation scheme about 27

times higher than that in the plain reprocessing scheme. With the borosilicate glass option, however, the I-129 dose rate should be substantially lower than with the plain reprocessing scheme, corresponding to its lower release rate from the repository.

Since it was assumed in the transport model that the well does not perturb the aquifer, the concentrations and dose rates calculated here are those that would exist at the well location if there were no appreciable draw-off of water from the well. If the well were to supply large amounts of water to a sizable population, it would disturb the groundwater flow and result in a lower concentration of radionuclides in the well effluent. However, this would not affect the relationships between individual radionuclide dose rates, or between dose rates from spent fuel and from actinide-burning reprocessing wastes.

## Chapter 5

### Conclusions

Three possible disposal schemes for the proposed Yucca Mountain repository are described. They are: disposal of 96,500 Mg LWR spent fuel; disposal of wastes from reprocessing 84,000 Mg LWR spent fuel and from reprocessing 8517 Mg ALMR spent fuel; and disposal of wastes from reprocessing 84,000 Mg LWR spent fuel and from reprocessing 235,110 Mg ALMR spent fuel. In the first reprocessing scheme, reprocessing involves removal of 99.8% of the Np, Pu, Am, and Cm and 98.4% of the U from LWR spent fuel, and removal of 99.8% of the actinides from ALMR spent fuel. In the second reprocessing scheme, reprocessing involves this same actinide removal, along with 100% removal of Sr-90 and Cs-137 and their decay products from LWR and ALMR spent fuel. In all disposal schemes the heat generation rate of the wastes at emplacement is  $1.1 \times 10^8$  watts.

Waste forms, packages, and radionuclide inventories are specified<sup>28</sup> for the three disposal schemes. Per-package and repository release rates are calculated for the spent fuel scheme and the reprocessing scheme without Sr/Cs separation. Per-package release rates in the two reprocessing schemes are the same because the same types of packages are used. Repository release rates of Np-237 are calculated for all three disposal schemes. Per-package and repository release rates of I-129 and Cs-135 are calculated for an additional disposal scheme, identical to the reprocessing scheme without Sr/Cs separation, but in which all salt/zeolite waste forms are replaced with borosilicate glass.

With the wet-drip model used to calculate release rates, assumptions about the waste forms strongly affect release rates. Release rates for soluble fission products in salt/zeolite wastes are calculated assuming that the waste form is unstable and has no ability to contain radionuclides. As a result, these release rates are initially very

high and drop off rapidly, as most of the inventory is released shortly after water contact. This approach is extremely conservative. In reality, the waste form will probably prevent instant dissolution of the entire package inventory. Reprocessing waste forms are not yet established and may be changed from those adopted here if an actinide burning program is undertaken. If the soluble fission products are immobilized in borosilicate glass instead, their release rates are much lower than the early-time release rates from instant-dissolution waste packages.

The release rate of a solubility-limited species from a waste package does not depend on its inventory in the package. The most important parameter for such a species is its elemental solubility. Here it is assumed, somewhat arbitrarily, that the solubilities of actinides in reprocessing wastes are the same as those in spent fuel. Solubility data for reprocessing waste forms are needed if an accurate comparison of spent fuel and reprocessing waste release rates is to be made. These data are also needed to evaluate potential waste forms. However, as long as dissolution of an actinide is limited by its solubility, its package inventory will not affect its release rate.

With the wet-drip water-contact release rate model, the release rate of a solubility-limited species is proportional to the top area of the vertically emplaced container. Although the inventories of solubility-limited actinides in reprocessing waste packages adopted here are up to 100 times lower than in the spent fuel packages, the per-package release rates from waste containers with the same top area are equal. Total repository release rates of actinides are only a few times lower for our actinide-burning reprocessing scheme, because the total top area of all of the packages in this scheme is lower.

Curium is the only soluble actinide, and thus the only one for which decreasing the package inventory decreases the release rate. The release rates of curium in the reprocessing scheme without Sr/Cs separation are about 100 times lower than in the spent fuel scheme. This is due both to its lower inventory and to the placement

of a portion of the repository inventory in waste packages containing copper, which is expected to corrode very slowly.

If strontium and cesium are separated from the reprocessing wastes before disposal, the reduced heat generation rate of the wastes allows a greater loading of waste in the repository. If the additional waste packages placed in the repository are the same type as the original packages, release rates from the repository increase proportionately to the number of extra packages in the repository. With the repository loadings adopted here, the release rate of Np-237 in the Sr/Cs separation scheme is about ten times higher than that in the reprocessing scheme without Sr/Cs separation.

Radionuclide discharge rates at the water table, and concentrations and dose rates at the accessible environment are calculated for the spent fuel scheme and the reprocessing scheme without Sr/Cs separation. With the geologic and hydrologic parameters adopted here, the only actinides which reach the water table are U-234, U-238, Np-237, and Pu-242. Their discharge rates from spent fuel are only about one to six times higher than those from reprocessing wastes, corresponding to their higher repository release rates. Curium, the only actinide for which reducing the waste inventory reduces the release rate, decays before reaching the water table. The fission products Tc-99 and I-129 are highly mobile, and in both disposal schemes their discharge rates at the water table peak well before those of any of the actinides. The Tc-99 and I-129 discharge rates are also much higher than those of the actinides, because their repository release rates are much higher. Cs-135 decays before reaching the water table.

Relative radionuclide concentrations at the accessible environment approximately correspond to their relative discharge rates at the water table, and thus also with their release rates from the repository. Dose conversion factors for all species except Tc-99 are within an order of magnitude of each other; their relative dose rates also correspond roughly to their relative repository release rates. As a result, dose rates

of both fission products and actinides are only a few times lower in the reprocessing scheme than in the spent fuel scheme. In both schemes, dose rates of Tc-99 and I-129 are  $10^6$  to  $10^{18}$  times higher than those of the actinides.

Because release of actinides from spent fuel and reprocessing wastes is limited by their solubilities and unaffected by their per-package inventories, their removal from spent fuel before placement in the Yucca Mountain repository does not appreciably reduce the risks to future individuals from groundwater contamination. The fission products Tc-99 and I-129 pose a much higher risk than do any of the actinides. However, this study does not consider risk from the above-ground reprocessing plants, from repository releases of gaseous radionuclides such as C-14, or from human intrusion into the repository. A recent study of the Auriat repository site in France<sup>61</sup> estimated risks from human intrusion to be 10 to 100 times lower than risks from groundwater contamination, for spent fuel and high-level wastes.

In addition to radionuclide inventories, a number of other factors affect risk to future humans. These include the waste form, package geometry, and radionuclide transport characteristics. This leads to the possibility of using techniques other than, or in addition to, inventory reduction to limit radionuclide releases from waste packages. For example, since the total release rate of a solubility-limited species is proportional to the number of packages (assuming the same type of packages), the total release rate from a given amount of solubility-limited radionuclide can be minimized by storage in as few packages as possible. For soluble species, immobilization in a stable waste form can decrease the release rate.

As discussed in Chapter 1, the DOE actinide burning program has a number of possible benefits and drawbacks not all of which are related to risk reduction. A complete evaluation of the program will consider many additional issues before a decision on whether to implement actinide burning in the United States is made.

## References

1. Wicks, G. and D. Bickford, "Doing Something About High Level Nuclear Waste," *Technology Review*, 92, No. 8, 50-58, (1989).
2. U. S. Department of Energy, Office of Civilian Radioactive Waste Management, "Integrated Data Base for 1990: U. S. Spent Fuel and Radioactive Waste Inventories, Projections, and Characteristics." Rev. 6. DOE/RW-0006. Washington, D. C.: U. S. Government Printing Office, 1990.
3. U. S. Nuclear Regulatory Commission, "Disposal of High-Level Radioactive Wastes in Geologic Repositories." Title 10 *Code of Federal Regulations* 60.113(a)(1)(ii)(B). Washington, D. C.: U. S. Government Printing Office, 1983.
4. U. S. Department of Energy, Office of Civilian Radioactive Waste Management, "Site Characterization Plan Overview: Yucca Mountain Site, Nevada Research and Development Agency, Nevada." DOE/RW-0198. Washington, D. C.: U. S. Government Printing Office, 1988.
5. U. S. Environmental Protection Agency, "Environmental Radiation Protection Standards for Management and Disposal of Spent Nuclear Fuel, High-Level and Transuranic Radioactive Wastes." Title 40 *Code of Federal Regulations* 191. Washington, D. C.: U. S. Government Printing Office, 1987.
6. Griffith, J. D., U. S. Department of Energy, Office of Nuclear Energy, "Actinide Recycle: Presentation to National Research Council Committee on Future Nuclear Power Development," January 29, 1990.
7. Hecker, S. S., Los Alamos National Laboratory, "Science Making a Difference in the 21st Century," Testimony before the U. S. Senate Committee on Energy and Natural Resources, Subcommittee on Energy Research and Development, July 1990.

8. Croff, A. G., "Historical Perspective of Partitioning-Transmutation," in Forsberg, C. W. *et. al.*, "Historical Perspective, Economic Analysis, and Regulatory Analysis of the Impacts of Waste Partitioning-Transmutation on the Disposal of Radioactive Wastes." ORNL/TM-11650. October 1990.
9. Steinburg, M., G. Watsak, and B. Manowitz, "Neutron Burning of Long-Lived Fission Products for Waste Disposal." BNL-8558. September 1964.
10. Burkholder, H. C., "Nuclear Waste Partitioning Incentives," Proceedings of the Nuclear Regulatory Commission Workshop, The Management of Radioactive Waste: Waste Partitioning as an Alternative. NR-CONF-001, 444-469, June 1976.
11. Claiborne, H. C., "Neutron-Induced Transmutation of High-Level Radioactive Waste." ORNL/TM-3964. December 1972.
12. Croff, A. G., J. O. Blomeke, and B. C. Finney, "Actinide Partitioning-Transmutation Program Final Report I Overall Assessment." ORNL-5566. June 1980.
13. Davidson, W. and D. Klein, Editors, "Proceedings of the International Conference on Nuclear Waste Transmutation," Austin, Texas, July, 1980.
14. International Atomic Energy Agency, "Evaluation of Actinide Partitioning and Transmutation." Technical Report 214. Vienna, 1982.
15. Thompson, M. L., "Actinide Recycle in the Advanced Liquid Metal Reactor," Presentation at the University of California, Berkeley Industrial Liaison Program, March 13, 1991.
16. Johnson, T. R., L. Burris, N. M. Levitz, and R. N. Hill, "Use of Transuranic Elements from LWR Fuel in Integral Fast Reactors." ANL-IFR-127. 1990.
17. Wolfe, B. and B. F. Judson, "Fuel Recycle in the U. S. - Significance, Status, Constraints and Prospects," Proceedings of the fourth Pacific Basin Nuclear Conference. Canadian Nuclear Association, ISBN0-919307-30-2, 134-

136, Vancouver, Canada, September 1983.

18. Pigford, T. H., "Actinide Burning and Waste Disposal." UCB-NE-4176. Berkeley: University of California, October 1990.
19. Eriksson, L. G., "Is It Time to Reduce the Heat on the Concept of Geologic Disposal of High-Level Radioactive Waste?," *American Underground-Space Association News*, 5, No. 1, 18, (1990).
20. Eriksson, L. G. and D. L. Pentz, "Natural System Issues in the OCRWM Program," Proceedings of the International High Level Waste Management Conference. Vol. 1, 10-19, Las Vegas, Nevada, April 1990.
21. Cloninger, M. O., D. Short, and S. Stahl, "Waste Package for Yucca Mountain Repository: Strategy for Regulatory Compliance," Proceedings of Waste Management '89. Vol. 1, 537, 1989.
22. Ramspott, L. D., "The Constructive Use of Heat in an Unsaturated Tuff Repository." UCRL-JC-105868. January 1991.
23. Berglund, R. C., Y. I. Chang, S. Rosen, and C. E. Weber, "Actinide Recycle in Advanced Liquid Metal Reactors," Korean Atomic Industrial Forum, April 16, 1990.
24. Till, C. E. and Y. I. Chang, "The Liquid-Metal Reactor," Presentation to the National Academy of Sciences, Committee on Future Nuclear Power Development, August 1989.
25. Jourde, M. et. al., "Séparation et Transmutation des Actinides Mineurs." Commission Pour les Questions Scientifiques et Techniques Relatives à la Gestion des Déchets Radioactifs Auprès du Conseil Scientifique du C. E. A., Mars 1990.
26. Priem, T., F. Bretheau, and A. Cernes, "Effect of Minor Actinide Removal from Fission Products Before Vitrification on the Radiological Impact of a High Level Waste Deep Repository," Proceedings of the International High

Level Waste Management Conference. Las Vegas, Nevada, 1990.

27. U. S. Department of Energy, "Characteristics of Spent Fuel, High-Level Waste, and Other Radioactive Wastes Which May Require Long-Term Isolation." DOE/RW-0184. Washington, D. C.: U. S. Government Printing Office, 1987.
28. Thompson, M. L. and I. N. Taylor, "Projected Waste Packages Resulting from Alternative Spent Fuel Separations Processes." NP-7262. Electric Power Research Institute, 1991.
29. Pigford, T. H. and J. S. Choi, "Inventory Reduction Factors for Actinide-Burning Liquid-Metal Reactors," *Trans. American Nuclear Society*, 64, 123, (1991).
30. Young, W. H., "Office of Nuclear Energy (NE) Review of Conclusions in Professor T. H. Pigford's Paper." U. S. Department of Energy, March 5, 1991.
31. Rodwell, E., R. A. Shaw, and R. F. Williams, "An Evaluation of the Concept of Transuranic Burning Using Liquid Metal Reactors." NP-7261. Electric Power Research Institute, March 1991.
32. Lee, W. W.-L., J. S. Choi, and M. M. Sadeghi, "Releases from Exotic Waste Packages from Partitioning and Transmutation." LBL-31258. Berkeley: Lawrence Berkeley Laboratory, 1991.
33. Pigford, T. H., "Suggestions for Actinide-Burning Scenarios for Yucca Mountain." UCB-NE-4180. April 1991.
34. U. S. Department of Energy, Office of Civilian Radioactive Waste Management, "Site Characterization Plan: Yucca Mountain Site, Nevada Research and Development Agency, Nevada." DOE/RW-0199. Washington, D. C.: U. S. Government Printing Office, 1988.
35. O'Connell, W. J. and R. S. Drach, "Waste Package Performance Assessment:

Deterministic System Model Program Scope and Specification." UCRL-53761.

36. Sadeghi, M. M., T. H. Pigford, P. L. Chambré, and W. W.-L. Lee, "Equations for Predicting Release Rates for Waste Packages in Unsaturated Tuff." LBL-29254. Berkeley: Lawrence Berkeley Laboratory, 1990.
37. Wilson, C. N., "Results from NNWSI Series 3 Spent Fuel Dissolution Tests." PNL-7170. 1990.
38. Wilson, C. N. and C. J. Bruton, "Studies on Spent Fuel Dissolution Behavior under Yucca Mountain Repository Conditions." PNL-SA-16832. 1989.
39. Bruton, C. J. and H. Shaw, "Geochemical Simulation of Reaction between Spent Fuel Waste Form and J-13 Water at 25°C and 90°C," in *Scientific Basis for Nuclear Waste Management XI*, Editors M. J. Apted and R. E. Westerman, Materials Research Society, Pittsburgh, PA, 485, 1988.
40. Sadeghi, M. M., T. H. Pigford, P. L. Chambré, and W. W.-L. Lee, "Prediction of Release Rates for a Potential Waste Repository at Yucca Mountain." LBL-27767. Berkeley: Lawrence Berkeley Laboratory, October 1990.
41. Wilems, R. E. and J. G. Danna, "The Effects of Transuranic Separation on Waste Disposal." NP-7263. Electric Power Research Institute, 1991.
42. Burger, L. L., R. D. Scheele, and K. D. Wiemers, "Selection of a Form for Fixation of Iodine-129." PNL-4045, UC-70. 1981.
43. Benedict, M., T. H. Pigford, and H. W. Levi, "Nuclear Chemical Engineering." Second Edition. New York: McGraw-Hill, 1981.
44. Pigford, T. H., University of California, Berkeley, private communication, 1991.
45. Southwell, C. R., J. D. Bultman, and A. L. Alexander, "Corrosion of Metals in Tropical Environment- Final Report of 16-Year Exposures," *Materials*

*Performance*, 15, No. 7, 9-25, (1976).

46. Kim, C. L., P. L. Chambré, and T. H. Pigford, "Radionuclide Release Rates as Affected by Container Failure Probability," *Trans. American Nuclear Society*, 50, 136, (1985).
47. Abrajano, T. A., J. K. Bates, T. J. Gerding, and W. L. Ebert, "The Reaction of Glass During Gamma Irradiation in a Saturated Tuff Environment, Part III: Long Term Experiments at  $10^4$  rad/hr." ANL-88-14. 1988.
48. Harada, M., P. L. Chambré, M. Foglia, K. Higashi, F. Iwamoto, D. Leung, T. H. Pigford, and D. Ting, "Migration of Radionuclide Chains Through Sorbing Media: Analytical Solutions - I." LBL-10500. Berkeley: Lawrence Berkeley Laboratory, 1980.
49. Light, W. B., "UCB-NE-10.4 User's Manual." UCB-NE-4133. Berkeley: Lawrence Berkeley Laboratory, 1990.
50. Rundberg, R. S., "Assessment Report on the Kinetics of Radionuclide Adsorption on Yucca Mountain Tuff." LA-11026-MS. 1987.
51. de Marsily, G., "Quantitative Hydrogeology." Orlando: Academic Press, 1986.
52. Barnard, R. W. *et. al.*, "Summary Report on the PACE-90 Radionuclide Transport Problem for a "Nominal" Hydrogeologic Configuration." SLTR90-3001. 1990.
53. Sinnock, S., Y. T. Lin, and J. P. Brannen, "Preliminary Bounds on the Expected Postclosure Performance of the Yucca Mountain Repository Site, Southern Nevada," *Journal of Geophysical Research*, 92, No. B8, 7820-7842, (1987).
54. Chambré, P. L., T. H. Pigford, W. W.-L. Lee, J. Ahn, S. Kajiwara, C. L. Kim, H. Kimura, H. Lung, W. J. Williams, and S. J. Zavoshy, "Mass Transfer and Transport in a Geologic Environment." LBL-19430. Berkeley: Lawrence

Berkeley Laboratory, 1985.

55. Pigford, T. H., J. O. Blomeke, T. L. Brekke, G. A. Cowan, W. E. Falconer, N. J. Grant, J. R. Johnson, J. M. Matuszek, R. R. Parizek, R. L. Pigford, and D. E. White, "A Study of the Isolation System for Geologic Disposal of Radioactive Wastes." Washington, D. C.: National Academy Press, 1983.
56. Peters, R. R., E. A. Klavetter, I. J. Hall, S. C. Blair, P. R. Heller, and G. W. Gee, "Fracture and Matrix Hydrologic Characteristics of Tuffaceous Materials from Yucca Mountain, Nye County, Nevada." SAND-84-1471. Albuquerque: Sandia National Laboratory, 1984.
57. Charles, D. and G. M. Smith, "Conversion of Releases from the Geosphere to Estimates of Individual Doses to Man." I1802-10. INTERA-Exploration Consultants Ltd., 1990.
58. Swedish Nuclear Fuel Supply Company, KBS Division, "Final Storage of Spent Nuclear Fuel - KBS-3." May 1983.
59. Pigford, T. H., "Effect of Actinide Burning on Risk from High-Level Waste," *Trans. American Nuclear Society*, 69, 80, (1991).
60. National Cooperative for the Storage of Radioactive Waste, "Nuclear Waste Management in Switzerland: Feasibility Studies and Safety Analyses." NGB-85-09. June 1985.
61. Mobbs, S. F., M. P. Harvey, J. S. Martin, A. Mayhall, and M. E. Jones, "Comparison of the Waste Management Aspects of Spent Fuel Disposal and Reprocessing: Post-Disposal Radiological Impact." United Kingdom: National Radiological Protection Board, 1991.

END

DATE  
FILMED

8/27/92

